APPROVAL SHEET

Title of Dissertation: "Identification of Two Suppressors of CSG2Calcium Sensitivity, SCS7 and SUR2, as Genes Encoding Hydroxylases of the Sphingolipid Biosynthetic Pathway of Saccharomyces cerevisiae"

Name of Candidate: LTC Dale Haak
Doctor of Philosophy Degree
10 December 1997

Dissertation and Abstract Approved:

Troy Beeler, Ph.D.
Department of Biochemistry
Committee Chairperson

12/10/97
Date

Teresa Dunn, Ph.D.
Department of Biochemistry
Major Advisor

12/10/97
Date

Ishaiahu Shechter, Ph.D.
Department of Biochemistry
Committee Member

12-10-97
Date

Mark Adelman, Ph.D.
Department of Anatomy & Cell Biology
Committee Member

12/10/97
Date

Pat McGraw, Ph.D.
Department of Biology, UMBC
Committee Member

12/10/97
Date

ABSTRACT

Title of Dissertation: Identification of Two Suppressors of *CSG2* Calcium Sensitivity, *SCS7* and *SUR2*, as Genes Encoding Hydroxylases of the Sphingolipid Biosynthetic Pathway of *Saccharomyces cerevisiae*.

Dale Arthur Haak, PhD, 1997

Thesis directed by: Teresa Dunn, Associate Professor, Department of Biochemistry
Troy Beeler, Associate Professor, Department of Biochemistry

Sphingolipids are abundant constituents of the plasma membrane of many eukaryotic cell types from yeast to human and are known to function in numerous cellular metabolic processes. Sphingolipids have a wide range of structural diversity with respect to the composition of the head group and the hydroxylation state of the ceramide backbone. The biochemical significance of much of this structural variability is not well understood. The sphingolipids of the yeast *Saccharomyces cerevisiae* undergo the α-hydroxylation of the very long chain fatty acid (VLCFA) moiety of the ceramide backbone in the same manner as animal cells. Yeast sphingolipids are additionally hydroxylated on the long chain base (LCB) moiety and at a second position on the VLCFA. A connection between sphingolipid hydroxylation and calcium homeostasis in yeast is suggested by the phenotypic behavior of the calcium sensitive *csg2* mutant and its suppressors. This mutant cannot mannosylate the sphingolipid head groups and thus overaccumulates unmannosylated sphingolipids with hydroxylated ceramide backbones. Two secondary mutations, *sur2* and *scs7*, suppress *csg2* Ca^{2+} sensitivity and the corresponding double mutants overaccumulate unmannosylated sphingolipids with slightly higher thin layer

i

chromatography mobilities than those of *csg2* single mutants, consistent with the former species being ceramide unhydroxylated. Additionally, *sur2* and *scs7* single mutants accumulate species with mobilities predicted for unhydroxylated mannosylated sphingolipids. Sphingolipids and ceramides from *sur2* and *scs7* mutants in both wild-type and *csg2* backgrounds were purified by thin layer chromatography and subjected to acid methanolysis. TLC analysis showed that the acid-hydrolyzed *sur2* extracts contain the long chain base, dihydrosphingosine, while the *scs7* extracts contain nonhydroxylated VLCFA. This indicates that Sur2p and Scs7p are required for the LCB and VLCFA hydroxylations respectively. The wild-type *SCS7* gene was cloned by identifying plasmids from a wild-type yeast genomic library that complemented *scs7* suppression of *csg2* Ca^{2+} sensitivity when transformed into a *csg2 scs7* double mutant. The predicted Scs7p contains the topological and primary strutural features of a family of membrane diiron-oxo proteins that catalyze lipid desaturations and hydroxylations. These features include histidine rich primary sequence motifs in specific positions relative to hydrophobic membrane spanning domains. Sur2p also contains these histidine rich motifs which are thought to provide diiron center binding ligands at the active site. Taken together the sphingolipid structural characterizations and sequence analyses indicate that Sur2p and Scs7p are the hydroxylases responsible for the LCB and VLCFA hydroxylations of the yeast sphingolipid biosynthetic pathway.

IDENTIFICATION OF TWO SUPPRESSORS OF *CSG2* CALCIUM SENSITIVITY,

SCS7 AND *SUR2*, AS GENES ENCODING HYDROXYLASES OF THE

SPHINGOLIPID BIOSYNTHETIC PATHWAY OF *SACCHAROMYCES CEREVISIAE*

by

Dale Arthur Haak

Thesis submitted to the Faculty of the Department of Biochemistry Graduate
Program of the Uniformed Services University of the Health Sciences in
partial fulfillment of the requirements for the degree of
Doctor of Philosophy 1997

To the glory of the one who called it all into being *ex nihilo*

and

To Nellie, Leslie, Lindsey and Stephanie
who endured much so that I could do this

TABLE OF CONTENTS

Chapter

vi

FIGURES AND TABLES

ABBREVIATIONS

AcOH	Acetic acid
AlkB	Alkane ω-hydroxylase
AP-1	Activator protein 1
ATCC	American Type Culture Collection
BuOH	Butanol
CAPP	Ceramide-activated protein phosphatase
CAPK	Ceramide-activated protein kinase
CSG	Calcium sensitive growth genotype
CYTb5	Cytochrome b_5 locus
dNTP	Deoxynucleotidetriphosphate
DSC	Differential scanning calorimetry
DTPA	Diethylenetriaminepentacetic acid
EDTA	Ethylenediaminetetracetic acid
EGF	Epidermal growth factor
ER	Endoplasmic reticulum
FAME	Fatty acid methyl ester
FOA	5-fluoroorotic acid
GDA	Guanosine diphosphatase genotype
GPI	Glycerylphosphoinositol
HFA-CER	2-hydroxyfattyacid cerebroside
HVLCFAME	Hydroxylated very long chain fatty acid methyl ester
IκB	Inhibitor of nuclear transcription factor κB
IL-1	Interleukin 1
IP$_3$	Inositoltriphosphate
IPC	Inositolphorylceramide
LCB	Long chain (sphingoid) base
LCB	Long chain base genotype
MAP	Mitogen-activated protein
MAPK	Mitogen-activated protein kinase
MAT	Mating genotype
MIPC	Mannosylinositolphosphorylceramide
M(IP)$_2$C	Mannosyldiinositolphosphorylceramide
MMOH	Methane monooxygenase
NfκB	Nuclear transcription factor κB
NFA-CER	nonhydroxy fatty acid cerebroside
NVLCFAME	Nonhydroxylated very long chain fatty acid methyl ester
OD	Optical density
OLE	Oleic acid desaturation genotype
ORF	Open reading frame
PCR	Polymerase chain reaction

PDGF	Platelet-derived growth factor
PGE$_2$	Prostaglandin E$_2$
PI	Phosphatidylinositol
PIPLC	Phosphatidylinositol specific phospholipase C
PMA1	Plasma membrane ATPase genotype
SCS	Suppressor of calcium sensitivity genotype
SD	Synthetic Dextrose Culture Media
SEC	Secretory genotype
SLC	Sphingolipid compenstation genotype
SPP	Sphingosine-1-phosphate
TLC	Thin layer chromatography
TNF-α	Tumor necrosis factor
VLCFA	Very long chain fatty acid
VLCFAME	Very long chain fatty acid methyl ester
YPD	Yeast peptone dextrose culture media
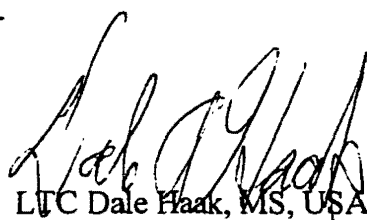
STRAIN LIST

TDY2037	*Matα lys2 ura3-52 trp1Δ leu2Δ*
TDY2038	*Matα lys2 ura3-52 trp1Δ leu2Δ csg2::LEU2*
TDY2010b	*Mata ura3-52 his4-619 csg2::LEU2*
CZ39R	*Matα lys2 ura3-52 trp1Δ leu2Δ csg2::LEU2 scs7-1*
TDY2050	*Matα ura3-52 ade2 leu2Δ csg1*
11224A	*Mata lys2 ura3-52 leu2Δ csg2*
5197d	*Mata lys2 ura3-52 trp1Δ leu2Δ ade2-101 csg2::LEU2 scs7-1*
G11-10	*Mata lys2 ura3-52 leu2Δ gda1::LEU2*
7gk36a	*Mata lys2 ura3-52 leu2Δ trp1Δ scs7::LEU2 gda1::LEU2*
TDY2037scs7k	*Matα lys2 ura3-52 trp1Δ leu2Δ scs7::LEU2*
6715b	*Matα lys2 ura3-52 trp1Δ leu2Δ csg2::LEU2 scs7::LEU2*
TDY239sur2k	*Mata ura3-52 trp1 leu2Δ his4-619 sur2::TRP1*
TDY239scs7k/sur2k	*Mata ura3-52 trp1 leu2Δ his4-619 scs7::LEU2 sur2::TRP1*
TDY240sur2k	*Mata lys2 ura3-52 trp1 leu2Δ his4-619 csg2::LEU2 sur2::TRP1*
6715b/sur2k	*Matα lys2 ura3-52 trp1Δ leu2Δ csg2::LEU2 sur2::TRP1*

The author hereby certifies that the use of any copyrighted material in the thesis manuscript entitled:

"Identification of Two Suppressors of CSG2Calcium Sensitivity, SCS7 and SUR2, as Genes Encoding Hydroxylases of the Sphingolipid Biosynthetic Pathway of <u>Saccharomyces cerevisiae</u>"

beyond brief excerpts is with the permission of the copyright owner, and will save and hold harmless the Uniformed Services University of the Health Sciences from any damage which may arise from such copyright violations.

LTC Dale Haak, MS, USA
Department of Biochemistry
Uniformed Services University of the Health Sciences

Chapter One

An Overview of Sphingolipid Metabolism

Metabolic Roles of Sphingolipids

In addition to their role as the chief structural components of cell membranes, phospholipids participate both directly and indirectly in cellular metabolism. Sphingolipids mirror many of the structural and metabolic phospholipid functions. The cell membrane can be thought of as a two dimensional fluid in which the protein components freely migrate in the performance of their various roles. This freedom of movement, and thus the physical state from which it is derived, is absolutely essential for membrane function.

The physical interactions among the phospholipid membrane components define this critical membrane property. These physical interactions are influenced by cellular environmental factors such as temperature, pressure and the concentrations of inorganic ions or chemicals, such as ethanol. The most widely studied of these factors is temperature with which the fluidity of the membrane varies directly. A wide variety of both prokaryotic and eukaryotic cells adjust the lipid composition of their membranes in order to stabilize fluidity in response to varying temperature (Thompson, 1992). The cell usually accomplishes this by inversely varying the concentration of lower melting point unsaturated phospholipids in response to temperature changes.

Counterbalancing the requirement for fluidity of the membrane is the need for structural integrity. Cells must be able to endure varying amounts of osmotic and

mechanical stress and maintain a specific state of permeability. Sphingolipids appear to have a role in mediating some of these properties in membranes as a consequence of their structure. Sphingolipids are more saturated than phospholipids which increases the hydrophobic interactions among the aliphatic chains. Additionally the sphingolipid structural backbone contains substituents that allow intra- and intermolecular hydrogen bonding.

The overall structure of the ceramide base of sphingolipids appears at first glance to be very similar to the diacylglycerol base of phospholipids (Figure 1). Both molecules have two long aliphatic chains that extend into the bilayer and are connected to a polar head group by a phosphodiester linkage. However the linkage of the aliphatic chains is different in the two molecules. In diacylglycerol two fatty acids are joined in an acyl ester linkage to a glyceryl moiety, while in ceramide one of the aliphatic chains is provided by a long chain base, (LCB; phytosphingosine in Figure 1), and the other is in amide linkage with the LCB. Ceramide therefore has many more proton donating groups capable of forming hydrogen bonds.

Hydrogen bonding is believed to be an important component of the physical properties and structure of membranes (Boggs, 1986). Single crystal X-ray diffraction analysis has shown that cerebroside (β-D-galactosylceramide) forms an extensive network of intra- and intermolecular hydrogen bonding that involves the hydroxyl groups of the galactosyl moiety as well (Pascher and Sundell, 1977). The ultimate effects of these cohesive lipid interactions is an overall increase in membrane rigidity.

2

····H–Ö–C   ····H–Ö–CH

C   CH

:O: N–CH   Ö–H····

H   CH₂

:O:

(R)

Ceramide

C=O

:O:

:O: C   CH₂

Ö–CH

CH₂

:O:

(R)
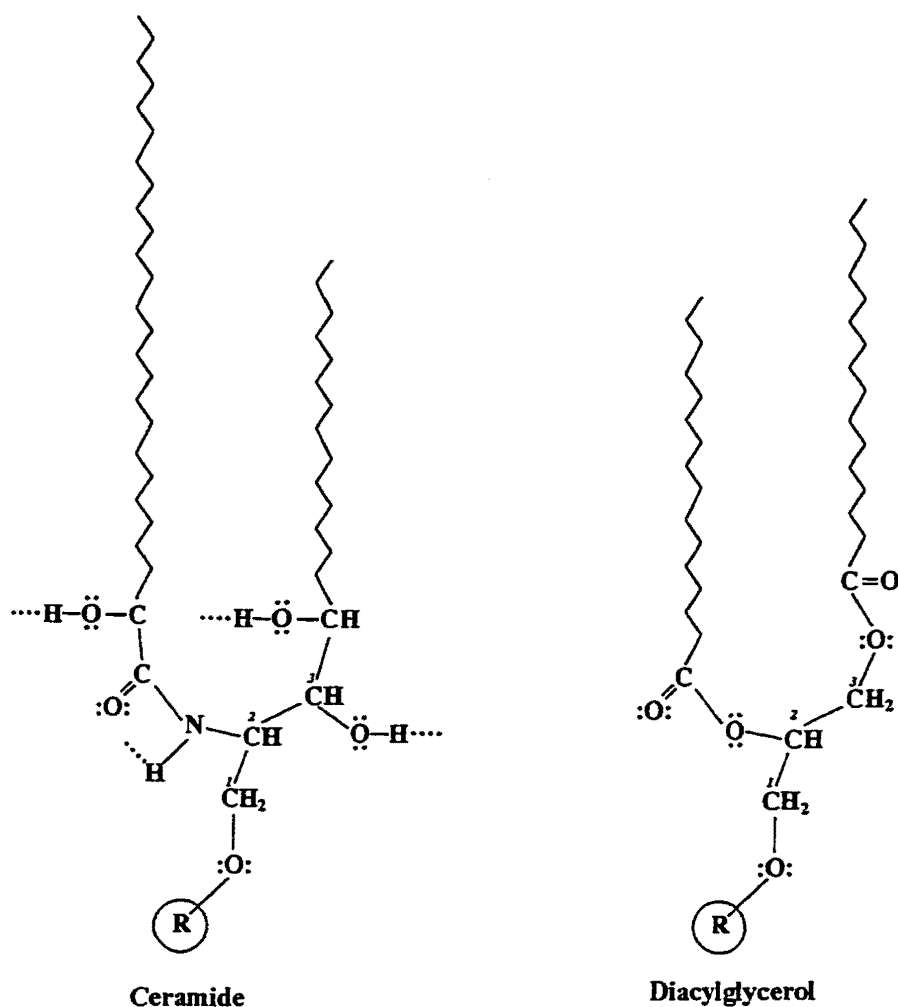
Diacylglycerol

Figure 1. Structure comparison of Ceramide and Diacylglycerol showing hydrogen bond capable substituents. The three labeled carbon atoms on the diacylglycerol structure are those of the glycerol backbone. In the ceramide structure they are the first three carbon positions of the ceramide long chain base, (phytosphingosine as drawn). Sphingosine differs from this in having a desaturation between C_4-C_5 instead of the hydroxylation at C_4. The C_2 carbon of the very long chain fatty acid can either be hydroxylated or unhydroxylated. Thus, depending on the species, ceramides have from 2 to 4 proton donor substituents compared to diacylglycerol which has none.

3

In many systems, the concentrations of the two choline containing lipids, phosphatidylcholine and sphingomyelin are reciprocally regulated, so that the total amount of these two species is maintained at near constant levels (Kolesnick, 1991). This phenomenon has been correlated with alterations in membrane fluidity. For instance, human erythrocytes from patients with the disease abetalipoproteinaemia have decreased membrane fluidity that results in an acanthocytic morphology. Their lack of deformability has been attributed to a decreased phosphatidylcholine / sphingomyelin ratio since liposomes designed to mimic the ratios found in these patients have similar physical properties (Cooper *et al.*, 1977). Reciprocally, increasing the phosphatidylcholine level of sheep erythrocytes resulted in increased membrane fluidity and osmotic fragility (Borochov, 1977).

The functions of many membrane proteins depend on the maintenance of a specific physicochemical environment in the membrane. For example the activity of the plasma membrane H^+-ATPase is significantly influenced by membrane sphingolipid composition. There is a strong correlation of phenotypes between sphingolipid deficient *Saccharomyces cerevisiae* sphingolipid compensation, (*SLC*), mutants and plasma membrane H^+-ATPase (*pma1*) mutants (Patton *et al.*, 1992). These phenotypes included inability to grow at 37° C, low pH, or high salt concentrations. Additionally *SLC* mutants exhibit irreversible inhibition of glucose-primed net proton exclusion after exposure to low pH, as well as increased proton permeability of the plasma membrane. These results suggest that sphingolipids are necessary for pH homeostasis in yeast cells under conditions of environmental stress. The nature of this requirement appears to involve sphingo-

4

lipid stabilization of the H$^+$-ATPase or other membrane proteins involved in pH homeo-

stasis. Further evidence for sphingolipid participation in the function of the plasma mem-

brane H$^+$-ATPase is the recent discovery that a gene required for normal expression of the

H$^+$-ATPase (García-Arranz, *et al.*, 1994) is a fatty acid elongase required for the synthesis

of the C$_{24-26}$ fatty acyl chains required for sphingolipid synthesis (Chan-Soek, *et al.*,

1997).

Membrane lipids, or their metabolytes, can also be directly involved in membrane

protein regulation. Sphingolipids participate in the regulation of a wide variety of cellu-

lar processes. Sphingolipids reside primarily in the outer leaflet of the plasma membrane,

where they function as both normal immune and tumor antigens, cell differentiation mar-

kers, proliferation modulators, receptor and receptor cofactors, and modulators of cell-cell

and cell-substrate interactions (Hannun and Bell, 1989). Many of these functions require

the transduction of an external signal into the cell interior suggesting a second messenger

role for the associated sphingolipid species. Recent studies have confirmed sphingolipids

acting in such roles.

First, agents such as 1α,25-dihydrovitamin D$_3$, Tumor Necrosis Factor (TNF-α)

and γ-interferon induce sphingomyelinase activity in HL-60 human leukemia cells.

Sphingomyelinase activity is also inducible in other cell lines by additional agents inclu-

ding IL-1, dexamethasone and complement components (Hannun, 1994). Sphingomy-

elinase cleaves the phosphocholine headgroup of sphingomyelin forming ceramide, and

as Figure 1 shows, the overall structure of ceramide is very similar to that of diacylgly-

cerol. Therefore, the presence of inducible sphingomyelinase in the plasma membrane

(Kolesnick, 1991), suggests the possibility that sphingomyelin, sphingomyelinase and ceramide form a second messenger system in a manner analogous to phosphatidylinositol triphosphate, phopholipase C, and diacylglycerol of the inositol triphosphate signaling pathway. Exogenously added ceramide duplicated the effects of TNF-α treatment in several cell lines including induced differentiation of HL-60 cells (Okazaki *et al.*, 1990) and apoptosis, in myeloid and lymphoid cells (Obeid, *et al.*, 1993). Stereoisomer specificity has been shown for these effects (Bielawska *et al.*, 1992.; Fishbein *et al.*, 1993.; Bielawska *et al.*, 1993).

Ceramide also performs as a second messenger in the immune response and protein secretion pathways. Interleukin-1 β (IL-1) induces sphingomyelinase activity in lymphocytes. Treatment of lymphocytes with ceramide duplicates IL-1-inducible secretion of prostaglandin E_2 (PGE2) (Ballou *et al.*, 1992) and IL-2 (Mathias *et al.*, 1993). C_6-ceramide inhibits secretion of vesicular stomatitis virus glycoprotein from infected Chinese hamster ovary cells (Rosenwald and Pagano, 1993). Brefeldin A, which acts to inhibit protein secretion by causing a collapse of the Golgi network into the endoplasmic reticulum, also stimulates a sphingomyelinase activity (Linardic, 1992).

Ceramide activity as a second messenger has been further established by the identification of many molecular downstream targets that are known signal transducers. These include ceramide activated protein kinase (CAPK; Mathias *et al.*, 1991; Joseph *et al.*, 1993), which upon activation by TNFα or C_8-ceramide, phosphorylates the epidermal growth factor (EGF) receptor (Goldkorn *et al.*, 1991), p42-MAP kinase in HL60 cells (Raines *et al.*, 1993), ceramide activated protein phosphatase (CAPP; Dobrowsky and

6

Hannun, 1992), and possibly a serine-like protease involved in IκB degradation. IκB is the physiologic inhibitor of NfκB, a TNFα responsive transcription factor that is activated in permeabilized Jurkat T-cells in response to exogenous sphingomyelinase and synthetic ceramide (Schultze *et al.*, 1992). In relation to this last finding, it is interesting to note that TNFα is a potent inducer of HIV provirus transcription and that such transcription induction by sphingomyelinase and C_8-ceramide has also been demonstrated, (Rivas *et al.*, 1994), suggesting that the sphingomyelinase pathway may be involved in HIV replication.

Although many questions remain, the sphingomyelinase pathways appear to induce antiproliferative, apoptotic and immune / inflammatory responses as well as playing an inhibitory role in protein trafficking and secretion. In contrast diacylglycerol second messenger pathways mediate tumor promotion, mitogenesis and activation of granule secretion and hormone release. Thus DAG and ceramide may define opposing pathways of regulation (Hannun, 1994). The sphingomyelinase pathway appears to be highly conserved as well, since a CAPP has recently been identified in *Saccharomyces cerevisiae* that mediates G1 growth arrest (Fishbein *et al.*, 1993).

The sphingolipid metabolites, sphingosine and sphingosine-1-phosphate (SPP) are also regulatory compounds. Sphingosine is formed by the deacylation of ceramide and SPP is formed by the subsequent phosphorylation of sphingosine at the hydroxyl group of the C1 carbon. Both molecules may play an early role in the MAP kinase cascade signal transduction pathway associated with cell growth, differentiation and neoplasia.

7

This pathway is initiated by the binding of platelet derived growth factor (PDGF) to its cognate receptor thus stimulating phospholipase D which hydrolyzes phosphatidylcholine to choline and phosphatidic acid (Ben-Av and Liscovitch, 1989). Phosphatidic acid stabilizes the active GTP bound form of Ras by inhibiting RasGAP the promoter of the GTPase activity of Ras (Tsai et al., 1989) and by stimulating cytoplasmic p21 ^{ras} GTPase inhibitory protein, another inhibitor of RasGAP (Tsai et al., 1990). GTP-Ras mediates a key step of the signaling cascade from the plasma membrane to the nucleus culminating in the activation of several transcription factors, including activator protein-1 (AP-1), that have been implicated in cell growth (Pelech and Sanghera, 1992). Sphingosine appears to increase phosphatidic acid levels by activation of both diacylglycerol kinase (Kanoh et al., 1989) and phospholipase D (Lavie and Liscovitch, 1990; Zhang et al., 1990), and by inhibition of phosphatidic acid phosphohydrolase (Jamal et al., 1991; Wu et al., 1993).

Sphingosine-1-phosphate (SPP), formed by phosphorylation of sphingosine, appears to mediate rapid release of calcium from intracellular stores in several types of intact and permeabilized cells (Zhang et al., 1991). SPP-induced calcium release is reminiscent of the calcium release caused by inositol triphosphate in the IP_3 signaling pathway and indeed evidence suggests that it is a receptor-mediated event (Spiegel and Milstien, 1995). A SPP-gated calcium channel with unique pharmacological and electrophysical properties has been characterized (Kindman et al., 1994), but whether this receptor is the mechanism by which SPP mediates calcium release has not been established.

8

Finally, sphingolipids also appear to be closely associated with protein trafficking. As will be discussed below, sphingolipids are transported to the cell surface via the protein secretory pathway. Additionally, it has been postulated that sphingolipid containing microdomains of intracellular membranes are involved in targeting glycosylphosphatidylinositol-anchored proteins to the apical cell surface in mammalian kidney cells (Brown and Rose, 1992). In yeast the fungal metabolite, myriocin, blocks ceramide synthesis and results in an inhibition of GPI-anchored protein transport (Horvath *et al.*, 1994).

Sphingolipids derive their name from the Greek myth of the sphinx and in many ways this name is still an appropriate expression of the magnitude of the riddle surrounding the function of these molecules. Yet the picture that is beginning to develop reveals the cell utilizing the full range of structural complexity of the sphingolipid species in cellular metabolism, both indirectly by the maintenance of critical physicochemical membrane properties and directly as effectors of multiple cellular processes. Although much of the sphingolipid riddle remains to be solved, there can be no doubt that these molecules are vitally important in multiple cellular processes and that their continued study can be expected to significantly advance our understanding of cell metabolism.

Sphingolipid Biosynthesis

The yeast *Saccharomyces cerevisiae* is a very useful system for studying sphingolipid metabolism. As a unicellular eukaryotic organism it is especially amenable to both genetic and biochemical analysis. In 1995 *S. cerevisiae* became the only eukaryotic organism for which the entire genomic sequence is known. Access to this infor-

mation has greatly facilitated genetic and biochemical investigation in this system. Yeast is also a useful model system because many molecular systems are less complex than their counterparts in animal or plant cells. The sophisticated molecular genetic approach that has been developed in *S. cerevisiae* has made it the most powerful model system for addressing basic questions in cell biology. As will be discussed below, the yeast sphingolipid biosynthetic pathway is an example of this.

Sphingolipid biosynthesis begins with the condensation of palmitoyl-CoA and serine (catalyzed by serine palmitoyltransferase) to form the long chain base 3-keto-sphinganine (Braun *et al.*, 1970). *S. cerevisiae* mutants defective in this first committed step of sphingolipid biosynthesis are long chain base auxotrophs (Pinto *et al.*, 1992; Zhao *et al.*, 1994), establishing sphingolipids as essential cellular components. Sphinganine is formed by the reduction of the 3-keto to a hydroxl group. Subsequently there is the conversion of sphinganine to either sphingosine, by a $\Delta 4,5$ desaturation, or to phytosphingo-sine, by hydroxylation at C_4, as well as attachment of the fatty acid in an amide linkage. Ong and Brady, (1973), reported that sphinganine is first acylated to form ceramide and that subsequently the sphinganine base is desaturated to form sphingosine, a result that has been confirmed by others (Michel *et al.*, 1997). The formation of phytosphingosine, which occurs in plants, yeast, and to a limited extent in animals, has been studied most extensively in the yeast *Hanenula ciferrii*. These studies have shown that the primary mechanism for formation of phytosphingosine is by incorporation of molecular oxygen as a C_4 hydroxyl in sphinganine. Water can apparently be added across the C_4-C_5 double bond of sphingosine as well, but this pathway is quantitatively less important (Kulmacz

10

and Schroepfer, 1978). Sphingolipids incorporate both the regular length fatty acid chains found in glycerylphospholipids, $C_{14}-C_{20}$, and very long chain fatty acids, $C_{22}-C_{30}$ (Kishimoto, 1983). Additionally, the fatty acid moiety of the ceramide can either be mono- or dihydroxylated.

The synthesis of sphingolipid is completed by the attachment of a polar headgroup via a phosphodiester linkage to the C_1 hydroxyl of the long chain base. *S. cerevisiae* makes only three species of sphingolipid (Figure 2); inositolphosphorylceramide (IPC), mannoseinositolphosphorylceramide (MIPC) and mannosediinositolphosphorylceramide $M(IP)_2C$ (Lester and Smith, 1974). The structural similarity of these molecules suggested a precursor product relationship with MIPC being formed by the addition of a mannose unit to the phosphoinositol head group of IPC followed by the addition of a second phosphoinositol to MIPC to form $M(IP)_2C$. This precursor-product relationship has been confirmed by pulse chase experiments with [^{3}H]myoinositol labeled cells (Hechtberger *et al.*, 1994).

The phosphoinositol of the IPC headgroup comes from phosphatidylinositol (Becker and Lester, 1980), in a one step transfer reaction catalyzed by IPC synthase. The IPC synthase reaction occurs in the endoplasmic reticulum based on studies with a collection of temperature sensitive yeast secretory (*sec*) mutants. Mutants blocked in the transfer of secretory vesicles from the endoplasmic reticulum to the Golgi continue to make IPC but fail to make MIPC and $M(IP)_2C$ (Puoti *et al.*, 1991). The same result is obtained from wild-type cells in the presence of ATPase inhibiting NaN_3. Considering the fact that secretory vesicle transport is an energy dependent process, the most likely

11
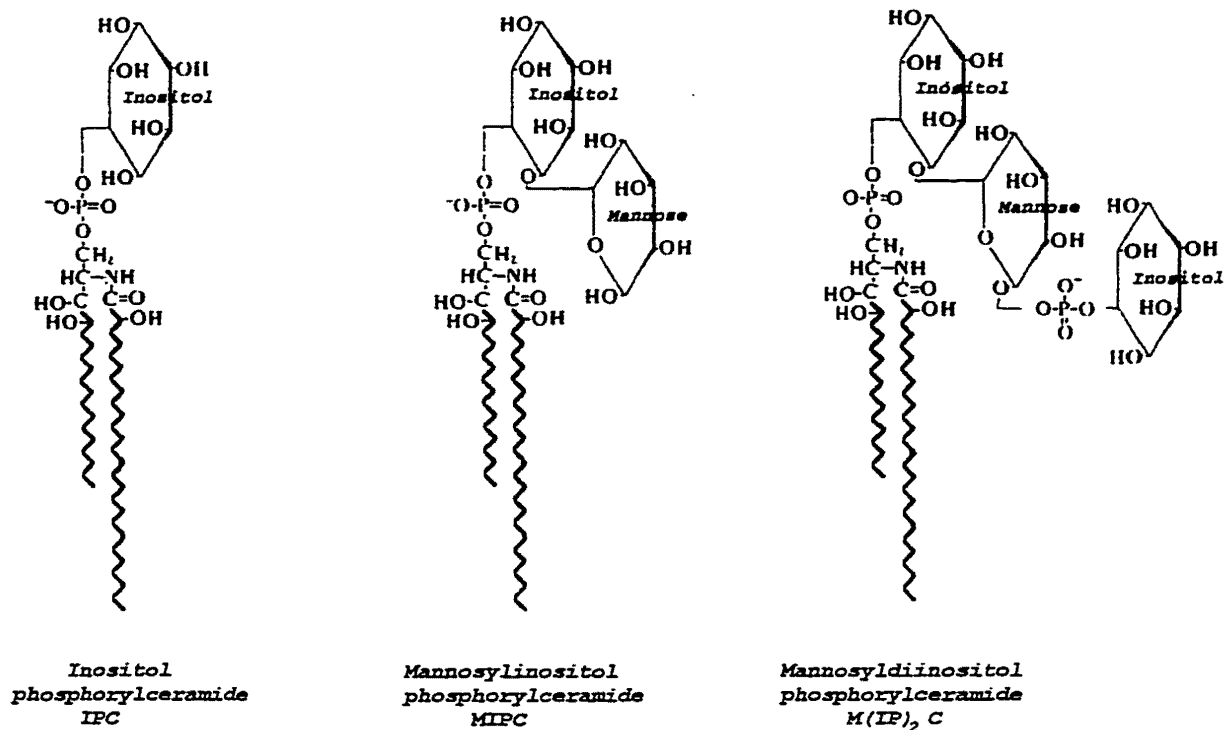
Figure 2. Structures of yeast sphingolipids.

12

explanation of these results is that IPC is synthesized in the ER and is subsequently

transported to the Golgi via the secretory pathway where it serves as a substrate for the

synthesis of MIPC and $M(IP)_2C$.

This model was further supported by studies that showed that MIPC and $M(IP)_2C$

were produced by *sec* mutants defective in late Golgi transport and in transport from the

Golgi to the plasma membrane (Hechtberger *et al.*, 1994). This study also confirmed that

the protein secretory pathway is utilized in the transport of sphingolipids between the

Golgi and the plasma membrane by isolating both plasma membrane and microsomal

fractions from a temperature sensitive, Golgi to plasma membrane-defective, *sec14* mutant

that was labeled with [^{3}H]myoinositol at both 24°C and 37°C. Mature MIPC and

$M(IP)_2C$ were present in the microsomal fraction from cells labeled at either temperature

but were only present in the plasma membrane fractions of cells grown at 24°C.

Sphingolipids were found in yeast secretory vesicles (Hechtberger *et al.*, 1994). Brefel-

din A, an inhibitor of Golgi function, reduces sphingolipid biosynthesis (Hechtberger and

Daum, 1995). Thus, taken together, the evidence consistently reveals that sphingolipid

trafficking occurs via the protein secretory pathway.

Most sphingolipids are localized to the plasma membrane in the form of $M(IP)_2C$

(Patton and Lester, 1991). The plasma membrane fraction also has significant amounts

of MIPC and lesser amounts of IPC. All three species were detected in Golgi and vacu-

olar membranes, secretory vesicles and microsomes with IPC being the predominant

species in Golgi and vacuolar membranes (Hechtberger *et al.*, 1994). This quantification

suggests that the previous commonly held assumption that IPC and MIPC serve primarily

13

only as intermediates on the pathway to mature $M(IP)_2C$ localized to the plasma membrane should be rethought. These "intermediate" forms may have significant functions at sites other than the plasma membrane.

.

Chapter 2

Cloning of SCS7

Introduction

Sphingolipid biosynthesis in *Saccharomyces cerevisiae* was investigated using the genetic suppressors of *csg2* mutants of that organism. *CSG2* was identified in a screen for calcium sensitive mutants (Beeler *et al.*, 1994). Spontaneous secondary suppressor mutations of the calcium sensitive phenotype of *csg2* were found to be in genes required for sphingolipid biosynthesis (Zhao *et al.*, 1994). These mutants were called *SCS* for suppressors of calcium sensitivity.

Genetic analysis revealed the *scs* mutants fall into seven complementation groups and that *scs* alleles are recessive to the wild-type alleles. Wild-type *SCS* genes can be cloned by complementation. Complementation refers to the restoration of a wild-type phenotype in a recessive mutant when the wild-type gene is introduced into the cell. Cloning by complementation involves transforming the mutant cells with a wild-type yeast genomic library and selecting transformants which revert back to the wild-type phenotype. The complementing fragment is used to make a ^{32}P-labeled probe that is hybridized to a commercially available membrane on which are bound contiguous DNA fragments covering the entire yeast genome. The sequence of the "contig" fragment to which the probe hybridizes is obtained from the *Saccharomyces* Genome Database. Restriction mapping can then be used to identify the specific open reading frame responsible for the complementation.

15

This procedure was used to clone the first member of the *SCS* mutant collection, *SCS1*. *Scs1* mutants are Ca^{2+} requiring and the complementation of this phenotype was used to select transformants containing the wild-type *SCS1* gene. When sequenced, *SCS1* was found to encode a pyridoxyl phosphate enzyme likely to catalyze condensation between the α-carbon of an amino acid and the carbonyl group of an acyl-CoA. *SCS1* was found to be about 60% homologous to *LCB1*. *LCB1* encodes a subunit of serine palmitoyltransferase (SPT). This enzyme catalyzes the first step in sphingolipid biosynthesis, the condensation of serine and palmitoyl-CoA to form 3-ketosphinganine. Therefore the *scs1* mutant was tested for phytosphingosine requirement and SPT activity. These studies demonstrated that *SCS1* encodes a novel subunit of SPT (Zhao *et al.*, 1994). Subsequently Lester and coworkers reported that *SCS1* is allelic to *LCB2* (Nagiec *et al.*, 1994).

The finding that reduced SPT activity suppresses the Ca^{2+} sensitivity of *csg2* mutants motivated a study of sphingolipid synthesis in *csg2* mutants. The sphingolipid content of yeast cells can be evaluated by labeling cells with [^{3}H]myoinositol, extracting the lipid fraction, and separating the extract using thin layer chromatography (Smith and Lester, 1974). Analysis of *csg2Δ* cells shows that they do not make the mannosylated sphingolipids MIPC and M(IP)$_2$C and overaccumulate their precursor, IPC-C. This raises the possibility that the Ca^{2+} sensitivity of *csg2* mutants is due either to failure to make mannosylated sphingolipids or to IPC-C overaccumulation. The finding that a decrease of serine palmitoyltransferase activity suppresses *csg2* indicates that IPC-C overaccumulation causes *csg2* Ca^{2+} sensitivity since an impairment in sphingolipid biosynthesis

upstream of mannosylation would be expected to remediate IPC-C overaccumulation but should have no effect on the inability to mannosylate.

Other *scs* mutants might identify other sphingolipid biosynthetic genes. The *scs7* allele was particularly interesting because it produces a distinct sphingolipid TLC profile that lacks IPC-C and overaccumulates an IPC species not seen in wild-type cells, which was named IPC-B. IPC-B has a higher mobility on TLC than IPC-C, indicating that it is the more hydrophobic of the pair. It was hypothesized that the difference between IPC-C and IPC-B is the hydroxylation state of the inositol phosphorylceramide. Therefore *SCS7* might encode a protein involved in the hydroxylation of yeast sphingolipids.

Materials and Methods

Materials. [α^{32}P]ATP was obtained from New England Nuclear. Polyethylene glycol was obtained from Fluka. Zymolase 100T was obtained from Seikagaku Corporation, Tokyo. TritonX-100 was from Cal Biochem. Glucuronidase was supplied by Boehringer Mannheim. Epicurean Coli Competent Cells were obtained from Stratagene and restriction endonucleases were from Gibco BRL or New England Biolabs. All other reagents were purchased from Sigma.

Strains, Growth Media, and Transformations. The strains used in this study are TDY2037 (*Matα ura3-52 lys2 leu2Δ trpΔ*), TDY 2010b (*Mat a SCS7 csg2Δ::LEU2 ura3-52 his4-619*), TDY2038 (Mat*α csg2Δ::LEU2⁺ ura3-52, lys2⁻ leu2Δ trp1Δ*), and CZ39R (*Matα csg2Δ::LEU2 scs7-1 ura3-52 lys2⁻ leu2Δ trp1Δ*). Yeast media was prepared according to Sherman *et al.*, 1974, using yeast extract, tryptone, peptone and bacto-

agar from Difco. Yeast were transformed by the method of Gietz *et al.*, 1995. Bacterial

strains AG1 and XL Blue (Stratagene) were used for propagation of plasmids.

Nucleic Acid Manipulation. DNA was prepared from yeast by the method of Holm *et al.*, 1986. Plasmid DNA was prepared from *Escherichia coli* by the method of Holmes

and Quigley, 1981. DNA probes were labeled utilizing the Gibco DNA labeling kit.

Sequence determination was accomplished by hybridization of $[\alpha^{32}P]$ATP-labeled DNA

probes to yeast genomic contiguous sequence membranes from ATCC. ATCC mem-

branes were incubated in a prehybridization solution of 0.9 M NaCl, 0.09 M sodium

citrate, 100 µg/ml denatured salmon sperm DNA, and 1mg/ml each of ficoll, polyvinyl-

pyrrolidone and bovine serum albumin, pH 7.0 at 68° C for 2-4 hours. An $[\alpha^{32}P]$ATP-

labeled *Sau3* digest of the fragment was added to the incubation chamber in a volume of

1 M EDTA sufficient to make the final solution 0.01 M EDTA.

The membranes were incubated with the labeled probe at 68° C overnight,

washed 2X in 0.3 M NaCl, 0.03 M sodium citrate and 0.5% SDS, pH 7.0, followed by 2

incubations; one in 0.3 M NaCl, 0.03 M sodium citrate and 0.1% SDS at room temper-

ature for 5 min and the other in 15 mM NaCl, 1.5 mM sodium citrate and 0.5% SDS at

68°C for 2 hr. The latter buffer was then changed and the membranes were incubated for

an additional 30 min at 68°C. The membranes were then dried, wrapped in Saran Wrap

and exposed to XAR5 X-ray film (Kodac).

The contiguous sequence identity number for the contiguous clone lit up by the

probe was obtained from its grid position on the autoradiogram. This number was used to

obtain the sequence of the contiguous DNA from the Saccharomyces Genome Database.

Alignment of the plasmid insert with the genomic sequence was accomplished by comparing a restriction map of the insert with that of the published sequence of the contiguous DNA fragment.

Results

Isolation of Complementing Fragment. *Csg2* mutants are unable to grow on 100 mM Ca^{2+} whereas a second mutation in the *SCS7* gene restores the ability of the double mutant to grow on 100 mM Ca^{2+} (Figure 3). The wild-type *SCS7* gene was cloned based on its ability to convert a *csg2 scs7* Ca^{2+} resistant double mutant back to Ca^{2+} sensitive. The logic behind this approach is that the introduction of a plasmid carrying a wild-type copy of the *SCS7* gene would result in the cell being heterozygous at the *SCS7* locus and the dominance of the wild-type allele would thus cause the normally Ca^{2+} resistant double mutant to become Ca^{2+} sensitive. Strain CZ39R *(csg2Δ::LEU2 scs7-1)* was transformed with a YCp50-based yeast genomic library (Rose *et al.*, 1987) and transformants were selected as uracil prototrophs.[1]

Approximately 5 X 10^5 ura^- transformants grew up on the minimal media, synthetic dextrose (SD) plates. These were replica-plated to YPD and YPD + 100 mM Ca^{2+} plates and screened for colonies which had grown on the permissive YPD media but were absent on the YPD + 100 mM Ca^{2+} plate. Four such candidates were identified. In order

---

[1]
The YCp50 plasmid contains the wild-type *URA3* gene and the bacterial ampicillin resistance gene. Therefore uracil prototrophy can be used to select for plasmid uptake in YCp50-transformed *ura3-52* yeast and ampicillin resistance can be used to select for plasmid uptake in YCp50-transformed *E coli* (Rose *et al.*, 1987).

19
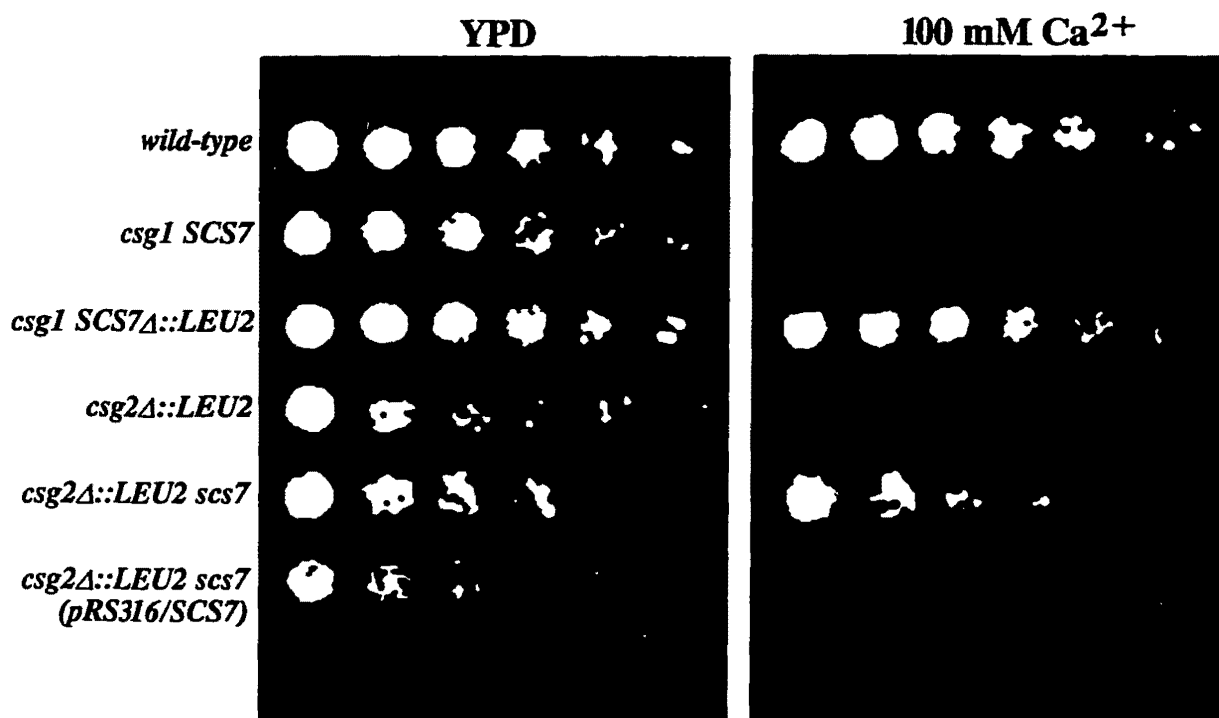
Figure 3. Calcium growth phenotypes for *csg* mutants and their *scs7* suppressors. Exponential growth phase liquid cultures of wild-type and mutant cells were standardized at 0.1 OD$_{600}$ and 100 μl of each was pipetted into the left well of a row on a microtiter plate. Serial dilutions (1:5) from left to right were made of these suspensions and a pronged transfer tool was used to inoculate a YPD (~0.25 mM Ca^{2+}) and a YPD + 100 mM Ca^{2+} plate from them. The plates were incubated for 3 days at 26°C. Wild-type cells, (row 1), grow equally well on both YPD and 100 mM Ca^{2+}, but *csg1* and *csg2* mutants, (rows 2 & 4), are unable to grow on 100 mM Ca^{2+}. However growth is restored on 100 mM Ca^{2+} in either mutant if the cell is also mutant at the *scs7* locus (rows 3 & 5). A plasmid containing a wild-type copy of the SCS7 gene transformed into a *csg2 scs7* double mutant compliments the *scs7* suppression of *csg2* calcium sensitivity causing the cell to be Ca^{2+} sensitive (row 6).

20

to verify that the Ca^{2+} sensitivity of these candidates was plasmid-linked, subcultures were allowed to segregate the plasmid by growth on YPD and ura⁻ segregants were selected on FOA.[2] For two of the candidates, loss of the plasmid resulted in restoration of Ca^{2+} resistance establishing that Ca^{2+} sensitivity depends on the presence of the plasmid. The plasmids from these two strains were purified by passage through *E coli* and restriction mapping indicated that they contained the same 11 kB genomic fragment.

Identification of the Complementing Open Reading Frame. The sequence of this fragment was obtained utilizing the *Saccharomyces cerevisiae* contiguous clone membranes from ATCC as explained above. The fragment hybridized to ATCC clone 8156. The sequence of this clone was accessed and the 11 kB complementing fragment was localized by comparison of its restriction map with that of the clone. The 11 kB fragment was found to contain eight open reading frames (ORFs). Subcloning was performed to locate the ORF responsible for the complementation. A 7 kB *EcoRI* subclone containing 2 ORFs was found to complement when transformed into the *csg2Δ scs7-1* mutant (Figure 4). Further subcloning and complementation included two deletions involving YMR273C. These were made by digesting pRS316 containing the 7kB *EcoRI* fragment

---

2

Orotic Acid is an intermediate of uracil and thymine biosynthesis. 5-Fluroorotic Acid (FOA) is an analog that is readily taken up by yeast cells and enters the uracil / thymine biosynthetic pathway being converted to 5flurouracil. However 5flurouracil irreversibly blocks the methylase that catalyzes the methylation of uracil at position 5 to form thymine. Therefore the cell dies of thymine insufficiency. However, a uracil auxotroph, i.e. a ura⁻ cell which has lost its *URA3* containing plasmid, does not die because it cannot transform the FOA to 5-fluorouracil and the cell survives on the minimal amount of uracil supplied in the FOA media (Boeke, *et al.*, 1984).
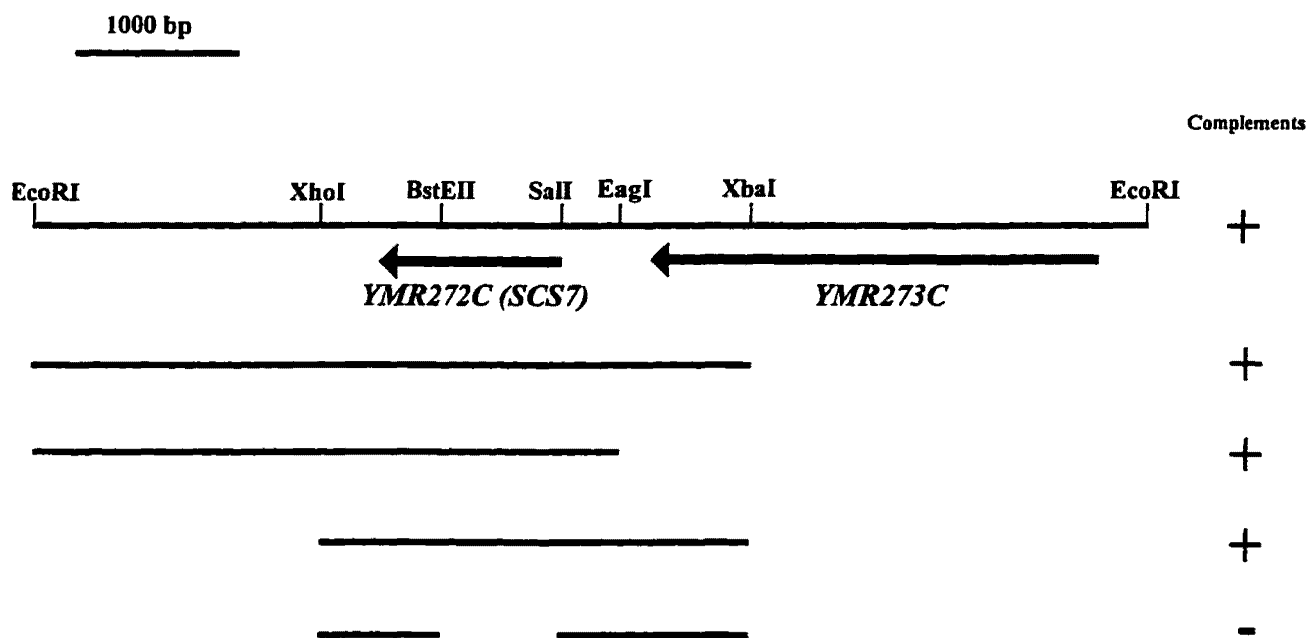
Figure 4. A restriction map of the 7 kB fragment that complemented *scs7* suppression of *csg2* Ca^{2+} sensitivity. Also shown are four subclones along with their respective complementation results. The positions of the two open reading frames encompassed by the fragment are as indicated by the arrows.

with either *EagI* or *XhoI* to cut out the intervening sequence between their respective

sites on the fragment and the vector polylinker. The plasmids were then recircularized

with DNA ligase. The *XhoI-XbaI* subclone was made by digestion of 7kB *EcoRI*

subclone with those enzymes followed by band isolation of the 2.7 kB *XhoI-XbaI* frag-

ment. This fragment was then ligated into pRS316. The resulting plasmid was used to

make a YMR272C deletion plasmid. The plasmid was digested with *BstEII* and the

sticky ends were blunt filled with dNTPs and klenow subunit. *SalI* linkers were ligated

to the blunt ends and the plasmid was recircularized by *SalI* digestion and religation of

the ends. The resulting plasmid had a *SalI* to *BstEII* deletion eliminating the first 780 bp

of YMR272C. These subclones were transformed into the CZ39R (*csg2Δ scs7-1*) double

mutant and the transformants were tested for growth on Ca^{2+}. The testing revealed that

the three subclones deleting portions of YMR273C continued to complement, while the

XhoI to *XbaI* subclone with a *BstEII* to *SalI* deletion, which eliminated the first two thirds

of the YMR272C sequence, failed to complement. This established YMR272C as the

ORF responsible for complementation of *scs7* suppression of *csg2* Ca^{2+} sensitivity.

Linkage Analysis of Complementing Fragment and SCS7 locus. The complementation of

a mutant phenotype by a cloned fragment cannot unequivocally establish that the clone

contains a wild-type copy of the mutant gene. A second possibility is that the clone con-

tains another wild-type gene that when overexpressed by the plasmid-supplied extra copy

allows the cell to overcome the mutant defect. Thus the genetic linkage of the cloned

DNA to the mutant locus must be established. The linkage of the cloned DNA to the

23

SCS7 locus was demonstrated by marking the locus of the cloned gene with *URA3*⁺ and

determining the segregation of the *URA3*⁺ and *scs7* phenotypes after meiosis.

An integrating plasmid was constructed by subcloning a 2750 bp *XhoI* to *XbaI*

fragment (see Figure 5) into pRS306. This plasmid was linearized with *BstEII* and used

to transform TDY 2010b, (*Mat a csg2Δ*), to uracil prototrophy. This haploid strain was

crossed to CZ39R, (*Matα scs7-1 csg2Δ*), and the resulting diploid was sporulated.

Ninety-nine spores were evaluated. All were either ura⁻, Ca^{2+} resistant (51) or ura⁺, Ca^{2+}

sensitive (48), indicating that the cloned fragment is linked to the *SCS7* locus (Figure 5).

Sequence Analysis of the SCS7 Open Reading Frame. The open reading frame implicated

as being *SCS7* by the above analysis is YMR272C on the right arm of Chromosome XIII.

It contains 1155 base pairs predicted to encode a 385 amino acid protein. In order to gain

insight into possible functions of *SCS7*, Basic Alignment Search Tool (BLAST) software

was used to search the GenBank database for sequences homologous to *SCS7*. The

search found a high degree of homology between a region near the N-terminus of *SCS7*

and the heme-binding domain of cytochrome b-5 (50% identity, 70% conserved).

Additionally the sequence showed the presence of 3 small histidine-containing regions

and two long hydrophobic domains capable of spanning the membrane twice. These

features were positioned in a manner that is characteristic of a family of enzymes that

appears to include all of the membrane fatty acid desaturases and at least two bacterial

hydroxylases (Shanklin *et al*, 1994). These findings, (discussed in detail in Chapter 5),

suggested that Scs7p could be a hydroxylase and considering the fact that *scs7* mutant

cells accumulate a presumed unhydroxylated sphingolipid intermediate, IPC-B, it

24

Figure 5. Linkage analysis of *SCS7* clone.

A). Diagram of the integration of the pRS306/*SCS7* candidate clone construct into the yeast chromosome. The construct is cut at a point internal to the cloned *XhoI-XbaI* fragment and transformed into a *csg2Δ* strain. The cell integrates the construct at the point on its chromosome homologous to the *XhoI-XbaI* sequence (Hinnen *et al.*, 1978). The result is the creation of two hybrid wild-type copies of the sequence which flank the plasmid sequence containing *URA3*. Thus URA3 will mark the chromosome location of the cloned fragment.

B). Diagram of the segregation the *scs7* and *URA3* marker. The marked *csg2Δ* strain was mated with *csg2Δ scs7-1* strain and the diploid was sporulated. If the cloned *XhoI-XbaI* fragment contains *SCS7* and the *SCS7* locus has been marked then, *URA3* will always segregate away from *scs7* during meiosis. Thus all tetrads should contain two ura+, Ca^{2+} sensitive (*csg2Δ::LEU2 SCS7::URA3*) spores and two ura⁻, Ca^{2+} resistant (*csg2Δ::LEU2 scs7-1*) spores [Case I]. However if the fragment does not contain *SCS7*, integration will occur at the non*SCS7* homologous site and when the diploid undergoes meiosis, recombination between *URA3* and *scs7* will be possible. Therefore some ura⁻, Ca^{2+} resistant spores as well as ura⁻, Ca^{2+} sensitive spores will be recovered [Case II].

25

A

= XbaI-XhoI

= pRS 306

Yeast Chromosome

URA3

URA3

B

Case I

Case II

■ = *SCS7* locus

□ = *URA3*-marked locus
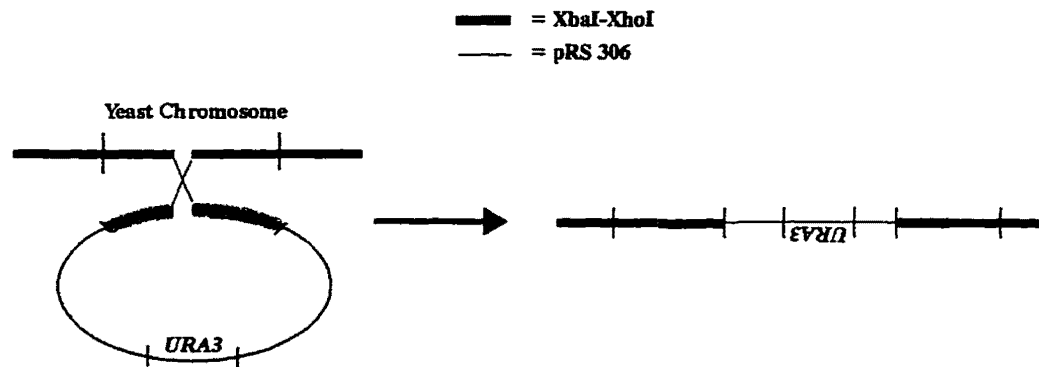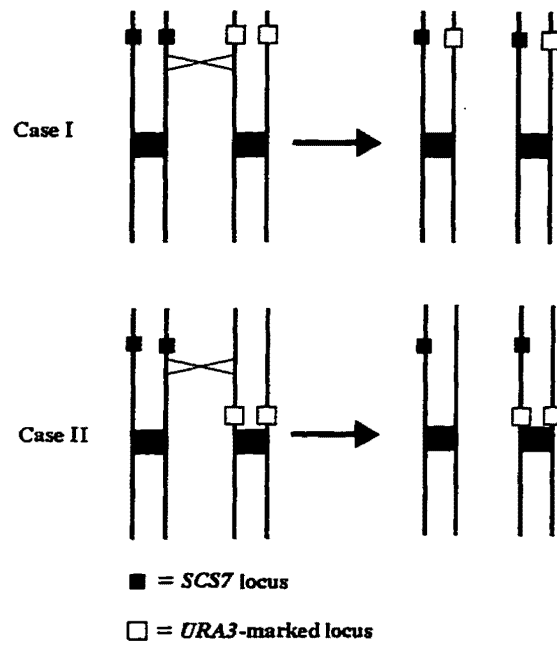
seemed highly likely that Scs7p is the hydroxylase responsible for the conversion of IPC-

B to IPC-C in wild-type cells.

SCS7 and SUR2 Null Mutant Construction and Sphingolipid Phenotype Evaluation.

Introduction

Generally, recessive gene mutation involves a loss of function. However, this is not always the case. There are many scenarios that can result in a gain of function, e.g. the mutation of an enzyme regulatory domain that causes constitutive activity of the enzyme. Additionally, even in the case of a loss of function mutation, varying degrees of residual activity can result in different phenotypes. Since it is impossible to know the nature of a spontaneous mutation without detailed knowledge of its genetic context, the ability to specifically generate null mutants is highly useful because it allows for phenotypic characterization of a precisely defined genetic state, the total lack of gene expression. Null mutants also identify essential versus nonessential genes.

As discussed in Chapter Two, *csg2* mutants and *csg2* suppressor mutants have defects in sphingolipid biosynthesis. *Csg2* mutants do not make mannosylated sphingolipids and most *csg2* suppressor mutants appear to have sphingolipid biosynthetic defects upstream of the synthesis of IPC-C, the precursor to the mannosylated sphingolipids, which lessen its overaccumulation by *csg2*. In the isolation of the *scs* suppressor mutants, more alleles of *scs7* were found than of any other complementation group (Zhao *et al.*, 1994). This suggested that the *scs7* alleles were loss of function mutations since that outcome is the most probable and therefore most likely to yield a large number of suppressors. The *scs7Δ* in *wild-type, csg2Δ*, and *csg1⁻* backgrounds was constructed to investigate its phenotype.

Recently a new gene family has been identified and found to be involved in sphingolipid synthesis; the *SUR* genes (Desfarges *et al.*, 1993). The *sur* genes were initially identified as <u>su</u>pressors of <u>r</u>vs161 which in turn was identified as a mutant with <u>r</u>educed <u>v</u>iability on <u>s</u>tarvation (Crouzet *et al.*, 1991). *Sur1* is allelic to the sphingolipid mannosylation mutant *csg1* (Takita, *et al.*, 1995), and *sur4* has been identified as one of two fatty acid elongases that produce the C_{26} fatty acid chain used in ceramide synthesis (Oh, *et al.*, 1997). The *sur2* mutant contains high homology to *scs7* including the histidine-containing domains. In light of this and the genetic connection of the *sur* genes to sphingolipid synthesis, it seemed a reasonable hypothesis that *sur2* could also encode a sphingolipid hydroxylase, perhaps the hydroxylase that catalyzes the hydroxylation of dihydrosphingosine to phytosphingosine. In order to address this question, *sur2Δ* mutants were constructed in wild-type, *csg2Δ*, *scs7Δ* and *csg2Δ scs7Δ* backgrounds to assess their sphingolipid phenotypes.

Materials and Methods

Materials. Glass beads were from Biospec Products, Inc., Bartlesville, OK. Silica Gel TLC plates were from Merck. Chloroform was purchased from Fisher Scientific and Methanol was obtained from J.T. Baker. All other reagents and chemicals were from Sigma.

Strains and Media. The strains used in this study in addition to those listed in Chapter Two were 1122 4A (*Mat a csg2⁻, leu2Δ, lys2⁻, ura3-52*), 2050 (*Matα csg1⁻ leu2Δ ade2⁻ ura3-52*), 5197d (*Mat a csg2::LEU2 scs7-1 ura3-52 trp1 Δ leu2Δ lys2⁻ ade2-101*), and G11-10 (*Mat a gda1::LEU2 ura3-52 lys2⁻ leu2Δ*). Inositol free synthetic minimal media

29

consisted of: 20 mg/ml glucose; 1 mg/ml KH_2PO_4; 0.5 mg/ml each of $MgSO_4$, NaCl, and $CaCl_2$; 0.35 mg/ml NH_4SO_4; 0.2 mg/ml riboflavin; 40 µg/ml lysine; 30 µg/ml each of leucine, tryptophan, and adenine; 20 µg/ml uracil and biotin; 2.0 µg/ml calcium pantothenate and folic acid; 0.4 µg/ml each of $ZnSO_4 \cdot 7H_2O$, $CuSO_4 \cdot 5H_2O$, niacin, pyridoxine HCl, thiamine HCl, and $MnCl_2$; and 0.2 µg/ml each of $FeCl_3 \cdot 6H_2O$ and amino benzoic acid.

Nucleic Acid Manipulation. Southern Blot Analysis (Southern, 1975) was performed as described in Maniatis *et al.*, 1982.

Selection of Diploids by Failure to Mate. Mated haploid strains for which unique auxotrophies for diploid selection were unavailable were streaked for isolated colonies and these were mated with *Mat a* and *Mat α* test strains on YPD plates. The resulting growth was streaked on minimal media without amino acids. Candidate isolates that did not grow after crossing with both tester strains were identified as diploids.

Sphingolipid Analysis by Inositol Pulse Labeling. Cells were grown in synthetic minimal medium without inositol to a density of 1-2 OD_{600} per ml. The cells were concentrated in 0.5 ml of fresh media at 10 OD_{600} per ml and incubated for 10 min with 25 µCi [^{3}H]myo-inositol (specific activity 20 Ci/mmole). The cells were diluted 6X in 2.5 ml of minimal media with 300 µM inositol and incubated for 90 min. The labeling was terminated by adding 330 µl of 50% trichloroacetic acid. The cells were washed twice with 10 ml of H_2O and resuspended in 0.6 ml chloroform:methanol (1:1). An equal volume of acid washed glass beads was added and the tubes were vortexed for 5 min followed by 5 min of bath sonication. The supernatant was taken off the glass beads to a new tube and the

beads were reextracted with chloroform:methanol:H$_2$O (1:1:0.3) by 5 min each of vortexing and sonication. The two organic supernatants were combined and evaporated to dryness.

The lipid extract was hydrolyzed with mild alkali by resuspending the pellet in 180 µl of hydrolysis solvent, EtOH:dH$_2$O:Ether:pyridine. (15:15:5:1). Twenty µl of 1 M KOH in methanol was added and the tubes were incubated at 37°C for 3 hours. The samples were neutralized with 20 µl of 1 M acetic acid and evaporated to dryness. To desalt the samples, the pellets were resuspended in 300 µl 1-butanol + 200 µl dH$_2$O. The butanol (upper) phase was removed to a new tube and the aqueous phase was reextracted with 300 µl 1-butanol. The two organic phases were combined and evaporated to dryness. The samples were resuspended in 10 µl chloroform:methanol (1:1) and spotted to the origin of a silica gel TLC plate. Plates were developed in a solvent solution of chloroform:methanol:acetic acid:dH$_2$O (16:6:4:1.6). The plates were sprayed with EN^{3}HANCE (Dupont) and used to expose an X-ray film for 3-7 days.

Sphingolipid Anaylysis by Steady State Inositol Labeling. Cells were grown in synthetic minimal medium containing 12 nM inositol and 1 µCi/ml of ^{3}H-myoinositol for several generations (OD$_{600}$ of 0.01 to 1.0). Cells (about 5 OD$_{600}$ units) were pelleted and washed in one volume of 4 mM sodium azide. Lipids were extracted, alkali-treated, BuOH desalted and chromatographed as described for pulse labeling.

Results

Construction of SCS7 knockout construct. The pRS316 plasmid with a 2.7 kB *XhoI* to *XbaI*, *SCS7*-containing fragment with a *Sal I* to *BstEII* deletion described in the previous

chapter was used to make an *SCS7* knockout construct for use in making scs7 null

mutants according to the method described by Rothstein, 1983[3]. This plasmid was

digested with *SalI* and a 2.2 kB fragment containing the *LEU2* gene with *SalI* ends was

ligated in. The resulting X*hoI-XbaI SCS7Δ::LEU2* knockout construct was cut out and

ligated into pRS306.[4] The resulting plasmid was digested with *XhoI* and *XbaI* and trans-

formed into 3 cell lines, TDY2037 (*Mat α CSG2⁺*), 1122 4A (*Mat a csg2⁻*) and 2050

(*Mat α csg1⁻*). The transformed cells were plated on SD plates without leucine to select

for integration. To check that the knockout constructs had integrated properly a Southern

blot analysis was performed on *BstEII*, *XhoI* digested genomic preparations from the

transformed strains (Figure 6).

Verification of 2037scs7k. In order to confirm that the 2037scs7k was really a *SCS7*

knockout, it was crossed with strain 5197d, (*Mat a csg2Δ scs7-1*). The resulting diploid

---

[3]

The one-step gene disruption method takes advantage of the observation that during yeast
transformation, free DNA ends are recombinogenic, stimulating recombination by
interacting directly with homologous sequences in the genome. Therefore when a DNA
construct whose ends contain homologous genomic sequences is transformed into the
yeast cell, it will perform a double crossover between the chromosome and the fragment,
essentially splicing out it's genomic DNA and replacing it with the construct at the
homologous site. In this case the disruption plasmid replaced the first 800 bp of the *SCS7*
sequence with *LEU2*. The *LEU2* sequence serves to mark the *SCS7* locus so that
successful transformation can be established by checking for leucine prototrophy. It also
helps insure that a functional *SCS7* transcript can not be made .

[4]

Recloning the fragment from pRS316 to pRS306 was necessary because pRS316
contains a centromeric sequence which allows it to be maintained episomaly. In this
procedure, the vector component of the knockout plasmid should be *cen⁻* (e.g. without the
yeast centromere sequence) otherwise any undigested transformed plasmid can be
maintained episomally causing a false positive when leucine prototrophy is used to select
for integration. Since pRS306 is *cen⁻*, the knockout construct was subcloned into it to
avoid this problem.

Figure 6. Southern blot verification of *SCS7* knockout strains.

A. Sequence of *BstEII* cut site and the *SalI* linker used in constructing the *SCS7* deletion plasmid, (see Figure 4) showing that the *BstEII* recognition sequence has a terminal G(5')C(3') base pair while the terminal base pair of the *SalI* linker is G(3')C(5'). The terminal GC base pair of the *BstEII* sequence is lost when the plasmid is digested with *BstEII* but it is added back by the *SalI* linker. This plasmid was used to construct the *SCS7Δ::LEU2* knockout plasmid; therefore, if the knockout sequence integrates into the chromosome, there will be both a *SalI* and a *BstEII* recognition sequence at the *BstEII* site within the *SCS7* ORF (see B. below).

B. Restriction Maps of *SCS7* Genomic and Knockout Sequences.

C. Southern Blot Analysis of *SCS7* Knockout Candidates. Genomic preps were prepared from two candidates from each transformed strain. The genomic preps were digested with *XhoI* and *BstEII* and separated on a 2% agarose gel. The gel was visualized by UV light (right panel) and used to make a Southern Blot using an [α^{32}P]ATP-labeled *XhoI* to *SalI* fragment as a probe. When compared to the *BstEII* λ phage ladder (lane 1), pRS316 with the 2.7kB *XhoI-XbaI* genomic fragment (lane 2) and pRS316/*SCS7Δ*::LEU2 (lane 3) yielded a 1.8 kB and 3.2 kB *BstEII-XhoI* fragment respectively as predicted by their restriction maps (see B. above). Both candidates from 2037, (wild-type; lanes 6&7) and 2050, (*csg1⁻*; lanes 8&9) yielded 3.2 kB fragments indicating that they are *SCS7* knockouts. However the 11224a(*csg2⁻*) candidates (lanes 4&5) yielded a 1.8 kB fragment like the untranformed wild-type control (lane 10). Therefore the 11224a candidates are not *SCS7* knockouts.

33

a.

$$5' \text{GGTNACC} \, 3'$$
$$3' \text{CCANTGG} \, 5'$$

$$5' \text{CGGTCGACCG} \, 3'$$
$$3' \text{GCCAGCTGGC} \, 5'$$

BstEII

SalI Linker

b.

XhoI   *BstEII*   *SalI*   *XbaI*

← SCS 7

SCS7 Genomic Map
BstEII - XbaI = 1.8 kB

SalI
XhoI   *BstEII*   *SalI*   *XbaI*

← *LEU2*
SCS 7

SCS7 Knockout Map
BstEII - XbaI = 3.2 kB

c.

34
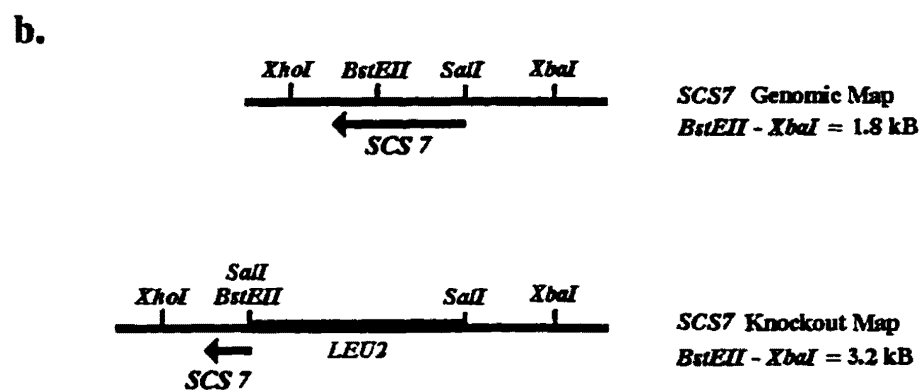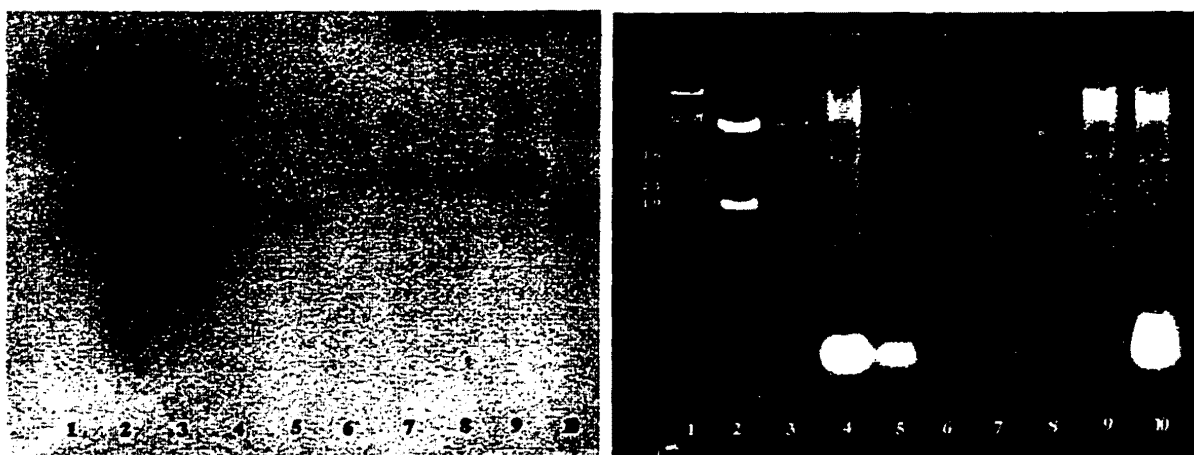
was sporulated and dissected. The four haploid offspring from twelve tetrads were tested

for Ca^{2+} sensitivity. All segregants were found to be Ca^{2+} resistant, proving that the

2037scs7k strain lacks the *SCS7* gene.

Isolation of 6715a and 6715b, as csg2Δ scs7Δ double knockouts. The 5197d X

2037scs7k cross described above was used to isolate a *csg2Δ scs7Δ* double mutant by

screening the tetrad dissection plates for nonparental ditype tetrads in which the *LEU2*

marker had segregated 2:2. Both leu⁺ spores from such a tetrad will be *csg2Δ::LEU2*

scs7Δ::LEU2 because that is the only way two leu⁻ spores can be isolated from a single

tetrad of this cross. Strains 6715a and 6715b were isolated in this manner.

Further crosses were performed to confirm the genotype of the 6715 strains. In

order to confirm that they had the *csg2Δ* allele, they were crossed to 2040, a *csg2Δ*

SCS7 strain. The resulting diploids were Ca^{2+} sensitive, indicating that they are

homozygous *csg2Δ* and heterozygous at the *SCS7* locus. This verified that the parent

6715 strains are *csg2Δ*.

To confirm that the 6715 strains were *scs7Δ*, they were backcrossed to 5197d

(*csg2Δ scs7⁻*). Both diploids in this case were Ca^{2+} resistant. Since the *csg2Δ* genotype

of the 6715 haploid parents is established by the previous cross, the Ca^{2+} resistance of

these diploids indicated that they are homozygous recessive mutant at both the *csg2* and

scs7 loci. Thus the confirmation crosses proved that the 6715 strains are *csg2Δ scs7Δ*

double mutants.

Sphingolipid phenotypes of SCS7 mutants. Sphingolipid biosynthesis in wild-type,

csg2Δ, scs7Δ, and csg2Δ scs7Δ cells was compared using the inositol pulse labeling

35

procedure described in Material and Methods above. Mild alkali hydrolysis was performed to eliminate phosphatidylinositol and lysophosphatidylinositol[5]. Figure 7 shows the analysis. The wild-type sphingolipid profile is shown in Lane 1. Hydroxylation decreases hydrophobicity, therefore the IPC's migrate in accordance with their hydroxylation state, the more hydroxylated, the less the migration. IPC- B, -C, and -D are un-, mono-, and dihydroxylated, respectively, on the long chain fatty acid moiety. The most hydrophobic unhydroxlated IPC-B runs the farthest and the least hydrophobic of the trio, dihydroxylated IPC-D, runs the least far. Likewise, MIPC and $M(IP)_2C$ migrate to positions consistent with the decrease in hydrophobicity conferred by the attachment of mannose and mannose-phosphoinositol to their respective head groups.

The inability of *csg2* mutants to mannosylate IPC's can be seen from the profile of the *csg2Δ* extract (lane 2) which lacks MIPC and $M(IP)_2C$. The predominant IPC of the *csg2Δ scs7Δ* extract is IPC-B as expected. *Saccharomyces cerevisiae* cells incorporate exogenous phytosphingosine into sphingolipids (Wells and Lester, 1983). Therefore sphingolipid biosynthetic defects upstream of the formation of phytosphingosine can be corrected by its addition to the growth media. The last step in phytosphingosine formation is the hydroxylation of C4 of dihydrosphingosine. If *SCS7* catalyzed this

---

[5]

The added inositol label incorporates into the sphingolipid species and phosphatidylinositol and lysophosphatidylinositol. Mild alkali treatment hydrolyzes the acylester linkage of the fatty acid chains to the glycerol moiety of PI and lysoPI forming labeled phosphoinositol glycerol which partitions in the aqueous phase during the desalt step. The amide linkage of the long chain fatty acid to the amine of the long chain base is stable to mild alkali, therefore sphingolipids are not degraded by this treatment.
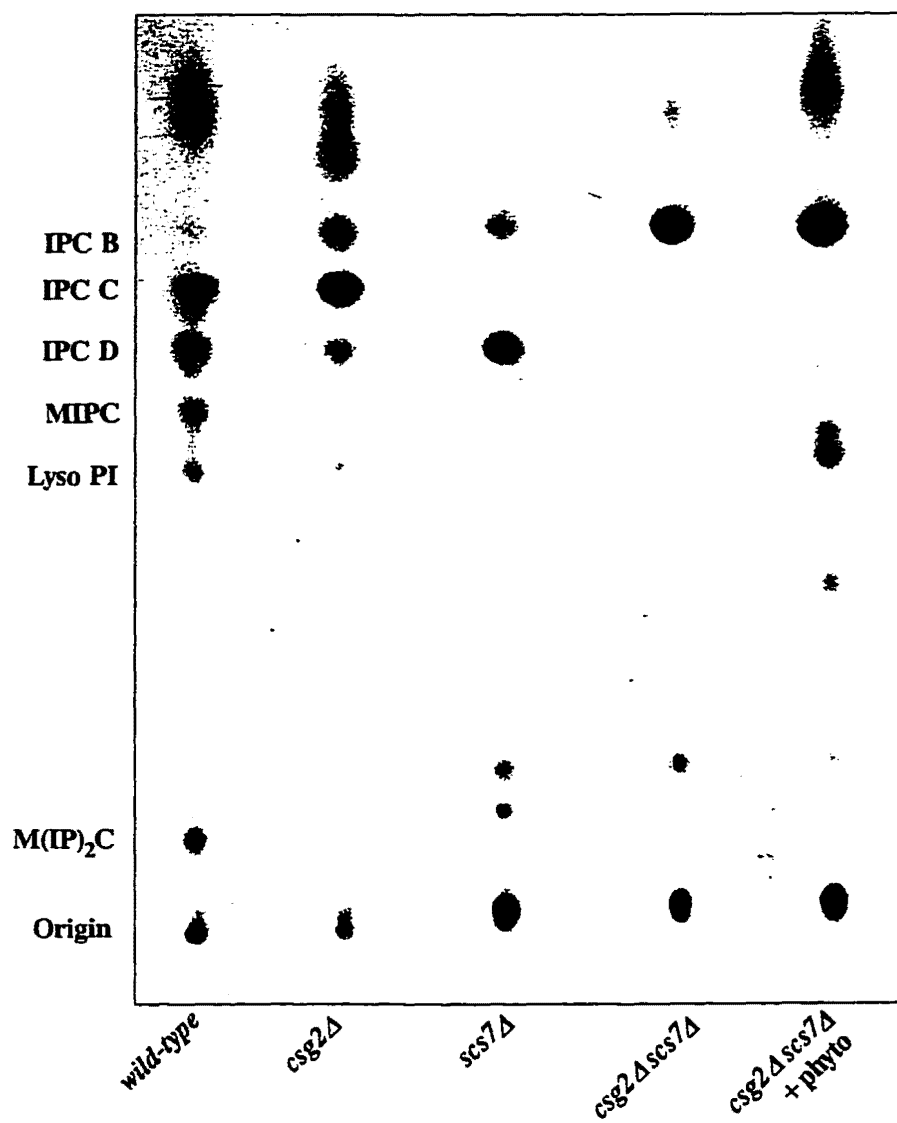
Figure 7. Sphingolipid analysis of *SCS7* knockout mutants.

hydroxylation, addition of phytosphingosine would bypass the hydroxylation defect and allow IPC-C formation. As seen in lane 5, the extract from *csg2Δ scs7Δ* cells grown in 12 μM phytosphingosine does not contain IPC-C, indicating that *SCS7* is not involved in the hydroxylation of dihydrosphingosine to form phytosphingosine.

The profile for the extract from *scs7Δ* cells, lane 3, showed very little IPC-B and a preponderance of the label in a species with mobility very similar to IPC-D. It was hypothesized that this species (migrating similarly to IPC-D) could be a mannosylated IPC-B. This would be consistent with the absence of this species in *csg2Δ scs7Δ* double mutants since *csg2Δ* is unable to mannosylate. Another mutant defective in mannosylation is *gda-1* (Abeijon *et al.*, 1993). The product of the *GDA1* gene is required for transport of GDP-mannose, the donor for mannosylation of IPC-C to MIPC, into the Golgi where mannosylation occurs (Berninsone *et al.*, 1994). Therefore the isolation of a *scs7Δ gda1Δ* mutant was undertaken in order to see if the putative MIPC-B species would be absent from its sphingolipid profile.

Construction of the scs7Δ gda1Δ mutant. An *scs7Δ gda1Δ* double knockout mutant was isolated by crossing the *scs7Δ* strain, 2037scs7k, with the *gda1::LEU2* strain, G11-10, and isolating a NPD tetrad that was phenotypically 2 leu⁺:2 leu⁻. The double knockout was confirmed by crossing it with the leu2Δ wild-type strain, 2037, and determining that the meiotic segregants from the diploid were not 2:2 leu⁺ / leu⁻. This strategy was necessary because there was not a simple growth phenotype of the *gda1* mutant to follow which would allow backcrossing the double knockout candidate to its parent haploid and checking for failure to revert back to the wild-type phenotype. Both *scs7Δ* and *gda1Δ*

loci were marked with *LEU2*. If the double knockout candidate strain is a single knockout then crossing it to a *leu2Δ* strain will result in a heterozygous *LEU2⁺/leu2⁻* diploid at the knockout locus. Dissection of this diploid will result in 100% 2:2 segregation of the leu⁺/leu⁻ phenotype. However if the strain is a *scs7Δ gdal Δ* double knockout, the diploid will be heterozygous for the *LEU2* gene at two independent loci and dissection will result in 4:0 and 3:1 as well as 2:2 leu⁺/leu⁻ segregation.

The candidate *scs7Δ gdal Δ* double knockout was crossed with strain 2037. The diploid was selected by its failure to mate with *Mat a/α* test strains, sporulated and dissected. As a result, of 14 four spore tetrads evaluated 7 were 4:0, 3 were 3:1, and 4 were 2:2 leu⁺/leu⁻, indicating that the *scs7Δ gdal Δ* candidate, named 7gk36a, is marked with *LEU2* at two independent loci.

Sphingolipid Phenotype of the scs7Δ gdal Δ Double Knockout. A sphingolipid analysis of the *scs7Δ gdal Δ* strain, 7gk36a, was performed in the same manner as described for the *scs7Δ csg2Δ* strains above. The results are shown in Figure 8. In this experiment the samples were not hydrolyzed with alkali and therefore contain PI and lyso-PI as indicated in the margin.[6] The *gdal* profile, lane 3, shows that although the amount of MIPC is greatly decreased in the *gdal* mutant as compared to the wild-type profile (lane 1), the mannosylation defect is not complete and it appears that the majority of the MIPC made is rapidly phosphoinositolated to form M(IP)$_2$C. The *scs7* profile, lane 2, shows the pre-

---

[6] Although performing the analysis without eliminating the phosphoglycerolipids by alkali treatment is not as clean as with it, omitting alkali hydrolysis is useful because the quantity of PI is not expected to be influenced by the sphingolipid mutations. Therefore PI can be used as an internal standard to verify even loading of the samples.
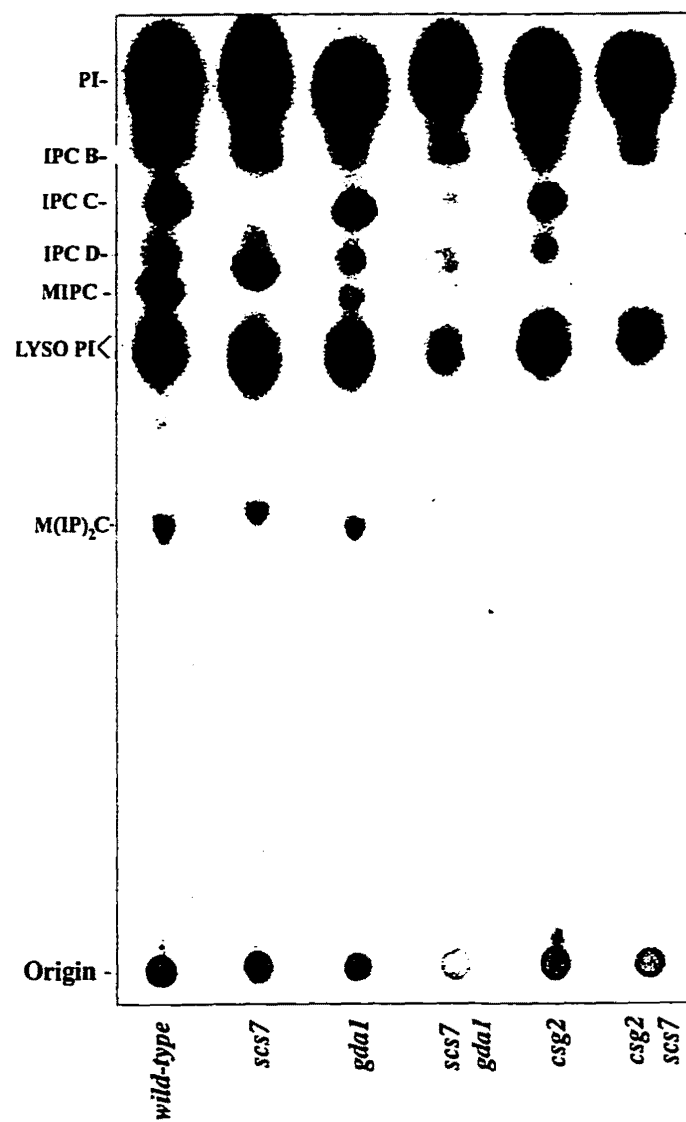
Figure 8. Sphingolipid profile of *scs7Δ* and *gda1 Δ* single and double mutants.

sence of the IPC-D-like species. This species is mostly absent in the *scs7Δ gdal Δ* double mutant (lane 4). This supports the hypothesis that the IPC-D-like species is not a hydroxylated IPC such as IPC-C or -D, but rather a mannosylated form of unhydrox-ylated IPC-B, MIPC-B. The *scs7* profile, lane 2, also indicates the presence of a species with slightly higher mobility than $M(IP)_2C$. This is believed to be an unhydroxlated form of $M(IP)_2C$.

Constructing the sur2Δ mutant. In an unrelated study we isolated a YCp50-based plas-mid containing a fragment of yeast DNA that included the amino terminus (through to a *Sau3A* site at codon 120) of the *SUR 2* gene. A restriction fragment extending from the *HindIII* site 367 basepairs upstream of the start codon of the *sur2* gene to the *SalI* site in Ycp50 was subcloned from this plasmid into pUC19. The resulting plasmid was line-arized at the *PstI* site in codon 9 of the *SUR2* gene, treated with *Bal31* to remove about 100 base pairs and incubated with dNTPs, Klenow, ligase and *XhoI* linkers. A candidate plasmid with a *XhoI* linker at the deletion junction that was missing about 50 basepairs from each side of the original *PstI* site was chosen to construct the disrupting plasmid. A *SalI* fragment carrying the *TRP1* gene was ligated into the *XhoI* site. The *SUR2* dis-rupting fragment was cut out of the pUC19 plasmid using *PvuII* and used in a one step gene replacement as described above. The disruption of *SUR2* was confirmed by PCR.

Steady state sphingolipid analysis of sur2Δ on wild-type, csg2Δ, scs7Δ, and csg2Δ scs7Δ backgrounds. As described in the introduction, *SUR2* is homologous to *SCS7* and the *SUR* genes are connected to sphingolipid metabolism. Therefore the sphingolipid study was extended to include *sur2* null mutants. The *sur2Δ* strain was crossed to wild-

41

type, *csg2Δ*, *scs7Δ* and *csg2Δ scs7Δ* strains and trp⁺ leu⁺ meiotic segregants were iso-
lated. The *csg2Δ sur2Δ* mutant was found to be Ca^{2+} resistant (data not shown). This
suppression of *csg2* Ca^{2+} sensitivity further implicated *sur2* in sphingolipid biosynthesis.

The strains indicated in Figure 9 were labeled, extracted, and chromatographed on
TLC using the steady state procedure as described in Materials and Methods. The steady
state wild-type profile is given in lane 1 and shows the positions of the IPC-C, IPC-D and
MIPC. In the *csg2Δ*, lane 2, the label is predominantly in IPC-C and the MIPC species is
absent consistent with previous results. Likewise the *scs7Δ* mutant, lane 4, contains the
fatty acid-unhydroxylated IPC-B and its mannosylated form, MIPC-B. The latter species
is absent in the *csg2Δ scs7Δ* double mutant (lane 7). The profiles are dramatically
altered by the addition of the *sur2Δ* mutation. The *sur2Δ scs7Δ* mutant (lane 5) makes 2
species with the same mobilities relative to each other as those of *scs7Δ* (lane 4); the
difference being that the *sur2Δ scs7Δ* pair is shifted slightly higher. This is consistent
with these species being the long chain base (LCB)-unhydroxylated forms of the of the
IPC-B and MIPC-B of *scs7Δ*. They are thus labeled IPC-A and MIPC-A respectively.

The *sur2*-dihydrosphingosine hypothesis predicts that a *sur2Δ SCS7* cell might
make an IPC species that is unhydroxylated on the dihydrosphingosine LCB moiety, but
hydroxylated on the fatty acid moiety. Such a species would have the same number of
hydroxylations as the IPC-B species of *csg2Δ scs7Δ*, and the two species should have
similar mobilities on TLC. The *csg2Δ sur2Δ* mutant, (lane 6), has a species with a
mobility very similar to the IPC-B species of the *csg2Δ scs7Δ* (lane 7) which is pre-
sumed to be the predicted LCB-unhydroxylated, fatty acid-hydroxylated IPC and is

	A	IPC-A
	B	IPC-B
	B'	IPC-B'
	C	IPC-C
	D	IPC-D
	MA	MIPC-A
	MB	MIPC-B
	MB'	MIPC-B'
	MC	MIPC-C
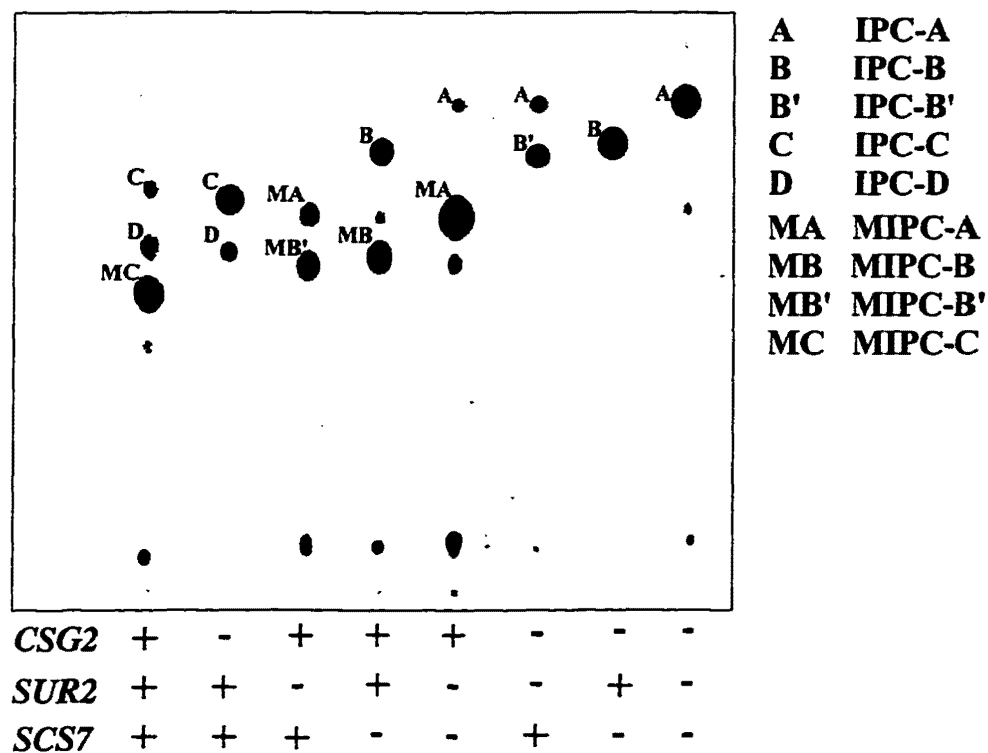
CSG2	+	-	+	+	+	-	-	-
SUR2	+	+	-	+	-	-	+	-
SCS7	+	+	+	-	-	+	-	-

Figure 9. Analysis of sphingolipids from wild-type (lane 1), *csg2Δ* (lane 2), *sur2Δ* (lane 3), *scs7Δ* (lane 4), *sur2Δ scs7Δ* (lane 5), *csg2Δ sur2Δ* (lane 6), *csg2Δ scs7Δ* (lane 7), and *csg2Δ sur2Δ scs7Δ* (lane 8) cells. Cells were labeled with [^{3}H]-inositol and sphingolipids were extracted and separated by silica gel TLC as described in Materials and Methods. The sphingolipids were visualized by autoradiography. The strains, designated only by the relevant gene disruptions are derivatives of TDY2037. The structures of the sphingolipid species, denoted as IPC-A, IPC-B, IPC-B', and IPC-C or MIPC-A, MIPC-B, MIPC-B' and MIPC-C are presented in Figure 16.

43

called IPC B'. The *csg2Δ sur2Δ* extract in lane 6 also contains a labeled species with higher mobility than IPC-B'. This species is also the sole species present in the *csg2Δ sur2Δ scs7Δ* triple mutant (lane 8) and its mobility is consistent with it being an IPC with hydroxylation on neither the fatty acid nor LCB moieties. Again, based on the hypothesized gene functions that have been deleted in the triple mutant, such a species is predicted, and it is thus labeled IPC-A.

Finally, the *sur2Δ* (lane 3) mutant produces a pair of species with mobilities relative to each other that are similar to the IPC-A/IPC-B' pair produced by the *csg2Δ sur2Δ* mutant (lane 6). The most likely explanation is that the wild-type CSG2 in the *sur2Δ* permits mannosylation of the IPC-A/IPC-B' species. Thus the upper and lower species of *sur2Δ* are labeled MIPC-A and MIPC-B' respectively.

Although, the above analysis does not unequivocally establish the structure of the various labeled species, there is a strong correlation of their actual TLC mobilities with those predicted based on the proposed gene functions. This establishes a very strong circumstantial case that the assignments made to these species, and thus the proposed gene functions, are correct.

Sphingolipid analysis with and without phytosphingosine and dihydrosphingosine. If *SUR2* is the gene encoding the dihydrosphingosine hydroxylase, then exogenously added phytosphingosine should bypass the block caused by *sur2Δ*, allowing the production of wild-type sphingolipids. Extracts from wild-type, csg2Δ, sur2Δ csg2Δ, and *csg2Δ scs7Δ* cells grown either with no supplementation or with supplementation of either phytosphingosine or dihydrosphingosine were prepared and analyzed as described in

Materials and Methods. Figure 10 shows the results of this experiment. Neither exogenously added phytosphingosine nor dihydrosphingosine affected the sphingolipid profiles of wild-type (lanes 1-3) or *csg2Δ* (lanes 4-6) cells. Lane 7 contains the profile of the unsupplemented *csg2Δ sur2Δ* mutant showing IPC-A and IPC-B' as in the previous experiment. The addition of phytosphingosine to this strain results in the production of IPC-C (lane 8) whereas the addition of dihydrosphingosine has no effect (lane 9) as the model predicts because dihydrosphingosine is upstream of the block. Conversely, as was seen in Lane 5, Figure 7, exogenous phytosphingosine has no effect on the profile of the *csg2Δ scs7Δ* double mutant because its block is in the hydroxylation of the fatty acid rather than the LCB. Further results from this experiment (not shown in Figure 10) are that IPC-B, but not IPC-C, was seen in the profile from *csg2Δ sur2Δ scs7Δ* triple mutant cells grown in the presence of phytosphingosine. In both cases, the addition of phyto-sphingosine to a *sur2Δ* changes the putative ceramide base of the terminal IPC from dihydroceramide to phytoceramide.

Growth Phenotypes of scs7Δ Mutants. In order to gain insight into the effect of the *scs7Δ* mutation on cell metabolism, the 2037scs7k and its parent 2037 were incubated under a variety of different conditions. The results are shown in Table 1. No differences were seen in the growth of 2037 and 2037scs7k at 26° C or 37° C. At both temperatures both strains grew well with no observable inhibition. At 14° C however, 2037scs7k grew markedly better than it's wild-type parent on all of the different medias tested. The effect appears to be a global one. In light of the findings described above showing that the *scs7Δ* mutant makes unhydroxylated IPCs with complete head groups and the reasonable

45
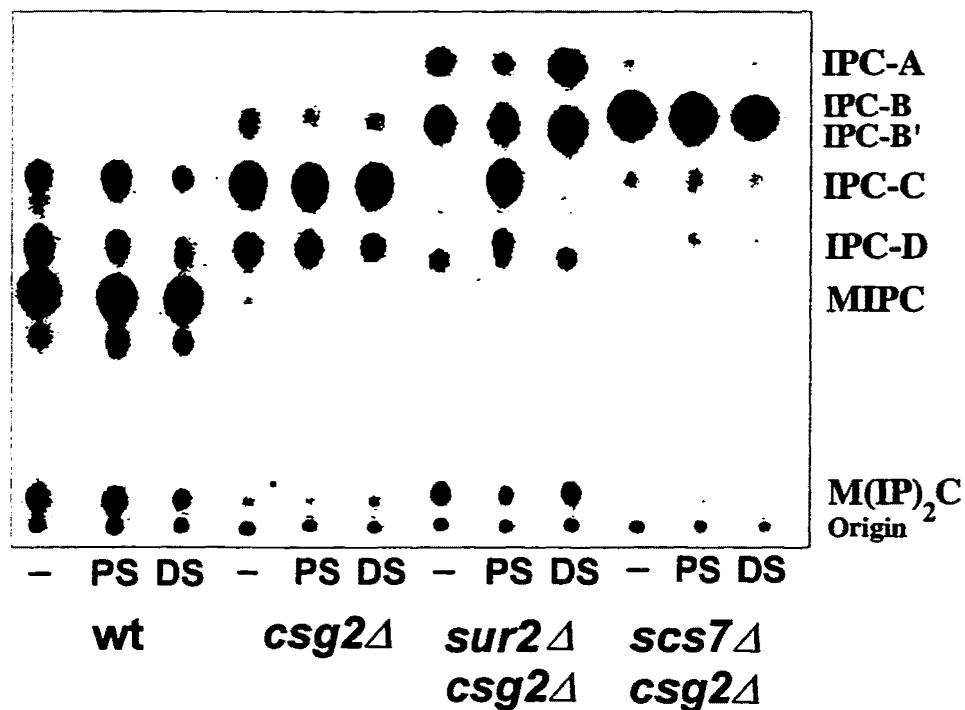
Figure 10. Effect of exogenous phytosphingosine on synthesis of IPC-C in the *csg2Δ* *sur2Δ* double mutant. Wild-type, *csg2Δ*, *csg2Δ sur2Δ*, or *csg2Δ scs7Δ* mutant cells were grown for several generations in synthetic medium containing 12 nM [^{3}H]-inositol at 1 μCi/ml. Where indicated, 25 μM phytosphingosine (PS) or dihydrosphingosine (DS) was included in the growth medium. Sphingolipids were extracted, alkali-treated, separated by TLC, and visualized by autoradiography. Structures of the sphingolipids are presented in Figure 16.

media	14° C 2037	scs7Δ	26° C 2037	scs7Δ	37° C 2037	scs7Δ	42° C 2037	scs7Δ
YPD	+	+++	+++	+++	+++	+++	+/-	+/-
5 mM EGTA	-	-	+++	+++	+++	+++	+/-	+/-
10 mM EGTA	-	-	+++	+++	+++	+	+/-	+/-
100 mM Ca^{2+}	+/-	+++	+++	+++	+++	+++	+	+
80 mM BCS	+/-	+++	+++	+++	+++	+++	+/-	+/-
80 mM BPS	+/-	++	+++	+++	+++	+++	+/-	+/-
1 mM Fe^{2+}	-	++	+++	+++	+++	+++	-	+/-
1 mM Cu^{2+} + 0.5 mM Ferizine	-	++	+++	+++	+++	+++	+/-	+/-
0.1 mM Cu^{2+}	-	++	+++	+++	+++	+++		
0.01 mM Zn^{2+}	+	+++	+++	+++	+++	+++		
30 mM Sr^{2+}	+	+++	+++	+++	+++	+++		
25 mM Sr^{2+}	+	+++	+++	+++				

Table 1. Growth phenotype study of scs7Δ mutant. Cell cultures were incubated for 7 days. - = no visible growth; +/- = light growth in the first streak; + = moderate to confluent growth in the first streak; ++ = confluent growth in first streak, pin point individual colonies in second streak; +++ = confluent growth in first streak; large individual colonies in second streak.

expectation that these sphingolipids will be heavily concentrated in the outer leaflet of the plasma membrane as are the hydroxylated sphingolipids of wild-type cells, this finding appears to be consistent with the possibility that the enhanced resistance to lower temperature of *scs7Δ* cells could be due to enhanced membrane fluidity resulting from this change in membrane sphingolipid composition in a manner analogous to the desaturation of phospholipids in response to varying temperature as discussed in Chapter One. This possibility is supported by other observations and will be discussed in detail in Chapter Five.

Conclusions

The studies described in this Chapter confirmed the construction of the *scs7Δ*, *sur2Δ* mutants both singly and together in wild-type and csg2Δ backgrounds. The *csg2Δ scs7Δ* mutant accumulates IPC-B, but makes no IPC-C or mannosylated sphingolipids. Thus, the *scs7Δ* mutation suppresses the Ca^{2+} sensitivity phenotype of *csg2Δ*, but does not suppress the mannosylation defect of *csg2Δ*. This is consistent with the hypothesis that *csg2Δ* Ca^{2+} sensitivity is due to overaccumulation of IPC-C and not due to the failure to mannosylate; and that the hydroxylation state of IPC-C is important to Ca^{2+} sensitivity.

The *csg2Δ sur2Δ* strain also makes an atypical IPC species and does not make mannosylated sphingolipids. However both *scs7Δ* and *sur2Δ* both individually and together result in the production sphingolipids with TLC mobilities consitent with their being mannosylated forms of the IPCs of the corresponding strains in a *csg2Δ* background. Phytosphingosine supplementation restores IPC-C synthesis in *sur2Δ* strains, but not in *scs7Δ* strains. This is consistent with the hypothesis that *SUR2* and *SCS7*

mediate the hydroxylations of LCB and VLCFA respectively. The *scs7Δ* mutant also

makes IPC-B, as well as a mannosylated IPC-B. Thus the Scs7p and Sur2p hydroxy-

lations are not required for mannosylation of yeast sphingolipids.

Chapter Four

Characterization of the Ceramide Content of *SCS7Δ* and *SUR2Δ* Mutants

Introduction

The work described in the previous chapters indicates that Scs7p mediates the hydroxylation of VLCFA to convert IPC-B to IPC-C. Additionally Sur2p is implicated as being necessary for the LCB hydroxylation at C_4. However, in order to establish these functions unequivocally it was necessary to structurally characterize the IPC species from these strains. This was the primary goal of the studies described in this chapter.

Secondly, one of the most fundamental questions in describing a biochemical pathway is establishing the order of reactions by which biomolecules are assembled. In the case of sphingolipids, the pathway order is well established through the production of dihydrosphingosine and this pathway appears to be common to all the sphingolipid species (Kishimoto, 1983). Likewise the pathway for the production of the ceramide base of sphingomyelin has been determined to involve first the addition of the very long chain fatty acid to the amine of dihydrosphingosine followed by the desaturation at C_4-C_5 of dihydrosphingosine (Ong and Brady, 1973). However the sequence of reactions in the construction of the phytoceramide molecule have not been firmly established. It was anticipated that examining the ceramide content of the *scs7Δ* and *sur2Δ* mutants would be useful in answering these questions.

Materials and Methods

Isolation of sphingolipids by preparative silica gel TLC. Sphingolipids were extracted from 600 OD$_{600}$ units of cells by bead beating in 100 mls of CHCl$_3$:MeOH (1:1). The

extract was dried, alkali-treated and BuOH-desalted as previously described (Zhao *et al.*, 1994). The sample was spotted in a line on a silica gel plate and developed using $CHCl_3$: MeOH:AcOH (95:4.5:0.5). In this system, fatty acids and ceramides migrate while sphingolipids remain at the origin. The material left at the origin was subjected to acid methanolysis for analysis of the fatty acid methyl esters (FAMES) and long chain bases (LCBs) as described below.

Ceramide Analysis. The cells were grown overnight at 26° C in minimal media containing inositol. The cells were beat with glass beads in hexane:ethanol (95:5) at 40 OD_{600}/ml. The supernatant was transferred to a fresh tube, the beads were washed with hexane:EtOH, and the pooled extract was dried. The lipid extract was alkali-treated as described in Material and Methods, Chapter 3, except that the concentration was ~40 OD_{600} / ml. The material was also desalted with butanol as described in Chapter 3 except that the concentration was ~60 OD_{600} / ml. The ceramides were analyzed by TLC on silica gel plates using $CHCl_3$:CH_3OH:AcOH (95:4.5:0.5) as the developing solvent (Imokawa *et al.*, 1991). Plates were sprayed with 10% copper sulfate in 8% orthophosphoric acid and heated for 20 min at 180° C to char the ceramides.

Isolation of ceramides by preparative silica gel TLC. Purified preparations of ceramides were obtained by TLC purifying ~600 OD_{600} units of the appropriate extracts [Strains 2037 (wild-type) and 2038 (*csg2Δ*) for C-ceramide; 240sur2k (*csg2Δ sur2Δ*) for B'-ceramide; 6715b (*csg2Δ scs7Δ*) for B-ceramide; and 6715b/sur2k (*csg2Δ sur2Δ scs7Δ*) for A-ceramide.] The extracts were applied in a line across the bottom of a TLC plate which was developed with the ceramide developing system described above. The plate

51

was sprayed with .01% 8-anilino-1-napthalene sulfonic acid and the lipids were visualized under ultraviolet light. The bands of interest were scraped and the ceramides were eluted by repeated sonication (5X for ten min in 2 ml of $CHCl_3:CH_3OH$ (1:1).

Acid Methanolysis of Ceramides and Sphingolipids and Isolation of FAMEs and LCBs.

Ceramides and sphingolipids were purified by silica gel TLC as described above. The purified ceramides or sphingolipids were subjected to acid methanolysis by resuspending in 2 ml $HCl:MeOH:H_2O$ (3:29:4) and incubating at 78° C for 18 hours (Bertello *et al.*, 1995). The FAMEs were recovered by extracting 3X with 2 ml of hexane (Hung *et al.*, 1995). The extracts were pooled, dried, and subjected to TLC using petroleum ether:Et_2O (17:3) as the developing solvent (Hung *et al.*, 1995). Plates were sprayed with 10% copper sulfate in 8% orthophosphoric acid and heated for 20 min at 180° C to char the FAMES.

The LCBs were recovered from the hydrolyzed ceramides or sphingolipids by adjusting the pH of the acid hydrolysate (after extraction of FAMEs) to 11.5 using 1 M NaOH (Hung *et al.*, 1995). The sphingoid bases were recovered by extracting 3X with 2 ml Et_2O. The pooled extracts were dried and the LCBs were separated by silica gel TLC using $CHCl_3:CH_3OH:2.0$ M NH_4OH (40:10:1) as developing solvent (Hung *et al.*, 1995). Plates were sprayed with 0.2% ninhydrin in ethanol and incubated at 100° C for 5-10 min to visualize the amine-containing LCBs.

Diacylglycerol kinase assay for measurement of ceramides. The lipid to be assayed was dried in a 10 ml round bottom screw cap glass tube and resuspended in 40 µl of 2.5x detergent solution consisting of 3.75%(w/v) β-octylglucoside, 12.5 mM dioleoylphospha-

52

tidylglycerol, and 1 mM diethylenetriaminopentacetic acid (DTPA). The tubes were

vortexed briefly and bath sonicated for 10 minutes. Fifty μl of 2x reaction buffer con-

sisting of 120 mM Hepes buffer pH 7.0, 100 mM LiCl, 25 mM $MgCl_2$, 2 mM EGTA, 2

mM dithiothreitol was added followed by 2 μl of CalBiochem purified E coli membranes.

The tubes were mixed and incubated at room temperature for 10 min. The reaction was

initiated by adding 5 μl of 20x ATP solution consisting of 20 mM ATP, 40 mM imidizole

pH 6.6, 2 mM DTPA and 0.5 μl [γ-^{32}P]ATP 10 mCi/ml and vortexing briefly. The tubes

were incubated at room temperature for 30 minutes and the reaction was stopped with 0.7

ml of 1% $HClO_2$. The reaction products were extracted by adding 3 ml chloroform/meth-

anol (1:2) followed by 1 ml each of chloroform and 1% $HClO_2$. The tubes were mixed,

centrifuged, and the upper phase was removed. The lower phase was washed twice with

2 ml 1% $HClO_4$:methanol (7:1) and then dried. The samples were chromatographed on

silica gel TLC plates using chloroform:pyridine:formic acid (60:30:7) as solvent. After

development, the plates were heated at 130° C for 10 min and then exposed to XAR5

film overnight at -70° C.

Phosphatidylinositol-specific phospholipase C (PIPLC) assay. The lipid to be digested

was dried in a 1.5 ml eppindorf tube and resuspended in reaction buffer containing 70

mM triethanolamine and 5 mM EDTA pH 7.2. Approximately 50 mU of PIPLC (Sigma)

was added to the reaction followed by bath sonication for 1 min. The reaction mixture

was then incubated overnight at 37° C.

Results

Acid hydrolysis of total IPCs from sur2Δ and scs7Δ mutants. The sphingolipid profiles of *Sur2Δ* and *scs7Δ* mutants (Figure 9) demonstrated the presence of unique IPC species that were consistent with an unhydroxylated LCB in the case of *sur2Δ* and an unhydroxylated VLCFA in the case of *scs7Δ*. In order to directly determine the structures of these species, total IPC preparations were made and subjected to strong acid methanolysis, as described in Materials and Methods above. This cleaves the sphingolipid amide bond forming the free very long chain fatty acid in the form of a methyl ester (VLCFAME) and the long chain base. The LCBs and VLCFA were then individually extracted and analyzed for their hydroxylation states by TLC as described in Materials and Methods. The results of this analysis are shown in Figure 11. The total sphingolipid extracts from *sur2Δ* mutants (lanes 3 & 5), contain a LCB species that migrates to the same position as the dihydrosphingosine standard (lane 7) and no material that has the mobility of the phytosphingosine standard (lane 6). Conversely all the samples from wild-type *SUR2* cells, (lanes 1,2 & 4), yield a LCB species with phytosphingosine mobility. This confirms that *SUR2* is necessary for the hydroxylation that converts dihydrosphingosine to phytosphingosine.

Acid hydrolysis of sphingolipids releases the VLCFAs in the form of methyl esters, which migrate to the indicated positions in the B panels of Figures 11. The acid-hydrolyzed extract from csg2Δ scs7Δ cells (Lane 4) does not contain HVLCFAME whereas the extracts from wild-type *SCS7* cells (Lanes 1-3) do contain HVLCFAME.

54

Figure 11. Analysis of the sphingoid moiety (panel A) and the VLCFA (panel B) of sphingolipids extracted from wild-type, *csg2Δ*, *csg2Δ sur2Δ*, *csg2Δ scs7Δ*, and *csg2Δ sur2Δ scs7Δ* mutants. Sphingolipids were isolated from the cells and purified by TLC as indicated in Materials and Methods. The sphingolipids were subjected to acid methanolysis and the liberated FAMEs were extracted with hexane and separated by silica gel TLC (panel B). Plates were sprayed with 10% copper acetate in 8% orthophosphoric acid and heated for 20 min at 180° C to char the fatty acid methyl esters. Hydroxylated C_{18} and C_{24} FAMEs (lanes 7 & 8) standards from Sigma were suspended at 4 μg/μl and 12 μg was spotted. The position of the NVLCFAME and HVLCFAME are indicated in the right margin. After extraction of the FAMEs, the pH of the remaining solution was adjusted to 11.5 with NaOH and the LCBs were extracted with diethylether and analyzed by TLC (panel A). The LCBs were visualized by spraying with 0.2% ninhydrin in ethanol and heating at 100° C for 5-10 min. Phytosphingosine (PS), dihydrosphingosine (DS), and sphingosine (S) standard from Sigma were suspended at 10 μg/μl and 10 μg were spotted.
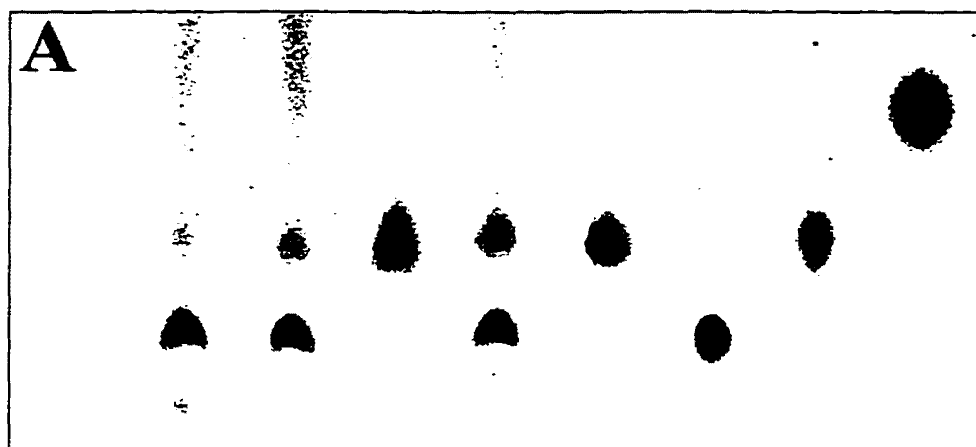
CSG2	+	-	-	-	-	PS	DS	S
SUR2	+	+	-	+	-			
SCS7	+	+	+	-	-			

NVLCFAME

HVLCFAME

←O

CSG2	+	-	-	-	C18 -OH	C24 -OH	C18	C24
SUR2	+	+	-	+				
SCS7	+	+	+	-				
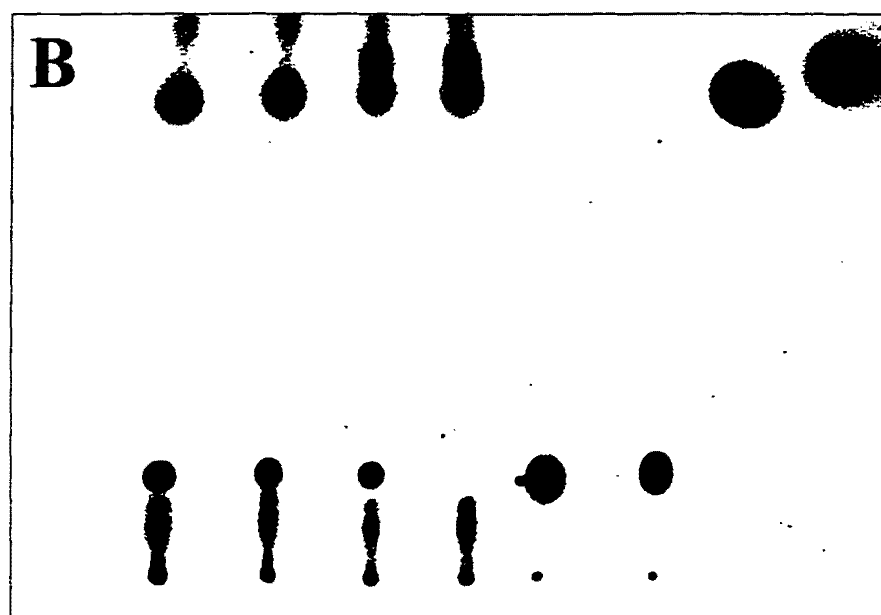
This result confirms that *SCS7* is required for the hydroxylation of the long chain fatty acid moiety of yeast sphingolipids.

Measurement of Yeast Ceramides using the Diacylglycerol Kinase Assay. Diacylglycerol kinase catalyzes the phosphorylation of diacylglycerol to form phosphatidic acid. In *E. coli*, it functions to salvage diacylglycerol generated by the inositol triphosphate signaling pathway and return it to phospholipid synthesis (Loomis, *et al.*, 1985). It will also phosphorylate ceramides *in vitro* and has been used widely to quantitate ceramides in a mixed micellar assay that uses $[\gamma^{32}P]ATP$ to quantitatively label ceramides (Van Veldhoven *et al.*, 1995). Therefore this assay was investigated for its potential to measure the ceramides produced by the sphingolipid mutants. Although the assay is well established for sphingosine based ceramides there were no reports of its use for the phytoceramides of yeast. Additionally, it was necessary to generate phytoceramide standards since they are not available commercially. This was accomplished by purifying the corresponding IPCs by TLC and treating with phosphatidylinositol specific phospholipase C (PIPLC). PIPLC cleaves the phosphoinositol head group yielding the free phytoceramide base. Figure 12, Lane 1 shows the position of the phosphatidic acid (PA) and lysophosphatidic acid produced by phosphorylation of the monoacyl and diacylglycerol contamination of the *E coli* membranes containing the diacylglycerol kinase. Alkali treatment was necessary to eliminate diacylglycerol contamination of the yeast extracts, but material from the membrane preparation could not be eliminated. The commercial TIII (lane 2) and TIV (lane3) bovine ceramide standards are unhydroxlated and hydroxylated respectively on the fatty acid moiety. In comparison, the unhydroxlated, IPC-B-derived (lane

57

Figure 12. Diacyglycerol kinase assay of *csg2Δ scs7Δ* mutant. Lane 1 contains no added

lipid. Lanes 2 and 3 are TypeIII (unhydroxylated; 0.5 μmole) and TypeIV (hydroxylated;

2 μmole) bovine ceramides. Lanes 4 and 5 contain "B" and "C" phytoceramide standards

prepared from extracts of strain 6715b, *csg2Δ scs7Δ*, and strain 2038, *csg2Δ*, respec-

tively. To prepare the standards, fifty OD_{600} units of cells were [^{3}H]myoinositol labeled,

extracted, and alkali hydrolyzed using the procedure described in Materials and Methods,

Chapter 3. The extracts were spotted to 4 lanes each on TLC plates and chromatographed

using the IPC solvent system described in Chapter 3. The IPC B and IPC C spots were

scraped and eluted from the 6715b and 2038 lanes respectively and eluted 5X with 2 ml

chloroform: methanol(1:1). This material was dried and treated with PIPLC as described

in Material and Methods (this chapter), dried, and butanol desalted. Approximately 50k

cpm of each sample was then used in the DG kinase assay. Lanes 6-8 and 9-11 contain

the indicated amounts of 2037 (wild-type) and 6715b (*csg2Δ scs7Δ*) alkali-treated

extract.
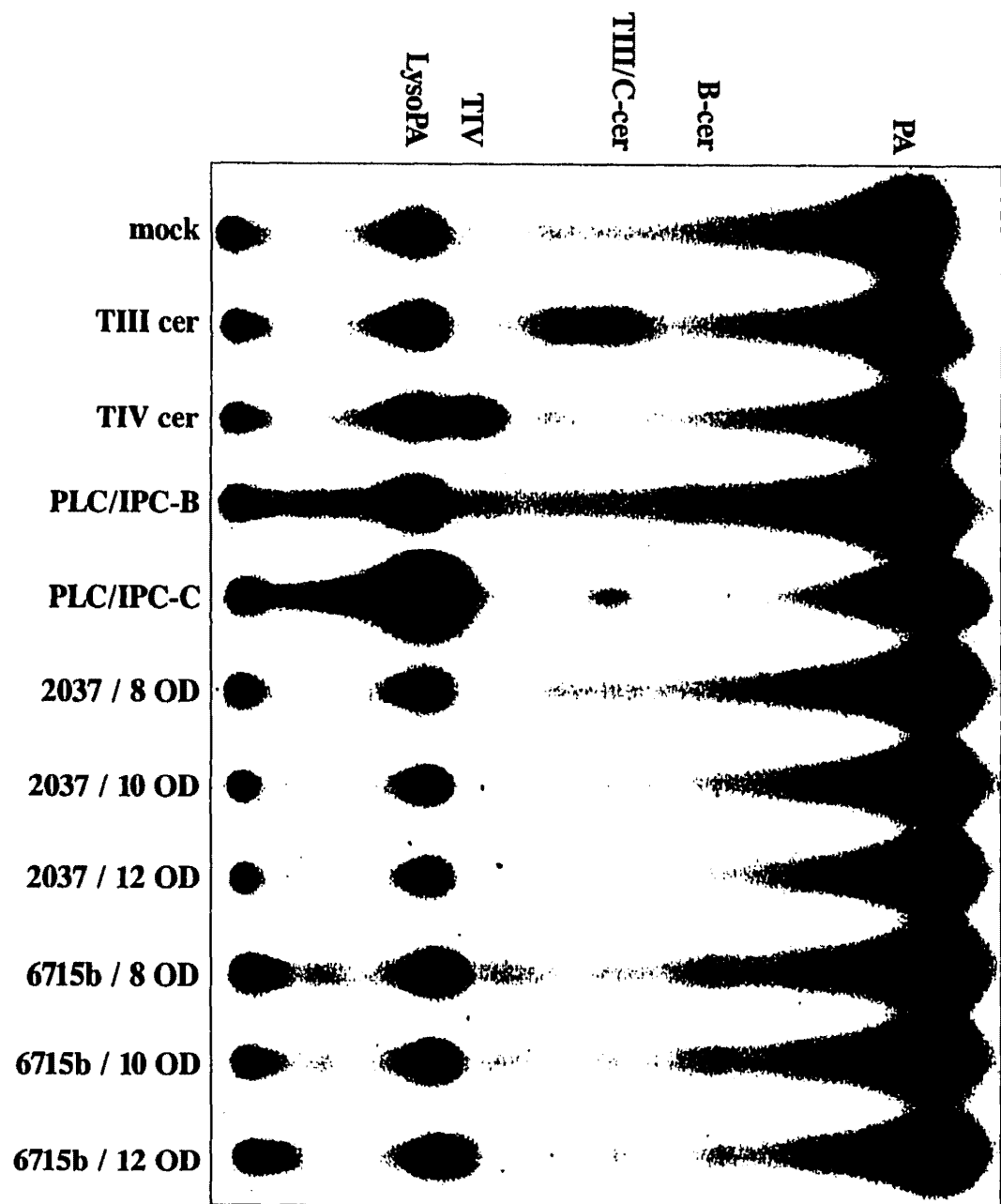
4), and hydroxylated, IPC-C-derived (lane5) phytoceramides are slightly more mobile upon phosphorylation. Lanes 9-11 contain the reaction products produced by increasing amounts of alkali-treated lipid extract from strain 6715b (*csg2Δ scs7Δ*) cells showing the presence of a putative phosphorylated, unhydroxylated B-ceramide in these cells. Similar attempts to show the presence of hydroxylated C-ceramide in wild-type 2037 cells were unsuccessful (lane 6-8). Lanes 9-11 show that increasing amounts of extract above 8 OD_{600} units actually resulted in diminution of an already weak signal. Perhaps yeast extracts contain an inhibiting factor that puts an upper limit on the signal that can be obtained.[7] Therefore the DG kinase assay could not be used to quantitate ceramide levels. However it did provide evidence that there is a buildup of unhydroxylated ceramides in *csg2Δ scs7Δ* mutants.

Isolation of Ceramides from scs7Δ and sur2Δ mutants. Thin layer chromatographic separation of ceramides was first described by Karlsson and Pascher in 1971. More recently it has been used to detect ceramide species in cell extracts from human skin (Imokawa *et al.*, 1991). Because of the above-described problems associated with cera-mide detection and measurement by the diacylglycerol kinase assay, it was reasoned that this simpler and more quantitative method would eliminate the limitations inherrent to an enzyme assay visa vis enzyme inhibition and differential substrate preference. Figure 13 shows the results of this analysis using extracts from wild-type, *csg2Δ*, *csg2Δ sur2Δ*,

---

[7]

The assay was also performed with less than 8 OD_{600} units of extract without any increase in signal. It therefore appears that approximately 8 OD_{600} units is the optimal amount of yeast extract, prepared as described, for this assay.
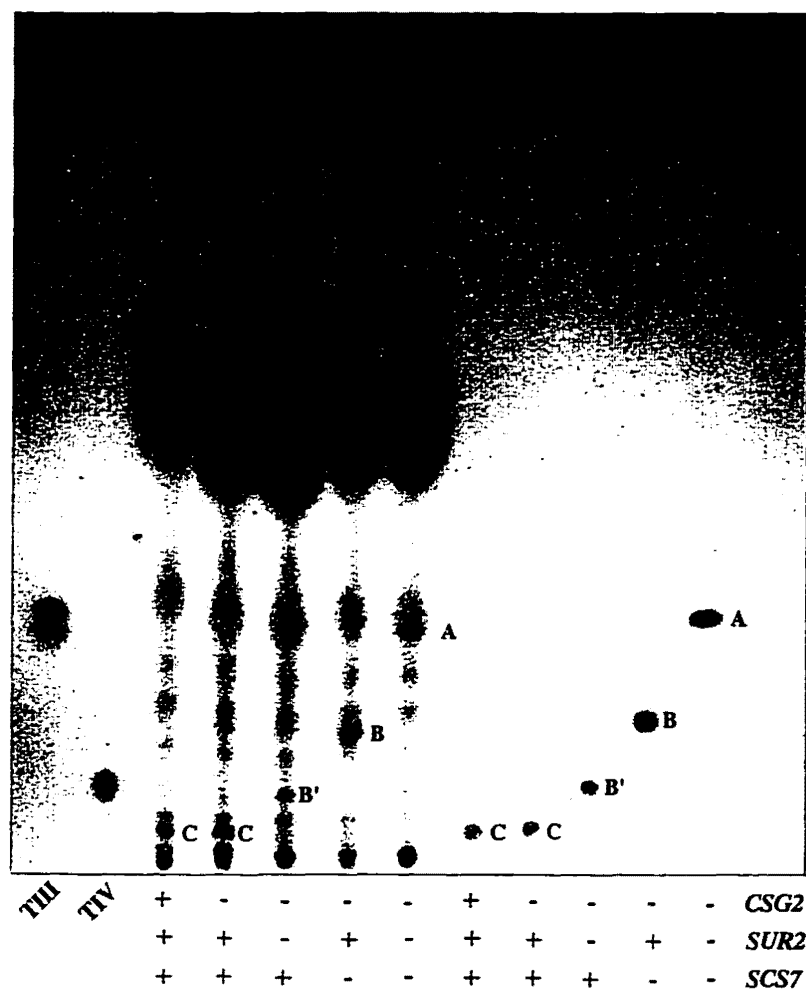
Figure 13. Analysis of ceramides from wild-type, *csg2Δ*, *csg2Δ sur2Δ*, *csg2Δ scs7Δ*, and *csg2Δ sur2Δ scs7Δ* cells. Nonpolar lipids were extracted from 10 OD_{600} units of wild-type (lane 3), *csg2Δ* (lane 4), *csg2Δ sur2Δ* (lane 5), *csg2Δ scs7Δ*(lane 6),or *csg2Δ sur2Δ scs7Δ* (lane 7) cells and separated by TLC as described in Materials and Methods. Four μg of bovine Type III (sphingosine and unhydroxylated FA, lane 1) and Type IV (sphingosine and hydroxylated FA, lane 2) ceramide standards were spotted. Ceramides from 100 OD_{600} units of cells were purified by preparative TLC and 6% were analyzed (lanes 8-12). The structures of the ceramide species are shown in Figure 16.

61

csg2Δ scs7Δ, and *csg2Δ sur2Δ scs7Δ* cells prepared as described in Material and Methods. In comparison to the diacylgycerol kinase method, this method essentially detects all lipid species on the plate and therefore has more background. On the other hand this lack of specificity allows for the detection of species of interest, specifically C-ceramide, that was not detected by the diacylglycerol kinase assay.

Tentative assignments for the ceramide spots were made based on comparison with the TIII and TIV bovine ceramide standards (lanes 1 and 2) and by comparison of the profiles with each other. The identity of the C-ceramide spot was assigned because of its presence in wild-type (lane 3) and *csg2Δ* extracts and absence in the extracts from *sur2Δ* or *scs7Δ* cells (lanes 5-6), which are deficient in the LCB and VLCFA hydrox-ylations respectively. The putative C-ceramide also migrated to a position lower than the hydroxylated Type IV bovine ceramide (lane 2) as would be expected based on the com-parative structure of the two species; both are hydroxylated on the VLCFA, but the LCB of the latter is the more hydrophobic desaturated sphingosine as opposed to the more hydrophilic hydroxylated phytosphingosine LCB of the former.

The spot labeled B'-ceramide was present only in extracts from *csg2Δ sur2Δ* cells (lane 5) which is the only cell line analyzed predicted to make a ceramide with a hydroxylated VLCFA, but unhydroxylated LCB. That this is the correct structure of this species is also suggesteded by the observation that it has the same mobility as the TIV bovine ceramide standard which has the same hydroxylations on its VLCFA and LCB.[8]

---

[8]

The solvent system used in Figure 12 does not separate ceramides that differ from each other only in the presence or absence of a double bond (Karlsson and Pascher, 1971).

The *csg2Δ scs7Δ* strain is predicted to make the LCB-hydroxylated, VLCFA-unhydroxy-lated B-ceramide. The extract of this strain (lane 6) contains a unique species that has a mobility consistent with its putative structure. Although the B-ceramide has the same hydroxylation state as B'-ceramide and TIV bovine ceramide, apparently positioning of the hydroxyl group on the LCB moiety as opposed to the VLCFA moiety makes the molecule more hydrophobic or alters its mobility with the silica gel matrix so that it migrates to a higher position than the latter two.

Finally, there is a species present in both the *csg2Δ sur2Δ* (lane 5) and the *csg2Δ sur2Δ scs7Δ* triple mutant that has the same mobility as the LCB-unhydroxylated, VLCFA-unhydroxylated TIII bovine ceramide standard (lane 1). This is the predicted structure of the putative A-ceramide predicted to be made by the triple mutant. The right side of the figure (lanes 8-12) contains purified preparations of these ceramide species obtained by TLC purification as described in Material and Methods. This material was used in further characterization studies including examining mobility alteration in the presence of arsenate and borate and in the acid methanolysis procedure described below. *TLC Analysis of Purified Ceramides on Arsenate and Borate Plates.* Further evidence concerning the hydroxylation states of the putative ceramide intermediates was obtained by observing the effect of arsenate and borate on their TLC mobilities. Species with vici-nal hydroxyl groups, like those of phytoceramide, form a mobile complex with arsenate that enhances their mobility relative to species without hydroxyl groups. The opposite is true with borate which forms a stationary complex with vicinal hydroxyl groups thus retarding the migration of phytoceramide (Karlsson and Pacher, 1971).

63

Figure 14 shows the results obtained when the purified ceramide samples were chromatographed on regular silica gel TLC plates and on plates treated with 1% sodium meta arsenate (panel B) or with 1% sodium borate (panel C). As compared to their migration on untreated plates (panel A), the putative phytoceramides, C-ceramide (lanes 1 and 2) and B-ceramide (lane 4), were accelerated on arsenate (panel B) and were retarded on borate, (panel C). Conversely, the mobility of the putative dihydroceramides, B'-ceramide (lane 3) and A-ceramide (lane 5) relative to the migration of the TIII and TIV (lanes 6 and 7) bovine ceramide standards, was unaffected by the presence of either arsenate or borate. This indicates that the C- and B-ceramides contain vicinal hydroxyl groups consistent with their being phytoceramides, whereas B'- and A-ceramides do not contain vicinal hydroxyl groups consistent with their being dihydroceramides.

Acid Methanolysis of Purified Ceramides and Isolation of FAMEs and LCBs. The analyses described above demonstrate that *sur2Δ* and *scs7Δ* mutants accumulate both IPC and ceramide intermediates with TLC mobilities consistent with their being LCB and VLCFA unhydroxylated in the case of *sur2Δ* and *scs7Δ* respectively. The analysis in Figure 11 confirmed that these are the correct structures for the IPC species. In order to structurally characterize the accumulated ceramide species, the purified ceramide samples shown in Figure 13, Lanes 8-12 , were subjected to acid hydrolysis and TLC separation as described in Materials and Methods. The LCB TLC (panel A, Figure 15) shows that the *sur2Δ* derived samples (lane 7 & 9) again yield only dihydrosphingosine, whereas the wild-type SUR2 derived samples (lanes 5, 6 & 8), contain phytosphingosine. Likewise the FAME TLC (Panel B, Figure 15) showed that the *scs7Δ*-derived FAMES

Figure 14. Effect of arsenite and borate on the relative chromatographic mobilities of the A-, B-, B'-, and C-ceramides. The isolated ceramides used in the expreriment described in Figure 12 were analyzed by TLC on silica gel plates without (panel A) or with either 1% sodium *meta* arsenite (panel B) or 1% sodium borate (panel C) as described by Karlsson and Pascher, 1971. The borate plate and the untreated plate were run 1X in $CHCl_3:CH_3OH$ (95:5) while the arsenite plate was run 2X in $CHCl_3:CH_3OH:AcOH$ (95:4.5:0.5).

	1	2	3	4	5	6	7
CSG2	+	−	−	−	−		
SUR2	+	+	−	+	−	TIII	TIV
SCS7	+	+	+	−	−		

66
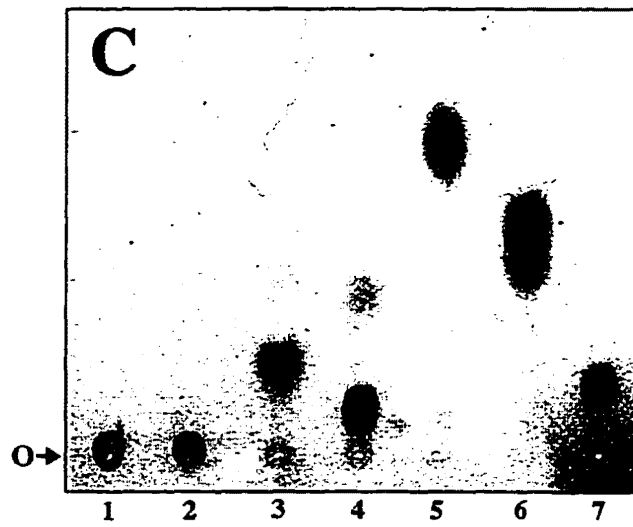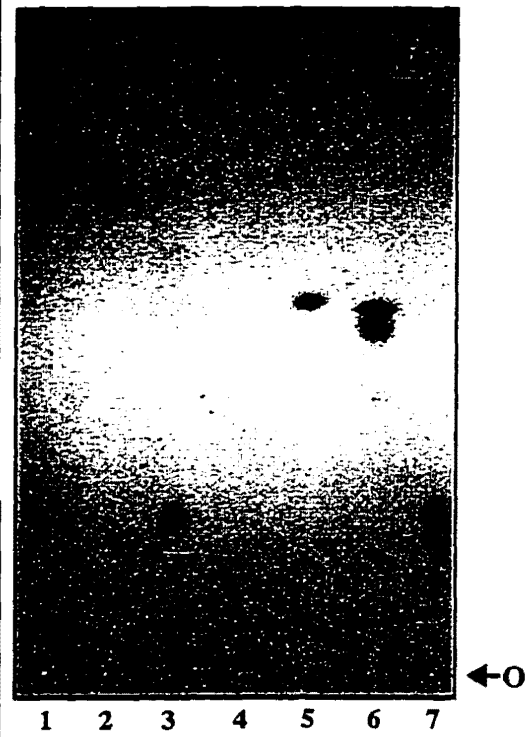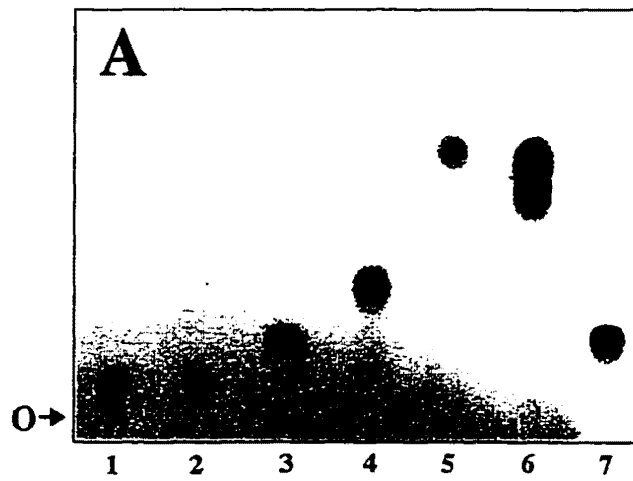
Figure 15. The LCBs and the FAMEs from A-, B'-, B-, and C-ceramides were analyzed

by silica gel TLC. Ceramides purified from 100 OD_{600} units of cells (see Figure 12) were

subjected to acid methanolysis and FAMEs and LCBs were extracted for analysis as

described in Materials and Methods.

A. The LCBs were separated by silica gel TLC. Standards were the LCB derived from

acid methanolysis of 4 μg of TIII bovine ceramide (lane 1) and 10 μg of sphingosine (S),

dihydrosphingosine (DS) and phytosphingosine (PS). The LCBs were visualized by

spraying with 0.2% ninhydrin in ethanol and heating at 100° C for 5-10 min.

B. The FAMEs were also separated by silica gel TLC. Standards were the FAMES

derived from acid methanolysis of Type III and Type IV bovine ceramides (4 μg) (lanes

1&2), and 10 μg of C_{18} FAME, C_{24} FAME and hydroxylated C_{24} FAME (lanes 3-5). The

plate was sprayed with 10% copper sulfate in 8% orthophosphoric acid and heated for 20

min at 180° C to char the FAMEs.

TIII	S	DS	PS	+	-	-	-	-	CSG2
				+	+	-	+	-	SUR2
				+	+	+	-	-	SCS7

A

←O

←NVLCFAME

←HVLCFAME

TIII	TIV	C18ME	C24ME	HC24ME	+	-	-	-	-	CSG2
					+	+	-	+	-	SUR2
					+	+	+	-	-	SCS7

B

←O

68
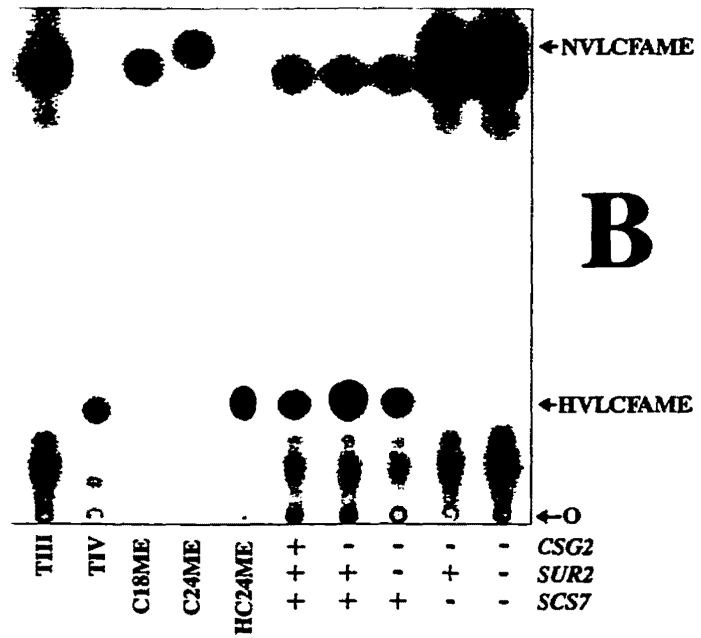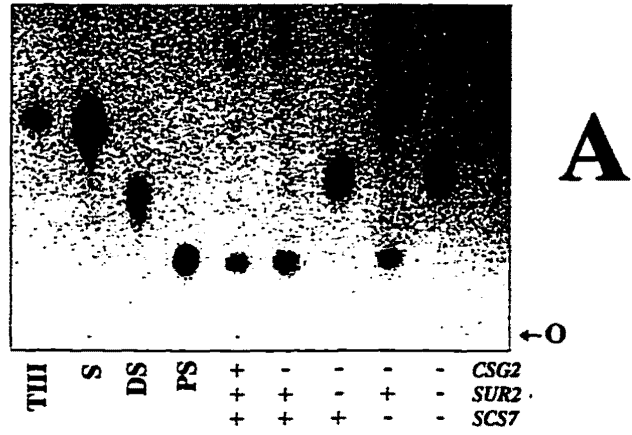
(Lanes 9 & 10) were unhydroxylated and the *SCS7*-derived FAMES (Lanes 5-7) were hydroxylated. These results correspond exactly with those presented in Figure 11 for the IPCs and further confirm *SUR2* and *SCS7* as being required for LCB and VLCFA hydroxylations respectively.

Epistatic Implications for the yeast Biosynthetic Pathway. As stated at the beginning of this chapter, one of the goals of the studies herein described was to gain insight into the order of steps in yeast sphingolipid biosynthesis. Figure 16 is a schematic of the yeast sphingolipid biosynthetic pathway that incorporates the conclusions that can be made in this regard based on examination of the above data. The diagram shows the possible routes of formation for mature wild-type sphingolipids as well as the species found in sphingolipid synthetic mutants.

The fatty acid acylation of the LCB to form ceramide apparently occurs before VLCFA hydroxylation. First, the presence of NVLCFAME in the FAME extract of total sphingolipid from *csg2Δ sur2Δ* cells (Figure 11, panel B, lane 3), suggests that the *SCS7* mediated fatty acid hydroxylation is less than optimal in the absence of *SUR2*, i.e. the presence of the C_4 hydroxyl group on the LCB influences the Scs7p-mediated hydroxylation of the VLCFA. This conclusion is consistent with the presence of unhydroxylated fatty acid IPC-A (Figure 9, lane 6) and A-ceramide (Figure 13, lane 5), in the *csg2Δ sur2Δ* mutant. The simplest explanation for these findings is that the *SCS7*-mediated fatty acid hydroxylation occurs at the level of ceramide. In the case of *sur2Δ* this ceramide is dihydroceramide, which apparently is not as good a substrate for the *SCS7*-mediated hydroxylation as phytoceramide. If the *SCS7* fatty acid hydroxylation occured

69

Figure 16. The mannosylinositolphosphoylceramide (MIPC) biosynthetic pathway in *S cerevisiae* is shown at the top and the structure of ceramide is shown at the bottom. Ceramide has five potential sites of hydroxylation, Hydroxyl groups on C-1 and C-3 are found on all long chain bases (LCBs). The other three sites are labeled I through III. Site I is on C4 of the LCB, site II is on C2 of the very long chain fatty acid (VLCFA) and site III is also on the VLCFA, but the position has not been determined. Five species (A, B, B', C, D) of ceramides, inositolphosphorylceramide (IPC) or MIPCs which differ according to which of the three sites are hydroxylated are synthesized. In this work, it is shown that hydroxylation of site I and II require Sur2p and Scs7p respectively.

Serine + Palmitoyl-CoA

Serine palmitoyltransferase
Scs1p/Lcb2p, Lcb1p

3-Ketosphinganine

3-Ketosphinganine reductase

Dihydrosphingosine

Sur2p

Phytosphingosine

C_{26}FA-CoA
Ceramide
Synthase

C_{26}FA-CoA
Ceramide
Synthase

A		B'	B		C		D
Ceramide	→	Ceramide	Ceramide	→	Ceramide	→	Ceramide
	Scs7p			Scs7p		Ccc2p / Cu²⁺	

Sur2p

A	B'	B	C	D
IPC-A	IPC-B'	IPC-B	IPC-C →	IPC-D
↓1	↓1	↓1	↓1	↓1
MIPC-A	MIPC-B'	MIPC-B	MIPC-C	MIPC-D

(2 for each IPC → MIPC step)

-OH

	A	B'	B	C	D
I	-	-	+	+	+
II	-	+	-	+	+
III	-	-	-	-	+

III
OH

II
O OH

H
N

HO-C-C-C
   H₂ H   OH
        OH

I

Ceramide

71

before ceramide formation the presence or absence of *SUR2* would be predicted to have no effect on the fatty acid hydroxylation state of yeast sphingolipids, because the two gene products would be acting independently of each other on two different molecules.

The deduced preference of SCS7p for phytoceramide additionally suggests that the latter is the natural substrate for the former. If so, then Sur2p-mediated LCB hydroxylation may occur upstream of Scs7p-mediated fatty acid hydroxylation. However these studies provided no evidence for the epistatic relationship between LCB hydroxylation by Sur2p and ceramide formation by ceramide synthase, since the latter enzyme seems to readily incorporate either dihydrosphingosine, [evidenced by the formation of A-ceramide by *sur2Δ* mutants (Figure 13, lanes 5 & 7)], or phytosphingosine [evidenced by the incorportion of exogenous phytosphingosine (Wells and Lester, 1983 & Figure 10, lane 8)] into sphingolipid. Therefore the diagram has a branch point at dihydrosphingosine with the two resulting pathways differing only in the order of the ceramide synthase and LCB hydroxylation reaction and converging at the formation of B-ceramide.

The presence of C-ceramide in wild-type cells (Figure 13, lane 3) suggests, as the diagram indicates, Scs7p-mediated fatty acid hydroxylation occurs before the transfer of the phosphoinositol head group from phosphatidylinositol to form IPC-C; because if it occurred after phosphoinositol transfer, C-ceramide would not be formed. However it cannot be ruled out that the source of the C-ceramide seen in wild-type cells is from the turnover of mature sphingolipids. Finally, all ceramides in Figure 13 appear to be substrates for the IPC synthase and all the IPC's appear to be subtrates for the mannosylating enzymes since mature mannosylated forms are present for all of them in Figure 9.

72

Chapter 5

Discussion of Results and Conclusions

Findings of the Sequence Analysis of *SCS7*

As mentioned at the conclusion of Chapter 2, examination of the *SCS7* open

reading frame sequence revealed similarities between Scs7p and two groups of proteins.

The first basis of similarity was the high homology of an N-terminal domain of Scs7p

with the cytochrome b_5 heme-binding fold. Cytochrome b_5 is part of the NADH-depen-

dent microsomal electron transport system that donates reducing equivalents from NADH

through cytochrome b_5 reductase for fatty acyl desaturation, cytochrome P450, and other

reactions, including hydroxylations. It is a small hemoprotein which has a cytoplasmic

domain of about 100 amino acid residues connected to a hydrophobic segment that

anchors it to the membrane (Ozols, 1989). Its N-terminus has a distinctive heme-con-

taining protein fold which is found in a wide variety of complex heme binding redox

proteins such as flavocytochrome b_2 reductase, sulfite oxidase and nitrate reductase

(Lederer, 1994). The discovery of an Scs7p b_5-like domain suggested that SCS7p is a

member of this family of proteins.

Additionally, examination of the *SCS7* sequences revealed the presence of three

histidine-rich motifs that have been found to be in common in all of the membrane fatty

acyl desaturases sequenced to date as well as two bacterial membrane hydroxylases,

alkane hydroxylase (ω-hydroxylase) and xylene monooxygenase (Shanklin *et al.*, 1994).

Hydropathy analysis of these proteins indicates that they contain three or more, long

73

hydrophobic domains of at least 40 residues that would be capable of spanning the membrane twice. A proposed topology for this protein family, based on this analysis is contained in Panel A of the Insert to Figure 17. In all of these proteins there is a consistent positioning between the membrane-spanning domains and the histidine-containing regions. Generally, there is a double-spanning membrane domain near the amino terminus followed by a $HX_{(3\text{ or }4)}H$ sequence and a $HX_{(2\text{ or }3)}HH$ sequence. A second double spanning membrane domain is followed by a second repeat of the $HX_{(2\text{ or }3)}HH$ sequence. The two histidine regions following the first membrane domain are termed Region Ia and Ib and the histidine containing sequence following the second membrane domain is called Region II. The spacing between the first domain and the following histidine sequence is highly conserved, being ten amino acids in the case of Region Ia and between 37 and 40 residues for Region IIa (Figure 17, Panel B of Inset).

Figure 17 shows a proposed topology for Scs7p based on a hydropathy plot of its sequence. The salient characteristics of the fatty acid desaturase/hydroxylase proteins are present. In addition to the cytochrome b_5 heme-binding domain at the N-terminus there are two long hydrophobic domains, capable of spanning the membrane twice, flanking Region Ia and Ib as described. The Scs7p sequence is unique in that it contains a third repeat of the $HX_{(2\text{ or }3)}HH$ motif not present in the others. Therefore the second and third repeats of the $HX_{(2\text{ or }3)}HH$ in SCS7p are labeled Regions IIa and IIb repectively.

All of the proteins sequenced to date with these features are either membrane desaturases or hydroxylases (Shanklin *et al.*, 1994). Thus their presence in the Scs7p sequence coupled with the sphingolipid phenotype data of the previous chapters strongly

74

Figure 17. Proposed Topology of Scs7p. The first 100 base pairs of Scs7p contain a

cytocrome b_5-like heme binding domain. SCS7p is predicted to be a membrane spanning

protein based on a Kyte-Doolittle hydropathy plot of its sequence. It contains two

hydrophobic regions each capable of spanning the membrane twice. It also contains, in

correct positioning to the membrane-spanning domains, the histidine-rich Regions Ia, Ib,

and IIa characteristic of Class III diiron-oxo proteins (see Inset).

Figure 17, Inset.

A) General topology model for Class III diiron-oxo proteins.

B) Comparison of the hydrophobic domain structure of Class III diiron-oxo proteins.

Gray boxes represent hydrophobic domains containing greater than 40 amino acid

residues, capable of spanning the membrane twice. The location of the the His-

containing regions Ia, Ib, and IIa are indicated by solid boxes. All sequences are aligned

relative to the conserved His residues in region Ia. rat, *R norvegicus* Δ^9 desaturase; yeast,

S cerevisiae Δ^9 desaturase; Bnfad3, *B napus* chloroplast Δ^{15} desaturase; Rcfad7, *R*

communis plastid Δ^{15} desaturase; Atfad2, *A thaliana* endoplasmic reticulum Δ^{12}

desaturase; SyndesA, *Synechocystis* sp. strain PCC 6803 Δ^{12} desaturase; Synd6,

Synechocystis sp. strain PCC 6803 Δ^6 desaturase; alkB, *P oleovorans* alkane hydroxylase;

xylM, *P putida* xylene monooxygenase. Reprinted with permission from Biochemistry,

Vol. 33, No. 43, page 12791. Copyright 1994 American Chemical Society.

```
1 MSTNTSKTLEIFSKKTVQEHNTANDCWVTYQNRKIYDVTRFLSEHPGGDESILDY
                  2                           4                              A
                  0                           0                              G
                                                                            K60
GDASLQVEVKHNKNTLLRAAEEDTALYGILYEDELIEYASDSHEHVDSDKMIETID
T                   1            8
E                   0            1            0
F                   0            4            CYTOCHROME B5-FAMILY
D                   0                                DOMAIN
STTFVKELPAEEKLSIATDYSNDYKKHK
                                F
                                L
HRPRH QDVYFDKKFDSRLIQMLLPRNLD
```

```
Y                                                                           3
G                          I A 260                       IIb                6
K 180                      N   F                                            0
G                          S   A         PFMRKLKKY HLEHH YKNYQLGFGVTSWFW
S                          E   T         P    3                             D
A                          P   H         L    4                             E
P                          L   F         K    0                             V
L                          W   L               EYKMKSLPADPGLYTGF
F                          D   L                      3
G                          D   H                      8
N                          F   G   330                0
F                          H   C
L                          F   H   IIa
E                          L   Y
P              Ia          F   L
L                          R   P
T                          H   M
K                          L   D
T                      240 G   D              320
```
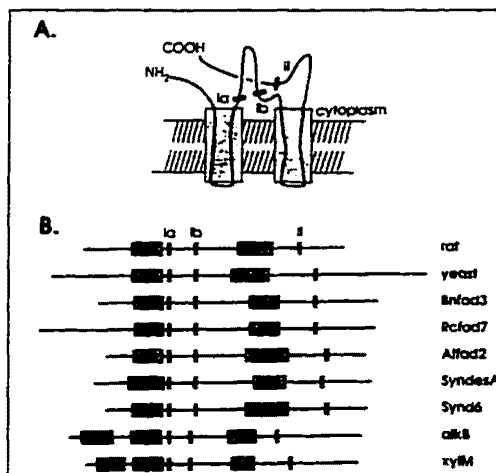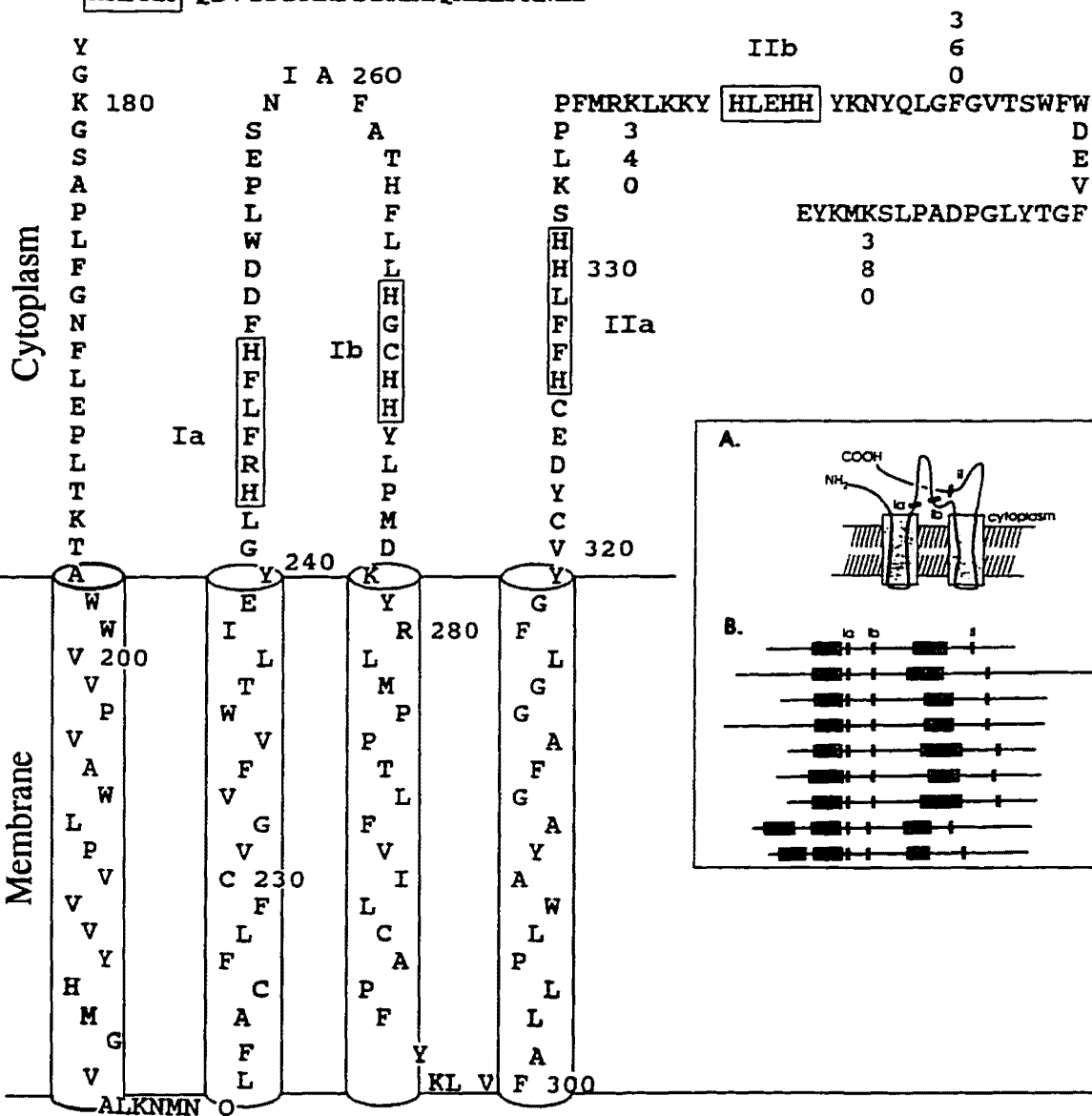
implies that Scs7p is the third hydroxylase member of this group of proteins and that its substrate is ceramide.

The histidine motif-containing desaturase/hydroxylase proteins are thought to comprise a third class of a recently identified family of proteins containing oxo- or hydroxo-bridged diiron clusters at the active site which are used to catalyze diverse reactions requiring O_2 activation chemistry (Shanklin et al., 1994). These clusters always contain two iron atoms connected by either an oxo- or hydroxo-bridging ligand and by at least one or more didentate carboxylate ligands from aspartate or glutamate. The remaining protein-derived iron ligands are histidine-derived N-atoms and either aspartate or glutamate-derived O-atoms that are provided by a protein secondary structural motif consisting of a bundle of four parallel α-helices (Holmes et al., 1991; Nordlund and Eklund, 1993; Rosensweig et al., 1993). Generally, two helices provide ligands for one of the iron atoms and the other two provide the ligands for the other iron atom. The diiron-oxo protein family is divided into three classes. The basis for this classification are differences in the primary structure motifs that provide the iron-binding ligands and structural differences elucidated by X-ray crystallography.

Hemethrin, an O_2 transport protein found in some invertebrates, is the best characterized class I diiron-oxo protein. It contains ligand-providing HX_3E, HX_3H, and HX_4D primary sequence motifs in helices B, C, and D, respectively, of its 4 α-helix bundle (Sanders-Loehr and Loehr, 1979), and its X-ray crystal structure shows that the diiron axis is oriented perpendicular to the long axis of the bundle (Holmes et al., 1991). On the other hand, the class II diiron-oxo proteins contain two copies of a ligand-providing

EX$_2$H primary sequence motif in each of two 4 helix bundle α-helices with an additional aspartate or glutamate-derived carboxylate ligand in each of the remaining two α-helices (Nordlund *et al.*, 1990). Additionally, X-ray crystallography of 2 representative proteins of this subclass, ribonucleotide reductase (R2) and methane monooxygenase (MMOH), has shown that the long axis of the diiron oxo-bridge is oriented parallel to the four helix bundle (Nordlund and Eklund, 1993; Rosenzweig *et al.*, 1993).

The two soluble fatty acid desaturases that have been identified to date are class II diiron-oxo proteins (Fox *et al.*, 1994). All other identified fatty acyl desaturases are membrane bound (Fulco, 1974). Despite these structural differences, as a group the fatty acyl desaturases share a number of biochemical similarities, including a catalytic requirement for iron (Nagai and Bloch, 1968), inhibition by metal chelators (Jaworski and Stumpf, 1974), stereospecificity of the desaturation reaction (Schroepfer and Bloch, 1965) and kinetic isotope effects observed for C-H bond cleavage (Morris, 1970). These similarities suggest a common catalytic mechanism which may include the requirement for a structurally related catalytic site. Although none of the membrane desaturases contain the EX$_2$H primary sequence motifs found in the soluble desaturases, all of them sequenced to date have the above-described HX$_{(2\ or\ 3)}$H and HX$_{(3\ or\ 4)}$HH primary sequence motifs. The similarity of these motifs to those already connected to diiron-oxo proteins makes them appear to be good candidates for ligand providing sequence motifs for an oxo-bridged diiron center. This is the basis for the proposal that membrane acyl desaturases/hydroxylases compose a third class of diiron-oxo proteins.

This hypothesis is supported by mutagenic and spectroscopic studies of stearoyal-CoA desaturase, the best characterized member of this protein class. In the mutagenic study, the finding that the transformed rat stearoyl-CoA gene complements the desaturation deficiency of an *S. cerevisiae ole1Δ* mutant (The yeast stearoyl-CoA desaturase homolog; Stuckey *et al.*, 1990), was used to show that all eight histidines contained in the three motifs are required for catalytic activity (Shanklin *et al.*, 1994). In an optical absorption spectroscopy study (Strittmatter *et al.*, 1974), the purified $\Delta 9$ stearoyl-CoA desaturase showed an absorption spectrum that is consistent with an oxo-bridged diiron center (Sanders-Loehr, 1989).

Recently the existence of a membrane bound, histidine motif-containing diiron-oxo protein class has been further established by demonstration of a diiron oxobridge in alkane ω-hydroxylase (AlkB), a membrane, histidine motif-containing, protein from *Pseudomonas oleovan* (Shanklin *et al.*, 1997). In this study the presence of the diiron-cluster was confirmed by Mössbauer spectroscopy analysis on an enzyme preparation from an AlkB overexpressing *E coli* strain. Additionally it was shown that reoxidation in air of the chemically reduced diiron center was octane substrate dependent and coupled to the production of 1-octanol. This established that catalytic activity was associated with the oxidation state of the oxo-bridged diiron center.

The class II and III diiron-oxo proteins have in common very similar overall reactions. The reaction involves the transfer of 2 electron equivalents from NADH through cytochrome b_5 reductase and cytochrome b_5 to reduce the iron atoms from FeIII to FeII. In the case of the desaturases, enzyme turnover results in the desaturation of the

fatty acid substrate with 4 electron equivalents being transferred to O_2 to form 2 moles of

water per mole of desaturated product:

$$\text{-CH}_2\text{CH}_2\text{-} + \text{NADH} + O_2 + H^+ \rightarrow \text{-CH=CH-} + \text{NAD}^+ + 2H_2O$$
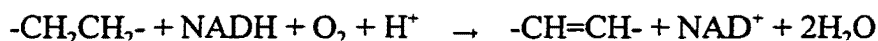
In the case of the hydroxylases, the reaction results in the splitting of the O_2 mole-

cule with one oxygen being incorporated into the substrate as a hydroxyl group and the

other being reduced to water:

$$\text{-CH}_2\text{-} + \text{NADH} + O_2 + H^+ \rightarrow \text{-CHOH-} + \text{NAD}^+ + H_2O$$
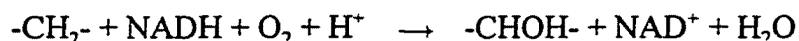
The hydroxylases are functionally classified as mixed function oxidases and as monooxy-

genases. They are "mixed function" because they mediate both fates of O_2-derived oxy-

gen; incorporation into substrate as a hydroxyl group and reduction to water. The term

oxygenase refers to oxidation using O_2 and monooxygenase means that only one oxygen

atom from the O_2 molecule is incorporated into the substrate as opposed to a dioxygenase

where both oxygen atoms are incorporated (Hayaishi, 1974).

It now appears that the general reaction scheme of electron flow from NADH

through cytochrome b_5 reductase and cytochrome b_5 to the diiron-oxo centers is modified

in some of the members of the membrane-bound diiron-oxo proteins. The presence of a

cytochrome b_5 heme-binding domain in the N-terminus of Scs7p quite logically suggests

the possibility that this domain is used by the protein for electron transfer in lieu of free

cytochrome b_5. That this is the case is supported by the discovery that the *S cerevisiae* Δ^9

fatty acid desaturase, Ole1p, also contains a cytochrome b_5 heme-binding domain, how-

ever in this case it is located near the C-terminus (Mitchell and Martin, 1995). In this

study the function of this domain was probed by evaluating the unsaturated fatty acid

80

auxotrophy of *cytb5Δ* and *cytb5Δ ole1Δ* knockout strains. It was discovered that the double knockout, like the *ole1Δ* single knockout, was an unsaturated fatty acid auxo-troph, but the *cytb5Δ* was not. Therefore cytochrome b_5 does not appear to be required for unsaturated fatty acid synthesis in yeast presumably because the electron transfer function of cytochrome b_5 is performed by the C-terminal b_5 heme-binding domain of Ole1p. To gain further evidence, the *ole1Δ* and *ole1Δ cytb5Δ* strains were transformed with plasmids containing either the rat Δ9 fatty acid desaturase gene or the *OLE1* gene and the transformants were evaluated for unsaturated fatty acid auxotrophy. It was found that both genes complement the desaturation deficiency of the *ole1Δ* mutant, but only the *OLE1* gene complements the *cytb5Δ ole1Δ* mutant. Finally, the *ole1Δ* and *ole1Δ cytb5Δ* strains were transformed with an *OLE1* gene construct with a C-terminal deletion of the cytochrome b_5 heme-binding domain. Both transformants failed to grow without unsatu-rated fatty acid supplementation. This result in the *ole1Δ cytb5Δ* strain confirmed that the heme-binding domain of OLE1p is required to support the fatty acid desaturase reac-tion. The result of the *ole1Δ* strain suggests that free cytochrome b_5 cannot not substitute for the heme-binding domain of OLE1p in the desaturase reaction.

An additional putative membrane desaturase with a cytochrome b_5 heme-binding domain has also been cloned recently from cDNA made from the RNA of ripening sun-flower embryos (Sperling *et al.*, 1995). Like Ole1p, the sequence of this protein has a faithful repetition of the hydrophobic and histidine domains of the class III diiron-oxo proteins and a cytochrome b_5 heme-binding domain, however this domain is near the N-terminus. The authors of this study investigated the functionality of this b_5 domain) by

overexpressing a truncated version of the cloned gene expected to code only for a soluble form of the b_5 domain in *E coli*. (Smith *et al.*, 1994). After 19 hours induction in liquid culture supplemented with the heme precursor 5-aminolevulinic acid to increase *de novo* heme synthesis, the transformed cells appeared reddish in color in contrast to control cells containing the expression vector alone indicating that the b_5 domain transformed cells were overexpressing a viable b_5 heme-binding domain. This further supports the hypothesis that the b_5 heme-binding domain of this protein participates in the electron transfer component of the desaturation reaction in the same manner as free cytochrome b_5.

Based on comparisons between the Scs7p sequence and the sequences of other characterized proteins coupled with the demonstrated role for Scs7p in sphingolipid hydroxylation it is reasonable to propose that Scs7p is a membrane ceramide hydroxylase member of the class III diiron-oxo protein family that contains a catalytically active N-terminal cytochrome b_5 heme-binding domain. Although no enzymological studies of Scs7p have been performed, the many shared biochemical features of the diiron-oxo proteins suggest that their mechanisms are similar and therefore some insight into the Scs7p mechanism might be obtained by examining the mechanisms of other studied members of this group. The bacterial methane monooxygenase is probably the best model for this purpose because: 1) it catalyzes the same reaction as Scs7p, the hydroxylation of a saturated carbon; 2) as a class II diiron protein it is closely related biochemically to the class III diiron protein, Scs7p; 3) its mechanism is well characterized.[9] Methane monooxygenase (MMOH), produced by methanotropic bacteria, catalyzes the

---

[9]The discussion of methane monooxygenase is based on the review by Lipscomb, 1994.

hydroxylation of methane, the first reaction in the oxidation of methane to carbon dioxide by these organisms. The reaction proceeds in the manner described above with molecular oxygen being split and each atom being alternatively added as a hydroxyl or reduced to water. The holoenzyme has a quartenary structure that consists of a 245 kDa hydroxylase containing nonheme iron, a 38.4 kDa reductase containing FAD and a $[Fe_2S_2]$ cluster, and a 15.8 kDa protein component with no cofactors called component B. The hydroxylase is a dimer of two $\alpha\beta\gamma$ subunit trimers. The α subunit contains the oxo-bridged diiron center. That this is the site of catalytic activity was confirmed by single turnover experiments which showed that only the reduced, diferrous hydroxylase component produced methanol upon reoxidation in the presence of methane (Fox *et al.*, 1989).

The structure of the active site, oxo-bridged diiron cluster of MMOH, as determined using data from a number of spectroscopic studies and by X-ray crystallography, is shown in Figure 18. The iron atoms are each coordinated by five ligands with a distorted square pyramidal geometry. The ligand residues provided by the two EX_2H sequence motifs characteristic of class II diiron-oxo proteins are Glu_{144} and His_{147} & Glu_{243} and His_{246}. The two additional carboxylate ligands are provided by Glu_{114} and Asp_{209}. A hydrogen bond exists between Asp_{242} and His_{147}; such bonds are also a common feature of these proteins. The evidence seems to indicate that the bridge oxygen is protonated.

Any proposed mechanism for MMOH must take into account two important features of the MMOH reaction. The first is that the reaction proceeds from the diferrous enzyme since only this form had catalytic activity in the single turnover experiment. Secondly, the only type of reagent known to attack unactivated hydrocarbons in biology is
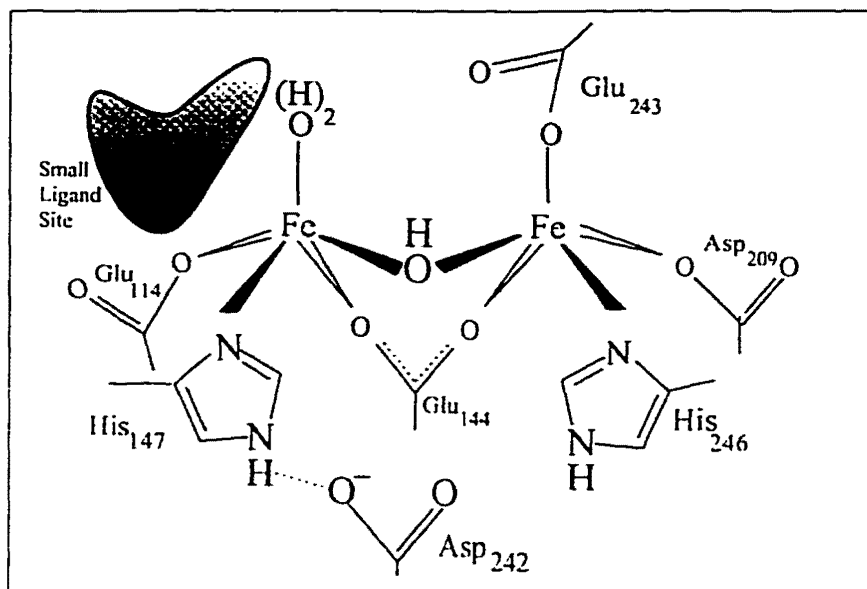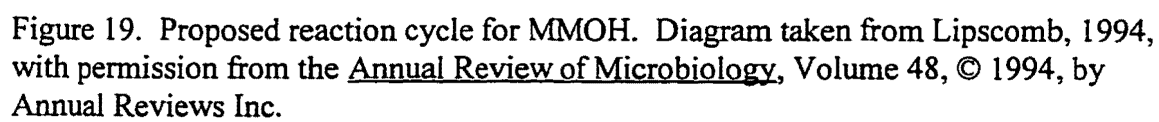
Figure 18. Hypothetical structure of the active-site, oxygen-bridged diron cluster of MMOH. Diagram taken from Lipscomb, 1994, with permission from the Annual Review of Microbiology, Volume 48, © 1994, by Annual Reviews Inc.

a metal-bound oxene, such as the highly reactive porphyrin π cation radical Fe(IV)=O

(oxene) species formed in cytochrome P450 catalyzed hydroxylations. Thus a mechan-

ism that invokes the formation/utilization of such a species would be most consistent with

what is known about the chemistry of these reactions. Figure 19 is a diagram of the pro-

posed mechanism of MMOH that encompasses these observations. The reaction pro-

ceeds by the reduction of diferric MMOH to the diferrous state by NADH. The binding

of O_2 to one or both of the iron atoms leads to heterolytic O-O bond cleavage to release

water. The resulting diiron, dioxygen complex would achieve its most stable resonance

form by the transfer of one electron from each iron to the O_2 derived oxygen to complete

its valence shell. This would form a [Fe(IV)●Fe(IV)]=O species, equivalent to the P-450

oxene species, that would be a powerful oxidizing agent of the type required to attack

methane. This oxidant is proposed to abstract a hydrogen atom from the substrate to form

a substrate radical and the iron-bound equivalent of a hydroxyl radical. Radical

recombination, or rebound, would yield the product alcohol and recycle the enzyme to

the diferric state.

The model suggests that there are two phases in the reaction, an oxygen activation

phase followed by a reaction phase wherein the actual chemistry of hydrocarbon oxida-

tion occurs. If this is the case, two reducing equivalents and O_2 could be provided in the

form of H_2O_2 to produce the activated oxene which could react with methane in the nor-

mal way. The existence of this putative peroxide shunt has been confirmed by recovering

methanol from the anaerobically-conducted reaction in the presence of H_2O_2 in lieu of

NADH, reductase and component B (Andersson *et al.*, 1991; Froland *et al.*, 1992).

Figure 19. Proposed reaction cycle for MMOH. Diagram taken from Lipscomb, 1994, with permission from the Annual Review of Microbiology, Volume 48, © 1994, by Annual Reviews Inc.

A key component of the mechanism is the existence of a free substrate radical as a reaction intermediate. Evidence for the existence of this intermediate was obtained by offering the enzyme chiral ethane (ethane with stereospecific placement of tritium and deuterium on one of the carbons). The logic of the experiment was that if a free radical does form, the subsequent hydroxylation can be on either side of the planar radical intermediate and the reaction products will be a racemic mixture of both retained and inverted stereospecificities. Conversely if the substrate intermediate remains bound through the course of the reaction, hydroxylation should occur consistently on the same side of the intermediate with respect to the side of proton extraction, resulting in either complete stereospecific retention or inversion in the reaction products. The former outcome was observed when this experiment was conducted confirming the presence of a free radical intermediate during the reaction course (Priestley *et al.*, 1992).

By these and other studies the two phase, methyl radical intermediate reaction mechanism for MMOH has been established. Considering that Scs7p catalyzes the same basic reaction as MMOH, and the many structural and biochemical similarities that Scs7p is known and expected to have by virtue of its membership in the diiron-oxo protein family, it is likely that the mechanism of Scs7p proceeds in a very similar fashion.

Biological Significance of Fatty Acid Hydroxylation

The state of knowledge concerning VLCFA hydroxylation in sphingolipids very much mirrors the situation for sphingolipids in general described in Chapter One. Despite some success in understanding, there seems to be much more that is not under-

stood. That VLCFA hydroxylation is important in sphingolipid function is suggested by several biochemical lines of evidence.

The most completely studied of these lines of evidence is the hydroxylation of lignoceric (C_{24}) acid to cerebronic acid in mammalian brain. Approximately 60% of brain cerebroside (1-β galactosylceramide), an abundant and indispensable myelin component, is hydroxylated on the α carbon of the VLCFA moiety. The α hydroxylation activity from rat brain has been isolated and extensively characterized (Singh and Kishimoto, 1979) and subsequently found to be very closely associated with the nerve myelination process. No α hydroxylase activity can be detected in immature rat brain before approximately 9 days of age when myelination begins. The activity increases in concert with myelination with both processes peaking at 21 days of age and then declining rapidly. Additionally two mutant mouse blood lines (Quaking and Jimpy) with autosomal recessive myelination deficiencies show decreases in α hydroxylation activity proportionate to the degree of neuropathy. The brains of newborn, myelin-deficient, Quaking mice have approximately 40% of the hydroxylation activity of their normal control littermates at all ages examined. Likewise, Jimpy mice, who have a much more severe myelination deficiency and do not survive beyond the 10 day myelination period, have only a few percent of normal hydroxylation activity (Murad and Kishimoto, 1975). In contrast, other neuropathy mutants such as Ducky, Weaver and Wabble-lethal show neither myelination deficiency nor decreased hydroxylation activity. Finally, the time window of the myelination process can adjusted by experimental alteration of thyroid status. Hyperthyroidism speeds up the time table while hypothyroidism retards it. When

the myelination window was advanced or retarded in newborn mice by the administration

of either triiodothyronine or methimazole respectively, the α-hydroxylation activity was

again shown to correlate exactly with the altered myelination (Murad *et al.* 1976).

As mentioned above, the α-hydroxylation system in rat brain is well characterized

and it is interesting to compare it to the yeast system. First of all α-hydroxylation is

closely tied to ceramide synthesis in both systems. Scs7p appears to hydroxylate the

VLCFA moiety after its attachment to phytosphingosine to form ceramide. An analogous

finding in rat brain is that no free cerebronic acid is ever recovered in the α-hydroxylase

assay. The hydroxylated product is only recovered as ceramide or cerebroside (Singh and

Kishimoto, 1979). However the reaction system does not hydroxylate exogenous cera-

mide (Hoshi and Kishimoto, 1973). This coupled with the finding that cerebronyl-CoA is

a substrate of ceramide synthesis (Ullman and Radin, 1972) has led to the speculation that

the actual substrate for the hydroxylation reaction is some type of activated lignoceric

acid as opposed to the free form.

In the previous chapter it was noted that the presence of hydroxylated ceramide

suggested that VLCFA hydroxylation occurs prior to head group assembly. An analo-

gous situation seems to exist in the rat brain system. When [1-^{14}C]lignoceric acid and

either [6-^{3}H]psychosine, (galactosyldihydrosphingosine), or [3-^{3}H]sphingosine were

added to an *in vitro* VLCFA hydroxylation assay, both the hydroxyceramide and the

hydroxycerebroside recovered from the reaction with labeled sphingosine contained both

^{14}C and ^{3}H in a 0.54 to 1 ratio, whereas no ^{3}H was recovered in the products of the reac-

tion with added labeled psychosine. This indicated that the galactosyl moiety is added

after completion of ceramide synthesis, since if the galactosyl moiety could be present on the sphingosine base prior to ceramide synthesis, recovery of ^3H would be expected in the presence of labeled psychosine. Additionally the identical label ratios of hydroxyceramides and hydroxycerebrosides suggests that the former is the sole source of the latter.[10]

There are also mechanistic parallels between the diiron-oxo hydroxylases and the rat brain α-hydroxylase system. The rat system is totally inhibited in a nitrogen atmosphere, suggesting that O_2 is required. Also there is a requirement for pyrimidine nucleotide, (Hoshi and Kishimoto, 1973) and, like the diiron-oxo proteins, the reaction is inhibited by cyanide, a microsomal electron transport inhibitor, but not by the cytochrome P-450 inhibitor, carbon monoxide. The reaction pathway for the rat brain lignoceroyl-α-hydroxylase was elucidated by a clever experiment that distinguished among 3 alternatives: 1) direct replacement of a hydrogen atom with a hydroxyl group on the α-methylene carbon, 2) dehydrogenation to desaturate the C_2-C_3 atoms followed by the addition of water across the double bond, 3) replacement of both H-atoms at C_2 with a keto group followed by reduction. Racemic mixtures of both [2-^3H] and [3-^3H] lignoceric acid were assayed and the reaction products were counted. The result obtained was that 50% of the label was lost from the product of the [2-^3H] lignoceric acid labeled reaction while all of the label was recovered in the [3-^3H] lignoceric acid labeled reaction. This indicates that

---

10

It is formally possible that the same results of this experiment could have been obtained if the reaction sequence had been ceramide synthesis followed by galactosylation, hydroxylation and cleavage of the galactose. This possibility was ruled out by additional purification of the enzyme preparation to remove UDP-galactose and showing that this preparation produced only hydroxyceramides and that the hydroxyceramide, hydroxycerebroside, reaction product mixture was restored by adding UDPgalactose.

pathway one is followed in the reaction course because it is the only one predicted to give this outcome. If the reaction followed pathway two, 50% of the label would have been lost in each reaction, whereas if pathway three was followed, all of the label would have been lost from the [2-^{3}H] lignoceric acid labeled reaction. Thus the rat brain α-hydroxy-lation reaction proceeds by direct replacement of a C_2 hydrogen atom by a hydroxyl group which is the same overall pathway followed by the diiron-oxo hydroxylases.

Myelin has a high concentration of both hydroxylated and unhydroxylated cerebroside which is undoubtedly central for its function. As discussed in Chapter One, increasing sphingolipid content in membranes generally results in increased rigidity due primarily to hydrophobic interactions of the fully saturated acyl chains and a presumed network of hydrogen bonding made possible by the presence of several proton donating and accepting groups in the ceramide backbone. Differential scanning calorimetry (DSC) studies have indicated that such hydrogen bonding networks between cerebroside (galac-tosylceramide) molecules may exist in solution (Ruocco, *et al.*, 1981). DSC detects lipid phase transitions by measuring relative heat capacity over a range of temperatures. These studies detected a phase transition that suggested cerebroside can exist in a metastable phase in addition to the stable gel and liquid crystal phases of phospholipids. X-ray diffraction comparison of the stable and metastable crystals indicated that the stable form (termed polymorph II) was more hydrated than the metastable form (termed polymorph I). It was therefore surmised that polymorph I represents a state wherein the cerebroside molecules are extensively involved in hydrogen bonding, similar to the situation seen in the X-ray diffraction study, and that poylmorph II represent a state wherein these inter-

molecular hydrogen bonds are disrupted and replaced by hydrogen bonds to water. Further evidence for this model is a DSC study of cerebroside in the presence of ethylene glycol and dimethylsulfoxide, two compounds that disrupt the hydrogen-bonded structure of water, that showed the elimination of metastable phase behavior presumably due to the disruption of intermolecular hydrogen bonding (Curatolo, 1985). Additionally, metastable phase behavior is also seen in certain sphingomyelins which possess hydrogen-bonding capability via the backbone amide (Barenholz et al., 1976) and in synthetic (carbamyloxy)phosphatidylcholine, which possesses hydrogen-bonding capability via the carbamyloxy group (R-NH-COO-; Curatolo et al., 1982).

With an eye toward understanding sphingolipid VLCFA α-hydroxylation, it is interesting to investigate the effect of α-hydroxylation on cerebroside metastable phase behavior. In this case, DSC analysis of HPLC fractionated 2-hydroxy fatty acid cerebrosides (HFA-CER) from bovine brain differed from their nonhydroxylated counterparts (NFA-CER) in two significant ways. First the transition temperature for the liquid crystal phase (T_M) was 12° C lower for HFA-CER (71° C) than for saturated NFA-CER (83° C). Secondly, the metastable to stable phase transition occurred much more readily for NFA-CER than for HFA-CER (Curatolo and Jungalwala, 1985)[11]. An analogous result was obtained in a study of the physical properties of hydroxylated and unhydroxylated ceramides by DSC and X-ray diffraction. Hydroxyceramides exhibited a simple phase beha-

----

[11]Initially it was thought that HFA-CER did not undergo metastable to stable phase transition at all (Curatolo, 1982). However on prolonged storage at low temperature conversion of some HFA-CERs did occur. Thus the barrier between metastable and stable phases in HFA-CER is kinetic rather than absolute.

vior that involved the interconversion of bilayer gel and hexagonal melted chain phases whereas unhydroxylated ceramide exhibited a more complex polymorphic phase behavior, involving two distinguishable gel phases in addition to the melted chain phase (Shah *et al.*, 1995).

As described above, this metastable phase behavior of sphingolipids is thought to be due to intra and intermolecular hydrogen bonding and the studies indicate that α-hydroxylation promotes this hydrogen bonding by stabilizing the metastable phase state. An intra, intermolecular hydrogen-bonding network in membranes would be expected to increase lipid order and membrane rigidity. These effects do seem to be characteristic of biological membranes containing these species.

The increased rigidity conferred by the high cerebroside content of myelin membrane ($\sim$24%; 60% of which is α-hydroxylated) is thought to decrease ion permeability of the membrane and thus promote its role as an insulator. This model is also consistent with the high cerebroside content of the brush border of the intestinal epithelium where mechanical strength and the maintenance of high ionic gradients are required (Pascher, 1976). The intestinal membrane also has an increased level of hydroxy ceramide, as do the membranes of kidney (Karlsson, 1977) and the stratum corneum of skin (Elias *et al.*, 1979). Exactly how α-hydroxylation stabilizes the hydrogen bond network is not known. The added hydroxyl group would certainly be expected to participate in hydrogen bonding, which in turn would be expected to strengthen the network. Nonetheless some physical properties of hydroxy versus unhydroxysphingolipids suggest a destabilizing effect for hydroxylation. For instance the greater rigidity and intermolecular attraction

caused by the additional hydrogen bonding should tend to raise the melting temperature, but as stated above, the T_M for hydroxylated cerebroside was found to be 12° C lower than the unhydroxylated form. Additionally, the Raman spectral parameters for the gel phase of unhydroxylated cerebroside are consistent with it being more highly ordered (Bunow and Levin, 1980). The reason for this destabilizing effect of hydroxylation also is not known but could be stearic interference with the acyl chain packing (Curatolo and Jungalwala, 1985). Alternatively, it has been proposed that the lower T_M of hydroxylated cerebroside may be due to a greater stabilization of the liquid crystal state relative to the gel state (Boggs, 1987).

Whatever their exact physical causes, the hydrogen-bonding network and α-hydroxylation-mediated destabilization of sphingolipids appear to be counterbalancing influences on membrane fluidity. In this light it is interesting to note that because of its high T_M, a membrane of pure cerebroside would be in the gel state at mammalian body temperature, which is generally not consistent with a functioning membrane (Curatolo, 1987b). It could be that α-hydroxylation-mediated destabilization of cerebroside bilayer structure is one of the moderating factors of rigidity in cerebroside containing membranes. On the other hand, lipids whose aliphatic chains have been altered from the saturated state generally confer a profoundly increased membrane fluidity compared to their saturated counterparts. For instance the introduction of a single double bond into the sn-2 position of phosphatidylcholine reduces its T_M 52° C from 49° C to -3° C (Curatolo and Jungalwala, 1985). In contrast, as stated above, the T_M of cerebroside falls only 11° C upon hydroxylation of the sn-2 position of the acyl chain.

Also to be determined is the extent to which a hydrogen-bonding network would exist and influence physical properties in an intact sphingolipid-containing membrane. Some investigations into this question have been undertaken. In an NMR study of phosphatidylcholine bilayers with 10% perdeuterated hydroxylated or unhydroxylated galactosylceramide, the results were mixed depending on membrane phase. There was a slight increase in motional freedom and / or conformational disorder of the hydroxylated versus unhydroxylated form in gel phase membranes, whereas in fluid membranes there was a slight increase in the order profile of the hydroxylated species near the membrane surface. The effect was largest for the D stereoisomer of galactosylceramide (Singh *et al.*, 1992). The liquid phase result was also obtained in a subsequent ^{2}H-NMR study with unsonicated multilamellar liposomes of phosphatidyl-choline with 8% galactosylceramide (Morrow *et al.*, 1995). The authors concluded that although there is some evidence that the hydroxyl group leads to strengthening of interlipid interaction near the membrane surface, the fluid membrane area requirements for glycosphingolipids with saturated fatty acids are not strongly influenced by the nature of that fatty acid when the glycosphingolipid is a minor component.

With respect to the influence of α-hydroxylation on membrane properties, Curatolo has proposed, that in addition to the presumed rigidifying effect, the maintenance of the membrane in a dehydrated state may be an important property. Since breakdown of the hydrogen-bonding network results in the formation of hydrogen bonds between the sphingolipid substituents and solvent water, network stabilization by α-

hydroxylation may prevent a membrane-destructive hydration-reyhydration cycle (Curatolo, 1982).

Although the evidence for these effects is clearly incomplete, two observations in living cells are consistent with the possibility that α-hydroxylation of sphingolipids is important in the maintenance of cell membranes. Firstly, in a quantitative analysis of the surface sphingolipids of the ciliated protozoan, *Tetrahymena pyriformis*, it was observed that the ratio of nonhydroxylated to hydroxylated ceramide, varied from 99.3:0.6 to 13:87 in cells grown at 15° C and 39° respectively (Kaya *et al.*, 1984). Although the specific purpose for the shift in membrane ceramide composition has not been established in this case, it certainly seems reasonable, in light of the above discussion, that this rather dramatic shift in ceramide hydroxylation state could be a cellular adjustment of membrane composition in order to maintain a certain physical state in response to the alteration in temperature. Higher temperature increases membrane fluidity and the expected response would be an alteration in lipid composition that would increase T_M. As discussed above, α-hydroxylation of cerebroside decreases the T_M of that species. However α-hydroxylation of cerebroside sulfate significantly increases the phase transition temperature (Boggs *et al.*, 1984). Therefore it appears that depending on overall molecular structure α-hydroxylation of the acyl moiety of sphingolipids can either increase or decrease membrane fluidity.

The second observation is the increased growth, relative to wild-type, of *scs7Δ* cells at 14° C reported in Chapter 3 of this work. Its been shown here that SCS7p is the hydroxylase that mediates the acyl α-hydroxylation of yeast IPCs and that in *scs7Δ*

mutants hydroxylated IPCs are not made. Thus in a manner directly analogous to the situation seen in *Tetrahymena pyriformis*, the absence of hydroxylated sphingolipids in *scs7Δ* cell membranes could be the cause of an increased membrane fluidity relative to wild-type cell membranes that would cause the mutants to grow better at the lower temperature.

Chapter One included a discussion of sphingolipid involvement in metabolic regulation, including protein trafficking. There is evidence that sphingolipid α-hydroxylation has a role in this process as well. This evidence was obtained by means of an apical / basolateral transport assay that uses exogenous radiolabeled ceramides with short (C_6) acyl moieties as probes. These ceramides have been shown to cross the plasma membrane and to be incorporated into the full complement of sphingolipids in human intestine Caco-2 cells and canine kidney MDCK cells. The relative amounts of the labeled products can be differentially recovered from the basolateral and apical surfaces of these cells (van't Hof *et al*, 1990). Using this assay with unhydroxylated and hydroxylated probes, it was shown that the hydroxylated glucosyl- and galactosyl-ceramides were found to be six-fold more abundant on the basolateral membrane surface of Caco-2 cells than on the apical surface relative to the unhydroxylated forms (van der Bijl, *et al.*, 1996). This was in sharp contrast to the results obtained in MDCK cells where glucosylceramide and galactosylceramide were each preferentially sorted to the apical and basolateral surfaces respectively, irregardless of hydroxylation state. The exact proper interpretation of these results cannot be made at this point since not enough is known about the determinants of vesicle trafficking. But based on the results, it does

appear that vesicular sorting to the apical and basolateral surfaces is a complex, cell specific process in which sphingolipid hydroxylation may have a determinant role.

Finally, based on the work of this laboratory, there seems to be a connection between sphingolipid hydroxylation and Ca^{2+} homeostasis. The $csg2\Delta$ mutants have a defect in Ca^{2+} homeostasis that causes them to be sensitive to Ca^{2+} and overaccumulate Ca^{2+} in a nonvacuolar pool (Beeler et al., 1994). They also have as their primary defect an inability to mannosylate sphingolipids that leads to IPC-C overaccumulation and their Ca^{2+} sensitivity is suppressed by mutants of the biosynthetic pathway upstream of the mannosylation step (Zhao, et al., 1994). This points to IPC-C overaccumulation as the cause of the Ca^{2+} sensitivity, as opposed to the failure to mannosylate sphingolipids, because decreasing the pathway flux upstream of mannosylation would be expected to remediate IPC-C overaccumulation, but would not have any effect on the mannosylation defect.

This work has shown that two mutations that suppress $csg2\Delta$ Ca^{2+} sensitivity, sur2 and scs7, are in genes required for sphingolipid LCB and VLCFA hydroxylation. Scs7Δ csg2Δ cells overaccumulate the VLCFA unhydroxylated form of IPC, (IPC-B), and sur2Δ csg2Δ overaccumulate the LCB unhydroxylated form of IPC (IPC-B'). Thus it would seem that either the dihydroxylated IPC-C or C-ceramide is toxic to the cell in the presence of elevated Ca^{2+}.

It is interesting to speculate on the nature of the connection between Ca^{2+} homeostasis and IPC-C / C-ceramide levels. In light of the involvement of both sphingolipids and Ca^{2+} in signal transduction it tempting to speculate that a critical Ca^{2+}

signaling pathway may be perturbed by IPC / C-ceramide imbalance. Alternatively the unmannosylated, dihydroxylated IPC-C may confer an unsuitable physical property to the plasma membrane which might be lethal in the presence of high calcium. Answering these questions will be a goal of future studies with the *csg* and *scs* cell lines and will undoubtedly provide key pieces to the puzzle of sphingolipid metabolism.

Appendix

Characterization of the Species with Short Chain FAME Mobility from Sphingolipid Extracts

The B panels of Figure 11 (lanes 1-4) and Figure 15 (lanes 6-10) show the TLC mobility of hydroxylated and nonhydroxylated FAME standards. It demonstrates the TLC system used in this study provides good separation based on hydroxylation state but not on fatty acid chain length. The analyses of the FAME extracts was complicated by the presence of a species with C_{16} FAME mobility in all sphingolipid and purified ceramide samples. The nature of this material is puzzling. It could be some type of contamination product of the acid hydrolysis or it could be C_{16} fatty acid in the form of ceramide, diacylglycerol or free fatty acid present in the lipid extracts prior to acid hydrolysis. In regard to the former possibility, the species is absent from the FAME extract of acid hydrolyzed TIV bovine ceramide (Figure 15, panel B, lane 2). Thus it seems that the material is not a product of the acid hydrolysis but is something brought along in the yeast extracts. The presence of material with short chain FAME mobility from the acid hydrolyzed TIII bovine ceramide standards (lane 1) does not contradict this conclusion because these ceramides contain both unhydroxlated stearic and nervonic acids as their fatty acid moiety, therefore the presence of a spot with short unhydroxylated FAME mobility is expected.

The FAMEs are chromatographed in petroleum ether:diethylether (17:3). In this system, the charged free fatty acids remain at the origin. However, as shown in Figure 20, if one part acetic acid is added to this system, free fatty acids are protonated and run

Figure 20. Free fatty acid analysis of purified ceramide extracts. TIII and TIV bovine ceramides (4 μg; lanes 1 & 2), palmitic and tetracosanoic acids, (10 μg; lanes 3 & 4), and both untreated (lane 6) and KOH treated (according to Materials and Methods, Chapter 3) purified C-ceramide from approximately 10 OD_{600} wild-type cells were spotted to a TLC plate. The plate was developed with petroleum ether:diethylether:acetic acid (17:3:1).

101

with very similar mobilities as their methylester counterparts when chromatographed without acetic acid (Figure 15, panel B, lanes 3 & 4). In order to investigate whether short chain fatty acid was contained in the purified ceramide extracts, both un- (lane 6) and KOH- (lane 5) treated C-ceramide extract was run on this system. As shown, both samples contain approximately equal amounts of a species with short chain fatty acid mobility. These results suggest that there is short chain fatty acid in the purified ceramide extracts. This material appears to be in the form of free fatty acid and not diacylglycerol because its presence does not depend on KOH hydrolysis.

BIBLIOGRAPHY

Abeijon, C., Yanagisawa, K., Mandon, E. C., Hausler, A., Moreman, K., Hirschberg, C. B., Robbin, P. W. 1993. Guanosine diphosphatase is required for protein and sphingolipid glycosylation in the Golgi lumen of *Saccharomyces cerevisiae*. Journal of Cell Biology. 122:307-323.

Andersson, K. K. Froland, W. A., Lee, S-K, and Lipscomb, J. D. 1991. Dioxygen independent oxygenation of hydrocarbons by methane monooxygenase hydroxylase component. New Journal of Chemistry. 15:411-415.

Ballou, L. R., Chao, C. P., Holness, M. A., Barker, S. C. and Raghow, R. 1992. Interleukin-1-mediated PGE$_2$ production and sphingomyelin metabolism. The Journal of Biological Chemistry. 267:20044-20050.

Barenholz, Y., Suurjuusk, J., Mountcastle, D., Thompson, T. E., and Biltonen, R.L. 1976. A calorimetric study of the thermotropic behavior of aqueous dispersions of natural and synthetic sphingomyelins. Biochemistry. 15:2441-2447.

Becker, G. W. and Lester, R. L. 1980. Biosynthesis of phosphoinositol-containing sphingolipids from phosphatidlyinositol by a membrane preparation from *Saccharomyces cerevisiae*. Journal of Bacteriology. 142:747-754.

Beeler, T., Gable, K., Zao, C. and Dunn, T. 1994. A novel protein, CSG2p, is required for Ca^{2+} regulation in *Saccharomyces cerevisiae*. The Journal of Biological Chemistry. 269:7279-7284.

Ben-Av, P. and Liscovitch, M. 1989. Phospolipase D activation by the mitogens platelet-derived growth factor and 12-O-tetradecanoylphorbol 13-acetate in NIH 3t3 cells. FEBS Letters. 259:64-66.

Berninsone, P., Miret, J. J., and Hirschberg, C. B. 1994. The guanosine diphosphatase is required for transport of GDP-mannose into the lumen of *Saccharomyces cerevisisae* Golgi vessicles. The Journal of Biological Chemistry. 269:207-211.

Bertello, L. E., Goncalvez, M.F., Colli, W., and deLederkremer, R. M. 1995. Structural analysis of inositol phospholipids from *Trypanosoma cruzi* epimastigote forms. Biochemistry Journal. 310:255-261.

Bielawska, A., Linardic, C. M., and Hannun, Y. A. 1992. Ceramide-mediated biology. The Journal of Biological Chemistry. 267:18493-18497.

Bielawska, A., Crane H. M., Liotta, D., Obeid , L. M. and Hannun,Y. A. 1993. Selectivity of ceramide-mediated biology. The Journal of Biological Chemistry. 268: 26226-26232.

Boeke, J. D., LaCroute, F. and Fink, G. R. 1984. A positive selection for mutants lacking orotidine-5'-phosphate decarboxylase activity in yeast: 5-fluoro-orotic acid. Molecular and General Genetics. 197:345-346.

Boggs, J. M., Koshy, K. M., and Rangaraj, G., 1984. Effect of fatty acid chain length, fatty acid hydroxylation, and various cations on phase behavior of synthetic cerebroside sulfate. Chemistry and Physics of Lipids. 36:65-89.

Boggs, J. M. 1986. Lipid intermolecular hydrogen bonding: influence on structural organization and membrane function. Biochimica et Biophysica Acta. 906:353-404.

Borochov, H., Zahler, P., Wilbrandt, W. and Shinitzki, M. The effect of phosphatidylcholine to sphingomyelin ratio on the dynamic properties of sheep erythrocyte membrane. Biochemica et Biophysica Acta. 470:382-388.

Braun, P. E., Morrell, P., and Radin, N. S. 1970. Synthesis of C_{18}- and C_{20}-dihydrosphingosines, ketodihydrosphingosines, and ceramides by microsomal preparations from mouse brain. The Journal of Biological Chemistry. 245:335-341.

Brown, D. A., and Rose J. K. 1992. Sorting of GPI-anchored proteins to glycolipid-enriched membrane subdomains during transport to the apical cell surface. Cell. 68:533-544.

Bunow, M. R. and Levin, I. W. 1980. Molecular conformations of cerebrosides in bilayers determined by Raman spectroscopy. Biophysical Journal. 32:1007-1022.

Cooper, R. A., Durocher, J. R., and Leslie, M. H. 1977. Decreased fluidity of red cell membrane lipids in abetalipoproteinemia. Journal of Clinical Investigation. 60:115-121.

Crouzet, M., Urdaci, M., Dulau, L., and Aigle, M. 1991. Yeast mutant affected for viability upon nutrient starvation: characterization and cloning of the RVS161 gene. Yeast. 7:727-743.

104

Curatolo, W. 1982. Thermal behavior of fractionated and unfractionated bovine brain cerebrosides. Biochemistry. 21:1761-1764.

Curatolo, W., Bali, A., and Gupta, C. M., 1982. Metastable phase behavior of a sphingolipid analogue. Biochica and Biophysica Acta. 690:89-94.

Curatolo, W. 1985. The effects of ethylene glycol and dimethyl sulfoxide on cerebroside metastability. Biochimica et Biophysica Acta. 817:134-138.

Curatolo, W. and Jungalwala, F. B. 1985. Phase behavior of galactocerebrosides from bovine brain. Biochemistry. 24:6608-6613.

Curatolo, W. 1987a. The physcial properties of glycolipids. Biochimica et Biophysica Acta. 906:111-136.

Curatolo, W. 1987b. Glycolipid Function. Biochimica et Biophysica Acta. 906:137-160.

Desfarges, L., Durrens, P., Juguelin, H., Cassagne, C., Bonneu, M., Aigle, M. Yeast mutants affected in viability upon starvation have a modified phospholipid composition. Yeast. 9:267-277.

Dobrowski, R. T. and Hannun, Y. A. 1992. Ceramide stimulates a cytosolic protein phosphatase. The Journal of Biological Chemistry. 267:5048-5051.

Elias, P. M., Brown, B. E., Fritsche, P., Goerke, J., Gray, P. M., and White, R. J. 1979. Localization and composition of lipids in neonatal mouse stratum granulosum and stratum corneum. Journal of Investigative Dermatology. 73:339-348.

Fishbein, J. D., Dobrowski,R. T., Bielawska, A., Garrett, S., and Hannun, Y. A. 1993. Ceramide mediated growth inhibition and CAPP are conserved in *Saccharomyces cerevisiae*. The Journal of Biological Chemistry. 268:9255-9261.

Froland, W. A., Andersson, K.K., Lee S-K., Liu, Y., and Lipscomb, J. D. 1992. Methane monooxygenase component B and reductase alter the regioselectivity of the hydroxylase component-catalyzed reactions. The Journal of Biological Chemistry. 267:17588-17597.

Fox, B. G., Foland, W. A., Dege, J., and Lipscomb, J. D. 1989. Methane monooxygenase from *Methylosinus trichosporium* OB3b: purification and properties of a three component system with high specific activity from a type II methanotroph. The Journal of Biological Chemistry. 264:10023-1033.

Fox, B. G., Shanklin, J., Jingyuan A., Loehr, T. M., and Sanders-Loehr, J. 1994. Resonance raman evidence for an Fe-O-Fe center in stearoyl-ACP desaturase. Primary sequence identity with other diiron-oxo proteins. Biochemistry. 33:12776-12786.

Fulco, A. J. 1974. Metabolic alterations of fatty acids. Annual Review of Biochemistry. 43:215-241.

Gietz, R. D., Schiestl, R. H., Willems, A. R. and Woods, R. A. 1995. Studies on the transformation of intact yeast cells by LiAc/SS-DNA/PEG procedure. Yeast. 11:355-360.

Goldkorn, T., Dressler, K. A., Muindi, J., Radin, N. S., Mendelsohn, J., Menaldino, D., Liotta, D., and Kolesnick, R. N. 1991. Ceramide stimulates epidermal growth factor receptor phosphorylation in A431 human epidermoid carcinoma cells. The Journal of Biological Chemistry. 266:16092-16097.

Hannon, Y. A. and Bell, R. M. 1989. Functions of sphingolipids and sphingolipid breakdown products in cellular regulation. Science. 243:500-507.

Hannon, Y. A. 1994. The sphingomyelin cycle and the second messenger function of ceramide. The Journal of Biological Chemistry. 269:3125-3128.

Hayaishi, O. 1974. General Properties and Biological Functions of Oxygenases. Molecular Mechanisms of Oxygen Activation. pp 1-28. Academic Press:New York.

Hechtberger, P., Zinser, E., Paltauf, F. and Daum, G. 1994. Assembly of sphingolipids into membranes of the yeast Saccharomyces cerevisiae. Biological Membranes: Structure, Biogenesis and Dynamics. Op den Kamp, J.A.F., Ed. NATO ASI Series,VolH82:23-31. Berlin Heidelberg:Springer-Verlag.

Hechtberger, P. 1994. Characterization, quantification and subcellular localization of inositol-containing sphingolipids of the yeast, Saccharomyces cerevisiae. European Journal of Biochemistry. 235:641-649.

Hechtberger, P. and Daum, G. 1995. Intracellular transport of inositol-containing sphingolipids in the yeast Saccharomyces cerevisiae. FEBS Letters. 367:201-204.

Hinnen, A., Hicks, J. B., and Fink, G. B. 1978. Transformation of Yeast. Proceedings of the National Academy of Sciences USA. 75:1929-1933.

Holm, C., Meeks-Wagner, D., Fangman, W. and Botstein, D. 1986. A rapid, efficient method for isolating DNA from Yeast. Gene. 42:169-173.

Holmes, D. S. and Quigley, M. 1981. A rapid boiling method for the preparation of bacterial plasmids. Analytical Biochemistry. 114:193-197.

Holmes, M. A., Le Trong, I., Turley, S., Sieker, L. C., and Stenkamp, R.E. 1991. Structures of deoxy and oxy hemerythrin at 2.0 Å resolution. Journal of Molecular Biology. 218:583-593.

Horvath, A., Sütterlin, C., Manning-Krieg, U., Movva, N. R. and Riezman, H. 1994. Ceramide synthesis enhances transport of GPI-anchored proteins to the Golgi apparatus in yeast. Cell. 550:3687-3695.

Hung, C-Y., Ko, Y-G., and Thompson, G.A. 1995. Temperature-induced alteration of inositolphosphorylceramides in the putative glycosylated lipid precursors of *Tetrahymena mimbres* glycosylphosphatidylinositol-anchored proteins. Biochemistry Journal. 307:107-113.

Imokawa, G., Abe, A., Jin, K., Higaki, Y., Kawashima, and Hidano, A. 1991. Decreased level of ceramides in stratum corneum of atopic dermatitis: An etiologic factor in atopic dry skin? Journal of Investigative Dermatology. 96:523-526.

Jamal, Z., Martin, A., Munoz, A. G. and Brindley, D. N. 1991. Plasma membrane fractions from rat liver contain a phosphatidate phosphohydrolase distinct from that in the endoplasmic reticulum. The Journal of Biological Chemistry. 266: 2988-2996.

Jacobs, C. W., Adams, A. E. M., Szaniszlo, P. J. and Pringle, J. R. 1988. Functions of microtubules in the *Saccharomyces cerevisiae* cell cycle. The Journal of Cell Biology. 107:1409-1426.

Jaworski, J. G. and Stumpf, P. K. 1974. Fat metabolism in plants. Properties of a soluble stearyl-acy carrier protein desaturase from maturing *Carthamus tinctorius*. Archives of Biochemistry and Biophysics. 162:158.

Joseph, C. K., Byun, H.-S., Bittman, R., and Kolesnick, R. N. 1993. Substrate recognition of ceramide-activated protein kinase. The Journal of Biological Chemistry. 268:20002-20006.

Kanoh, H., Keiko, Y. and Sakane, F. 1990. Diacylglycerol kinase: a key modulator of signal transduction? Trends in Biochemical Science. 15:47-50.

Karlsson, K.-A. and Pascher, I. 1971. Thin-layer chromatography of ceramides. Journal of Lipid Research.12:466-472.

Karlsson, K.-A. 1977. Aspects on structure and function of sphingolipids in cell surface membranes. Structural Biology of Membranes. 245-274.

Kaya, K., Ramesha, C. S., and Thompson, G. A. 1984. Temperature-induced changes in the hydroxy and non-hydroxy fatty acid-containing sphingolipids abundant in the surface membrane of *Tetrahymena pyriformins* NT-1. Journal of Lipid Research. 25:68-74.

Kindman, L. A., Kim, S., McDonald, T. V. and Gardner, P. 1994. Characterization of a novel intracellular sphingolipid-gated Ca^{2+}-permeable channel from rat basophilic leukemia cells. The Journal of Biological Chemistry. 269:13088-13091.

Kishimoto, Y. 1983. Sphingolipid Formation. The Enzymes. Boyle, P. Ed. VolXVI:372.

Kolesnick, R. 1991. Sphingomyelin and derivatives as cellular signals. Progress in Lipid Research. 30:1-38.

Kulmacz., R. J. and Schroepfer, G. J. Jr. 1978. Sphingolipid base metabolism. Concerning the origin of the oxygen at the carbon atom 4 of phytosphingosine. Journal of the American Chemical Society. 100: 3963.

Lavie, Y., Piterman, O., and Liscovitch, M. 1990. Inhibition of phosphatidic acid phosphohydrolase activity by sphingosine. FEBS Letters. 277:7-10.

Lederer, F. 1994. The cytochrome b$_5$ fold: An adaptable module. Biochimie. 76:674-692.

Linardic, C. M., Jayadev, S., and Hannun, Y. A. 1992. Brefeldin A promotes hydrolysis of sphingomyelin. Journal of Biological Chemistry. 267:14909-14911.

Lipscomb, J. D. 1994. Biochemistry of the soluble methane monooxygenase. Annual Review of Microbiology. 48:371-399.

Loomis, C. R., Walsh, J. P., and Bell, R. M. 1985. *sn*-1,2-Diacylglycerol kinase of *Escherichia coli*. The Journal of Biological Chemistry. 1985:4091-4097.

Maniatis, T., Fritsch, E. F. and Sambrook, J. 1982. Southern transfer. Molecular Cloning A laboratory manual. Cold Spring Harbor, New York:Cold Spring Harbor Laboratory. p382-389.

Mathias, S., Dressler, K. A., and Kolesnick, R. N. 1991. Characterization of a ceramide-activated protein kinase: stimulation by tumor necrosis factor α. Proceedings of the National Academy of Science. 88:10009-10013.

Mathias, S., Younes, A., Kan, C,-C., Orlow, I., Joseph, C.,and Kolesnick, R. N., 1993. Activation of the sphingomyelin signaling pathway in intact EL4 cells and in a cell free systemby IL-1β. Science. 259:519-522.

Mitchell, A. G. and Martin, C. E. 1995. A novel cytochrome b_5-like domain is linked to the carboxyl terminus of the Saccharomyces cerevisiae Δ-9 fatty acid desaturase. The Journal of Biological Chemistry. 270:29766-29772.

Morris, L. J. 1970. Mechanisms and stearochemistry in fatty acid metabolism. Biochemical Journal. 118:681.

Morrow, M. R., Singh, D., and Grant, C. W. M. 1995. Glycosphingolipid acyl chain order profiles: substituent effects. Biochemica et Biophysica Acta. 1235:239-248.

Murad, S. and Kishimoto, T. 1975. Alpha hydroxylation of lignoceric acid to cerebronic acid during brain development. Diminished hydroxylase activity in myelin-deficient mouse mutants. The Journal of Biological Chemistry. 250:5841-5846.

Murad, S., Strycharz, G. , and Kishimoto, T. 1976. Alpha-Hydroxylation of lignoceric and nervonic acids in the brain. Effects of altered thryoid function on postnatal development of the hydroxylase activity. The Journal of Biological Chemistry. 251:5237-5241.

Nagai, J. and Bloch, K. 1968. Enzymatic desaturation of stearyl acyl carrier protein. The Journal of Biological Chemistry. 243:4626-4633..

Nageic, M. M., Baltisberger, J. A., Wells, G. B., Lester, R. L., and Dickson, R. C. 1994. The LCB2 gene of Saccharomyces and the related LCB1 gene encode subunits of serine palmitoyltransferase, the initial enzyme in sphingolipid synthesis. Proceedings of the National Academy of Science USA. 91:7899-7902

Nordlund, P., Sjöberg, B.-M., and Eklund, H. 1990. Three-dimensional structure of the free radical protein of ribonucleotide reductase. Nature. 345:593-598..

Nordlund, P., and Eklund, H. 1993. Structure and function of the Escherichia coli ribonucleotide reductase protein R2. Journal of Molecular Biology. 232:123-164.

Obeid, L. M., Linardic, C. M., Karolak, L. A., and Hannun, Y. A. 1993. Programmed cell death induced by ceramide. Science. 259:1769-1771.

Oh, C. S., Toke, D. A., Mandala, S., and Martin, C. E. 1997. *ELO2* and *ELO3*, homologues of the *Saccharomyces cerevisiae ELO1* gene, function in fatty acid elongation and are required for sphingolipid formation. The Journal of Biological Chemistry. 272:17376-17384.

Okazaki, T., Bielawska, A., Bell, R. M. and Hannun, Y. A. 1990. Role of ceramide as a lipid mediator of $1\alpha,25$-dihydroxyvitamin D_3-induced HL-60 cell differentiation. The Journal of Biological Chemistry. 265:158230-15831.

Ong, D. E. and Brady, R. N. 1973. *In vivo* studies on the introduction of the 4-t-double bond of the sphingenine moiety of rat brain ceramides. The Journal of Biological Chemistry. 248:3884-3888.

Ozols, J. 1989. Structure of cytochrome b_5 and its topology in the microsomal membrane. Biochimica et Biophysicca Acta. 997:121-130.

Pacher, I. 1976. Molecular arrangements in sphingolipids. Conformation and hydrogen bonding of ceramides and their implications on membrane stability and permeability. Biochimica et Biophysica Acta. 455:433-451.

Pascher, I. and Sundell, S. 1977. Molecular arrangements in sphingolipids. The crystal structure of cerebroside. Chemistry and Physics of Lipids. 20:175-191.

Patton, J. L. and Lester R .L. 1991. The phosphoinositol sphingolipids of *Saccharomyces cerevisiae* are highly localized in the plasma membrane. Journal of Bacteriology. 173:3101-3108.

Patton, J. L., Srinivasan, B., Dickson, R. C. and Lester, R. L. 1992. Phenotypes of sphingolipid-dependent strains of *Saccharomyces cerevisiae*. Journal of Bacteriology. 174:7180-7184.

Pelech, S. L., and Sanghera, J. S. 1992. MAP kinases: charting the regulatory pathways. Science. 257:1355-1356.

Pinto, W. J., Srinivasan, B., Shepherd, S., Schmidt, A., Dickson, R. C. and Lester, R. L. 1992. Sphingolipid long-chain base auxotrophs of *Saccharomyces cerevisiae*: Genetics, physiology, and a method for their selection. Journal of Bacteriology. 174:2565-2574.
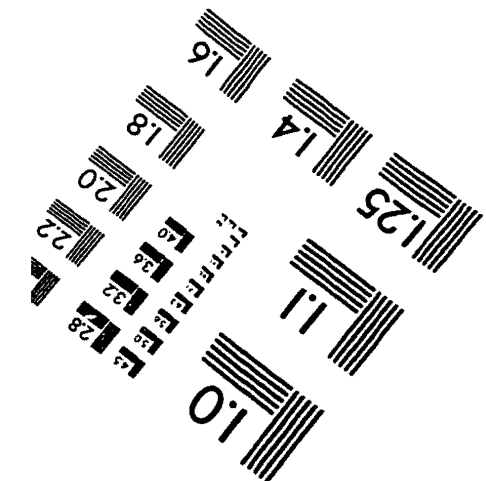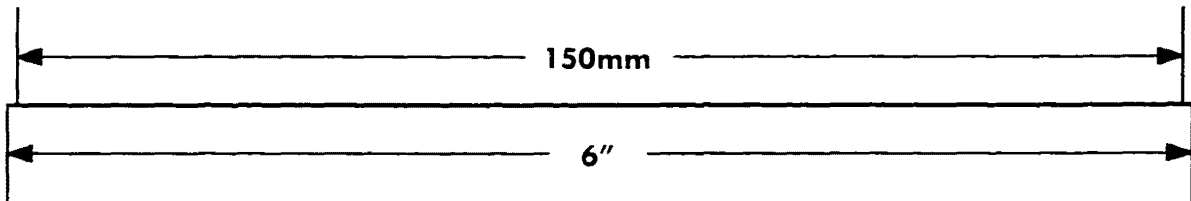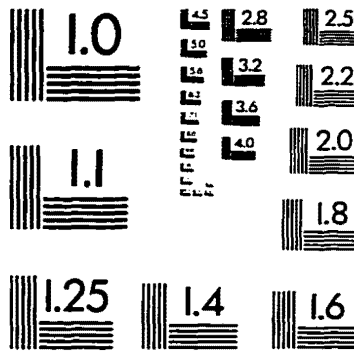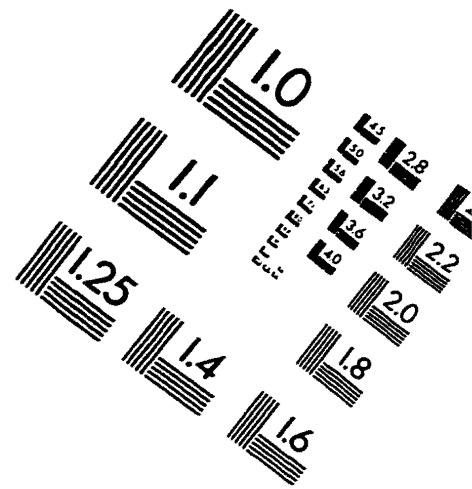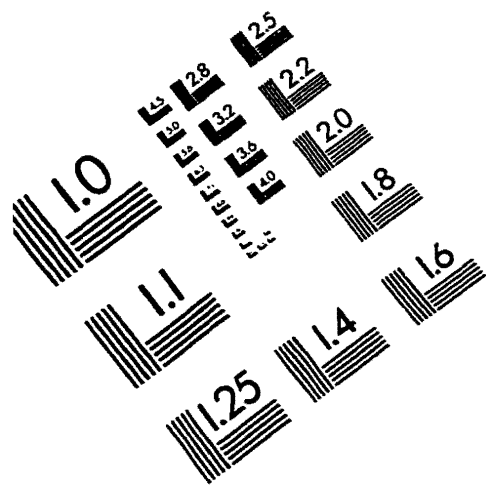
Priestley, N. D., Floss, H. G., Froland, W. A., Lipscomb, J. D., Williams, P. G., and Morimoto, H. 1992. Cryptic stereospecificity of methane monooxygenase. Journal of the American Chemical Society. 114:7561-7562.

Puoti, A., Desponds, C., and Conzelmann, A. 1991. Biosynthesis of mannosylinositol-phosphoceramide in *Saccharomyces cerevisiae* is dependent on genes controlling the flow of secretory vesicles from the endoplasmic reticulum to the golgi. The Journal of Cell Biology. 113:515-525.

Raines, M. A., Kolesnick, R. N., and Golde, D. W. 1993. Sphingomyelinase and ceramide-activated mitogen-activated protein kinase in myeloid HL-60 Cells. Journal of Biological Chemistry. 268:14572-14575.

Rivas, C. I., Golde, D. W., Vera, J. C. and Kolesnick, R. N. 1994. Involvement of the sphingomyelin pathway in autocrine tumor necrosis factor signaling for human immunodeficiency virus production in chronically infected HL-60 cells. Blood. 83:2191-2197.

Rose, M. D., Novick, P., Thomas, J. H. and Fink, G.R. 1987. A *Saccharomyces cerevisiae* genomic plasmid bank based on a centromere-containing shuttle vector. Gene. 60:237-243.

Rosenzweig, A. C., Frederick, C. A., Lippard, S. J., and Nordlund, P. 1993 Crystal structure of a bacterial non-haem iron hydroxylase that catalyses the biological oxidation of methane. Nature. 366:537.

Rosenwald, A. G. and Pagano, R. E. 1993. Inhibition of glycoprotein traffic through the secretory pathway by ceramide. Journal of Biological Chemistry. 268:4577-4579.

Rothstein, R. J. 183. One-step gene disruption in yeast. Methods in Enzymology. 101:202-211. New York: Academic Press Inc.

Ruocco, M. J., Atkinson, D., Small, D. M., Skarjune, R. P., Oldfield, E., and Shipley, G. G. 1981. X-ray diffraction and calorimetric study of anhydrous and hydrated N-palmitoylgalactosylsphingosine (cerebroside). Biochemistry. 20:5957-5966.

Sanders-Loehr, J. and Loehr, T. M. 1979. Hemerythrin. A review of structural and spectroscopic properties. Advances in Inorganic Biochemistry. Eichhorn, G. and Marzilli, L., Eds. 1:235-252. Elsevier:New York.

Sanders-Loehr, J. 1989. Binuclear Iron Proteins. Iron Carriers and Iron Proteins. Loehr, T.M., Ed. 5:375-466. VCH Publishers:NewYork.

Schroepfer, G. J., Jr., and Bloch, K. 1965. The stereospecific conversion of stearic acid to oleic acid. The Journal of Biological Chemistry. 240:54.

Schutze, S., Potthof, K., Machleidt, T., Berkovic, D., Wiegmann, K. and Kronke, M. 1992. TNF activates NFκB by phosphatidylcholine-specific phospholipase C-induced "acidic" sphingomyelin breakdown. Cell. 71:765-776.

Sharom, F. J., and Grant, C. W. M. 1977. Glycosphingolipids in membrane architecture. Journal of Supramolecular Structure. 6:249-258.

Shanklin, J., Whittle, E., and Fox, B. G. 1994. Eight histidines residues are catalytically essential in a membrane-associated iron enzyme, stearoyl-CoA desaturase, and are conserved in alkane hydroxylase and xylene monooxygenase. Biochemistry. 33:12787-12794.

Shanklin, J., Achim, C., Schmidt, H., Fox, B., and Münck, E. 1997. Mössbauer studies of alkane ω-hydroxylase: Evidence for a diiron cluster in an integral-membrane enzyme. Proceedings of the National Academy of Science USA. 94:2981-2986.

Sherman, F., Fink, G. and Lawrence, C. 1974. Methods in Yeast Genetics. Cold Spring Harbor Laboratory:Cold Spring Harbor, New York.

Shah, J., Atienza, J. M., Rawlings, A. V., and Shipley, G. G. 1995. Physical properties of ceramides: effect of fatty acid hydroxylation. Journal of Lipid Research. 36:1945-1955.

Singh, I. and Kishimoto, Y. 1979. α Hydroxylation of lignoceric acid in brain. The Journal of Biological Chemistry. 254:7698-7704.

Singh, D., Jarrell, H. C., Florio, E., Fenske, D. B., and Grant, C. W. M. 1992. Effects of fatty acid alpha-hydroxylationon glycosphingolipid properties in phosphatidyl-choline bilayers. Biochemica et Biophysica Acta. 1103:268-274.

Smith, M. A., Napier, J. A., Stymne, S., Tatham, A. S., Shewry, P. R. and Stobart, A. K. 1994. Expression of a biologically active plant cytochrome b_5 in *Escherichia coli*. Biochemical Journal. 303. 73-79.

Smith, S. W. and Lester, R. L. 1974. Inositol phosphoceramide, a novel substance and the chief member of a major group of yeast sphingolipids containing a single inositol phosphate. The Journal of Biological Chemistry. 249:3395-3405.

Southern, E. 1975. Detection of specific sequences among DNA fragments separated by gel electrophoresis. Journal of Molecular Biology. 98:152.

Sperling, P., Schmidt, H., and Ernst, H. 1995. A cytochrome-b_5-containing fusion protein similar to plant acyl lipid desaturases. European Journal of Biochemistry. 232:798-805.

Spiegel, S. and Milstien, S. 1995. Sphingolipid metabolites: members of a new class of lipid second messengers. The Journal of Membrane Biology. 146:225-237.

Stuckey, J.E., McDonough, V. M., and Martin, C. E. 1990. The *OLE1* gene of *Saccharromyces cerevisiae* encodes the Δ9 fatty acid desatruase and can be functionally replaced by the rat strearoyl-CoA gene. The Journal of Biological Chemistry. 265:20144-20149.

Strittmatter, P., Spatz, L., Corcoran, D., Rogers, M. J., Setlow, B., and Redline, R. 1974. Purification and properties of rat liver microsomal stearyl coenzyme A desaturase. Proceedings of the National Academy of Science U.S.A.. 71:4565.

Takita, Y., Ohaya, Y., and Anraku, Y. 1995. The *CLS2* gene encodes a protein with a multiple membrane-spanning domains that is important Ca^{2+} tolerance in yeast. Molecular and General Genetics. 1995:269-281.

Thompson, G. A. 1992. Response of membrane lipid composition to environmental perturbation. The Regulation of Lipid Metabolism. 2:14-16. CRC Press: Boca Raton, FL..

Tsai, M., Yu, C., Wei, F. S. and Stacey, D. W. 1989. The effect of GTPase activating protein upon Ras is inhibited by mitogenically responsive lipids. Science 243:7581-7590.

Tsai, M., Yu, C., and Stacey, D. W. 1990. A cytoplasmic protein inhibits the GTPase activity of H-Ras in a phospholipid-dependent manner. Science. 250:982-985.

Ullman, M. D. And Radin, N. S., 1972. Enzymatic formation of hydroxy ceramides and comparison with enzymes forming nonhydroxy ceramides. Archives of Biochemistry and Biophysics. 152:767-777.

van Blitterswijk, W. 1985. Membrane fluidity in normal and malignant lymphoid cells. Membrane fluidity in biology. Aloia, R. and Boggs J., Eds. 3:85. New York: Academic Press.

Van der Bijl, P., Lopes-Cardozo, M., and van Meer, G. Sorting of Newly synthesized galactosphingolipids to the two surface domains of epithelial cells. The Journal of Cell Biology. 132:813-821.

van't Hof, W. and van Meer, G. 1990. Generation of lipid polarity in intestinal epithelial (Caco-2) cells; sphingolipid synthesis in the Golgi complex and sorting before vesicular traffic to the plasma membrane. Journal of Cell Biology. 111:977-986.

Van Veldhoven, P. P., Bishop, W. R., Yurivich, D. A., and Bell, R. M. 1995. Ceramide quantitation: evaluation of a mixed micellar assay using *E coli* diacylglycerol kinase. Biochemistry and Molecular Biology International. 36:21-30.

Wells, G.B. and Lester, R.L. 1983. The isolation and characterization of a mutant strain of *Saccharomyces cerevisiae* that requires a long chain base for growth and for synthesis of phospholipids. The Journal of Biology Chemistry. 258:10200-10203.

Wu, W.I., Lin, T. P., Wang, E., Merrill, A. H. and Carman, G. M. 1993. Regulation of phosphatidate phosphatase activity from the yeast *Saccharomyces cerevisiae* by sphingoid bases. The Journal of Biological Chemistry. 268:13830-13837.

Zhang, H., Desai, N. N., Murphey, J. M.., Spiegel, S. 1990. Sphingosine stimulates cellular proliferation via a protein kinase C-indepenent pathway. The Journal of Biological Chemistry. 265:76-81.

Zhang, H., Desai, N. N., Olivera, A., Seki, T., Brooder, G. and Spiegel, S. 1991. Sphingosine-1-phosphate, a novel lipid, involved in cellular proliferation. Journal of Cell Biology. 114:155-167.

Zhao, C., Beeler, T. and Dunn, T. 1994. Suppressors of the Ca^{2+}-sensitive yeast mutant (*csg2*) identify genes involved in sphingolipid biosynthesis. The Journal of Biological Chemistry. 269:21480-21488.

IMAGE EVALUATION
TEST TARGET (QA-3)

150mm

6"